

**ESTIMATION OF PROBABILITY OF FAILURE FOR  
DAMAGE-TOLERANT AEROSPACE STRUCTURES**

---

A Dissertation  
Submitted to  
the Temple University Graduate Board

---

in Partial Fulfillment  
of the Requirements for the Degree of  
DOCTOR OF PHILOSOPHY

---

by  
Keith Halbert  
May, 2014

©

by

Keith Halbert

May, 2014

All Rights Reserved

**ABSTRACT**ESTIMATION OF PROBABILITY OF FAILURE FOR  
DAMAGE-TOLERANT AEROSPACE STRUCTURES

Keith Halbert

DOCTOR OF PHILOSOPHY

Temple University, May, 2014

Professor Richard M. Heiberger, Chair

The majority of aircraft structures are designed to be damage-tolerant such that safe operation can continue in the presence of minor damage. It is necessary to schedule inspections so that minor damage can be found and repaired. It is generally not possible to perform structural inspections prior to every flight. The scheduling is traditionally accomplished through a deterministic set of methods referred to as Damage Tolerance Analysis (DTA). DTA has proven to produce safe aircraft but does not provide estimates of the probability of failure of future flights or the probability of repair of future inspections. Without these estimates maintenance costs cannot be accurately predicted. Also, estimation of failure probabilities is now a regulatory requirement for some aircraft.

The set of methods concerned with the probabilistic formulation of this problem are collectively referred to as Probabilistic Damage Tolerance Analysis (PDTA). The goal of PDTA is to control the failure probability while holding maintenance costs to a reasonable level. This work focuses specifically on PDTA for fatigue cracking of metallic aircraft structures. The growth of a crack (or cracks) must be modeled using all available data and engineering knowledge. The length of a crack can be assessed only indirectly through evidence such as non-destructive inspection results, failures or lack of failures, and the observed severity of usage of the structure.

The current set of industry PDTA tools are lacking in several ways: they may in some cases yield poor estimates of failure probabilities, they cannot realistically represent the variety of possible failure and maintenance scenarios, and they do not allow for model updates which incorporate observed evidence. A PDTA modeling methodology must be flexible enough to estimate accurately the failure and repair probabilities under a variety of maintenance scenarios, and be capable of incorporating observed evidence as it becomes available.

This dissertation describes and develops new PDTA methodologies that directly address the deficiencies of the currently used tools. The new methods are implemented as a free, publicly licensed and open source R software package that can be downloaded from the Comprehensive R Archive Network. The tools consist of two main components.

First, an explicit (and expensive) Monte Carlo approach is presented which simulates the life of an aircraft structural component flight-by-flight. This straightforward MC routine can be used to provide defensible estimates of the failure probabilities for future flights and repair probabilities for future inspections under a variety of failure and maintenance scenarios. This routine is intended to provide baseline estimates against which to compare the results of other, more efficient approaches.

Second, an original approach is described which models the fatigue process and future scheduled inspections as a hidden Markov model. This model is solved using a particle-based approximation and the sequential importance sampling algorithm, which provides an efficient solution to the PDTA problem. Sequential importance sampling is an extension of importance sampling to a Markov process, allowing for efficient Bayesian updating of model parameters. This model updating capability, the benefit of which is demonstrated, is lacking in other PDTA approaches. The results of this approach are shown to agree with the results of the explicit Monte Carlo routine for a number of PDTA problems.

Extensions to the typical PDTA problem, which cannot be solved using currently available tools, are presented and solved in this work. These extensions

include incorporating observed evidence (such as non-destructive inspection results), more realistic treatment of possible future repairs, and the modeling of failure involving more than one crack (the so-called continuing damage problem).

The described hidden Markov model / sequential importance sampling approach to PDTA has the potential to improve aerospace structural safety and reduce maintenance costs by providing a more accurate assessment of the risk of failure and the likelihood of repairs throughout the life of an aircraft.

To my wife Kelly, for her patience.

## ACKNOWLEDGEMENTS

Thanks to my committee for seeing this through. Richard Heiberger, thank you for making a data analyst out of me and for forcing me to pay attention to details. Marc Sobel, thanks for suggesting that I read the particle filter literature. Frederic Murphy, thank you for encouraging me to pursue a PhD in the first place. Harry Millwater, thanks for your time and encouragement.

Special thanks to LeRoy Fitzwater for reading drafts, proofing slides, and giving great advice.

Thanks also to my parents Ken and Kathi for their love and support over the years.

# TABLE OF CONTENTS

ABSTRACT	iv
DEDICATION	vii
ACKNOWLEDGEMENT	viii
LIST OF FIGURES	xii
LIST OF TABLES	xxi
Glossary	xxvi
Acronyms	xxxii
<b>1 INTRODUCTION</b>	<b>1</b>
1.1 Motivation . . . . .	1
1.2 Original Contributions . . . . .	5
1.3 Chapter Overview . . . . .	5
<b>2 FATIGUE AND DAMAGE TOLERANCE ANALYSIS</b>	<b>8</b>
2.1 Introduction to Fatigue . . . . .	8
2.2 Crack Initiation . . . . .	11
2.3 Crack Growth . . . . .	13
2.3.1 Stress Intensity Factor, $K$ . . . . .	13
2.3.2 Fracture Toughness, $K_c$ . . . . .	14
2.3.3 Crack Growth Rate, $\frac{da}{dN}$ . . . . .	15
2.3.4 Initial Crack Size, $a_0$ . . . . .	17
2.4 Deterministic Damage Tolerance Analysis . . . . .	17
<b>3 PROBABILISTIC DAMAGE TOLERANCE ANALYSIS</b>	<b>20</b>
3.1 Typical Problem Specification for Probabilistic Damage Tolerance Analysis . . . . .	21

3.1.1	Single Flight Probability Of Failure . . . . .	22
3.1.2	Probability of Crack Detection . . . . .	24
3.1.3	Equivalent Initial Flaw Size . . . . .	25
3.1.4	Maximum Applied Stress Per Flight . . . . .	28
3.1.5	Probability of Detection Curve . . . . .	30
3.2	PROF Software . . . . .	31
3.2.1	PROF Software Methodology . . . . .	31
3.2.2	PROF Example Problems . . . . .	34
3.3	Explicit Monte Carlo Approach . . . . .	40
3.3.1	Analysis Routine . . . . .	40
3.3.2	SFPOF and PCD Estimation for the Monte Carlo Routine	43
3.3.3	Importance Sampling Modification . . . . .	44
3.3.4	Monte Carlo Results for CP4, CP6, CP7 and CP7ext . .	45
<b>4</b>	<b>HIDDEN MARKOV MODEL / SEQUENTIAL IMPORTANCE SAMPLING APPROACH TO PROBABILISTIC DAMAGE TOLERANCE ANALYSIS</b>	<b>51</b>
4.1	Hidden Markov Model (HMM) . . . . .	52
4.2	Importance Sampling (IS) . . . . .	53
4.3	Sequential Importance Sampling (SIS) . . . . .	54
4.3.1	Probability of Failure or Detection for a Single Particle	56
4.3.2	Calculating the Initial State . . . . .	58
4.3.3	Updating the Weights to Reflect Survival . . . . .	60
4.3.4	Scheduled Inspections . . . . .	60
4.3.5	SIS Routine Flow Chart . . . . .	62
4.4	Three Particle Example Problem . . . . .	64
4.5	Graphical Depiction of the SIS Approach . . . . .	68
4.6	Interval Version of the SIS PDTA Routine . . . . .	71
4.7	Convergence of the SIS Routine . . . . .	74
4.7.1	Running Independent Sequences . . . . .	78
4.7.2	Bootstrap Re-sampling . . . . .	81
4.8	SIS Results for Examples CP4, CP6, CP7 and CP7ext . . . . .	84
<b>5</b>	<b>COMPARISON OF PROBABILISTIC DAMAGE TOLERANCE ANALYSIS APPROACHES</b>	<b>91</b>
<b>6</b>	<b>IMPROVED REPAIR MODELING</b>	<b>96</b>
6.1	Modeling Multiple Repair Types . . . . .	97
6.2	Simple Modified Repair Example . . . . .	97
6.3	Complex Modified Repair Example . . . . .	99

<b>7</b>	<b>DIAGNOSTIC MODEL UPDATING</b>	<b>104</b>
7.1	Aircraft Usage . . . . .	105
7.1.1	Aircraft Usage Example . . . . .	106
7.2	Inspections . . . . .	107
7.2.1	Case 1: Uncertain Inspection . . . . .	109
7.2.2	Case 2: Uncertain Inspection Result . . . . .	110
7.2.3	Case 3: Known Repair Action . . . . .	111
7.2.4	Case 4: Inspection Result Obtained . . . . .	112
<b>8</b>	<b>CONTINUING DAMAGE</b>	<b>120</b>
8.1	Continuing Damage Using Explicit MC . . . . .	122
8.1.1	Inspection Modeling in Continuing Damage MC . . . . .	123
8.1.2	Importance Sampling in Continuing Damage MC . . . . .	124
8.2	Continuing Damage Using HMM/SIS . . . . .	124
8.2.1	Generating the Initial State in Continuing Damage SIS . . . . .	124
8.2.2	Flight-by-Flight Updating in Continuing Damage SIS . . . . .	125
8.2.3	Interval Weight Updating in Continuing Damage SIS . . . . .	127
8.2.4	Inspection Modeling in Continuing Damage SIS . . . . .	127
8.3	Continuing Damage Example Problem . . . . .	128
<b>9</b>	<b>MAINTENANCE COST MODELING</b>	<b>132</b>
9.1	Cost Modeling . . . . .	133
9.1.1	Inspection Costs . . . . .	134
9.1.2	Repair Costs . . . . .	135
9.1.3	False Call Costs . . . . .	136
9.1.4	Failure Costs . . . . .	137
9.2	NDE Cost Minimization Example . . . . .	138
9.3	Extensions to the Maintenance Cost Minimization Problem . . . . .	142
9.3.1	Variable POD Curve Detection Capability . . . . .	145
9.3.2	Automated Inspections of Inaccessible Locations . . . . .	145
9.3.3	Non-Typical Usage or Incorporation of Inspection Results . . . . .	146
<b>10</b>	<b>CONCLUSION</b>	<b>148</b>
10.1	Original Contributions . . . . .	148
10.2	crackR Software . . . . .	149
10.3	Future Work . . . . .	149
10.3.1	Other Types of Structural Deterioration . . . . .	150
10.3.2	Stochastic Crack Growth . . . . .	150
10.3.3	Crack Initiation . . . . .	151
10.3.4	Correlated Inspections . . . . .	152
	<b>REFERENCES</b>	<b>154</b>

# LIST OF FIGURES

1.1	Single Flight Probability Of Failure (SFPOF) estimates for an example problem using various approaches. Structural inspections are performed at flights 4615 and 6923 for this example, reducing the SFPOF estimates accordingly. A popular industry tool, PRobability Of Fracture v3.1 (PROF), overestimates and underestimates SFPOF as compared to an explicit Monte Carlo (MC) simulation. Note that importance sampling is used in the MC simulations prior to the first inspection. Sequential Importance Sampling (SIS), the focus of this work, yields SFPOF estimates similar to the benchmark MC estimates. . . . .	3
2.1	Typical $S-N$ diagram which relates the magnitude of the cyclic stress ( $S$ ) to the number of cycles to failure ( $N$ ). This is a fundamental relationship in fatigue analysis. This is a generic plot of an $S-N$ diagram, hence units are omitted. . . . .	10
2.2	Fatigue crack length versus applied loading cycles for three applied stresses, where $S_1 > S_2 > S_3$ . Crack growth speed $\left(\frac{\Delta a}{\Delta N}\right)$ is faster for higher applied stress. . . . .	15
2.3	Sigmoidal behavior of crack growth rate $\frac{da}{dN}$ versus $\Delta K$ , the stress intensity factor range. Region I is the crack initiation region. Region II is approximately linear. Region III, the failure region, shows crack growth rate going asymptotic near the fracture toughness, $K_c$ . . . . .	16
2.4	Results of the simplistic crack growth example. The time until failure calculated from the conservatively large initial size is used to schedule inspections in the traditional damage tolerance analysis approach. . . . .	18

3.1	Example analytical crack growth curve conservatively fit to the most extreme specimen from empirical data acquired through fatigue testing. The Equivalent Initial Flaw Size (EIFS) distribution is fit using the analytical “master” curve. . . . .	26
3.2	Master curve relating an Equivalent Initial Flaw Size (EIFS) distribution to a Time To Crack Initiation (TTCI) distribution. The crack is said to have initiated at length $a_{\text{init}}$ . The EIFS distribution is typically used in probabilistic damage tolerance analysis instead of the TTCI distribution. . . . .	27
3.3	The maximum applied stress per flight $\sigma_{\text{max}}$ is the peak stress applied during a single flight to the region containing the failure location. In this case, the failure location is a crack of length $a$ at a fastener hole. . . . .	29
3.4	Crack growth curves for Examples CP4, CP6, CP7 and CP7ext from the PRobability Of Fracture (PROF) v3.0 documentation. CP7ext contains input data at far larger crack sizes than do the other examples. . . . .	35
3.5	$K/\sigma$ curves for Examples CP4, CP6, CP7 and CP7ext from the PRobability Of Fracture (PROF) v3.0 documentation. CP7ext contains input data at far larger crack sizes than do the other examples. . . . .	36
3.6	Various input data for PROF Example CP7. The distribution family and parameters for each are given in Table 3.2. . . . .	38
3.7	PRobability Of Fracture (PROF) v3.1 Single Flight Probability Of Failure (SFPOF) estimates for Examples CP4, CP6, CP7 and CP7ext [23]. By default, PROF estimates SFPOF at 20 equally spaced points in each inspection interval, contributing to the jagged appearance prior to the first inspection at 6000 flight hours. Note that unlike the results of the other approaches used in this work, this plot uses flight hours instead of flight numbers. . . . .	39
3.8	Flow chart of an explicit Monte Carlo (MC) routine for a single trial, representing the complete life of the aircraft for one structural location on a single aircraft. This routine can also be used with importance sampling in the absence of scheduled inspections; see Section 3.3.3. . . . .	42

3.9	Explicit Monte Carlo (MC) Routine, Single Flight Probability Of Failure (SFPOF) flight-by-flight and interval estimates for Examples CP4, CP6, CP7 and CP7ext. Examples CP4 and CP6 use a sample size of 500 million, and Examples CP7 and CP7ext each use 1 billion samples. The SFPOF point estimate for each flight is shown as a dot. Interval estimates are acquired by partitioning all flights into 50 flight intervals and pooling the results, improving convergence. The methods of Section 3.3.2 can be used to estimate the MC error in SFPOF estimates for the flights of interest. . . . .	46
3.10	Importance Sampling (IS) Monte Carlo (MC) Single Flight Probability Of Failure (SFPOF) flight-by-flight and interval estimates for Examples CP4, CP6, CP7 and CP7ext. For the interval estimates all flights are partitioned into 50 flight intervals. Each example is run until the first scheduled inspection. SFPOF estimates have converged well at small failure probabilities, in contrast to the MC results of Figure 3.9. The methods of Section 3.3.3 can be used to characterize the MC error in these estimates. . . . .	47
4.1	Example actual and sampling Equivalent Initial Flaw Size (EIFS) distributions for Example CP7. The actual distribution is Weibull with scale 0.000219 and shape 0.575. The sampling distribution is also Weibull with shape 0.575, though the scale has been increased 100-fold to 0.0219. The increased scale parameter yields a distribution with the same support but which yields larger crack lengths more frequently. Larger initial crack sizes in the Sequential Importance Sampling (SIS) routine lead to more likely failure for these particles, contributing to improved convergence speed. . . . .	59
4.2	Flow chart of the Sequential Importance Sampling (SIS) routine using many simultaneous simulations. . . . .	63
4.3	Possible Sequential Importance Sampling (SIS) initial state for Example CP7ext with 1000 particles. . . . .	69
4.4	Changing state over 500 flights for Example CP7ext using 100 particles in the Sequential Importance Sampling (SIS) approach. Note the arrows appear to be all the same length; crack growth for Example CP7ext is an exponential function, so with the $x$ -axis on the log scale the growth appears to be uniform even though the larger cracks are growing at a much faster rate. Also note that the fracture toughness $K_c$ has not changed for any particle. . . . .	70

4.5 State for Example CP7ext before and after inspection using 1000 particles in the Sequential Importance Sampling (SIS) approach. Note the particles which had reached the critical crack length  $a_c$  are discarded. . . . . 72

4.6 Single Flight Probability Of Failure (SFPOF) estimates for Examples CP7 and CP7ext using the flight-by-flight Sequential Importance Sampling (SIS) routine. Because SFPOF is estimated for many flights, and the crack growth curve is generally a smooth function, SFPOF estimates should appear relatively smooth over the service life (except for at scheduled inspections where the SFPOF estimates decrease sharply). SFPOF estimates for CP7ext converge using far fewer particles than CP7. This is due to the fact that CP7 is dominated by the  $a > a_c$  failure mode and CP7ext is dominated by the  $K > K_c$  failure mode. . . . . 76

4.7 Single Flight Probability Of Failure (SFPOF) estimates for Examples CP7 using the flight-by-flight Sequential Importance Sampling (SIS) routine. CP7 is dominated by the  $a > a_c$  failure mode and convergence is slow using flight-by-flight estimates of SFPOF. By pooling results in 50 flight intervals, convergence is improved. . . . . 77

4.8 Single Flight Probability Of Failure (SFPOF) estimates for Example CP7 using Sequential Importance Sampling (SIS), comparing the flight-by-flight and interval routines. Flight-by-flight results are pooled at 50 flight intervals, and the interval routine proceeds 50 flights at-a-time. Similar SFPOF results can be obtained by proceeding several flights-at-a-time rather than flight-by-flight, requiring fewer calculations to do so. For larger intervals, runtime is further reduced though increasingly approximate. . . . . 78

4.9 Examining convergence for Example CP7 using five sequences run in parallel in the flight-by-flight Sequential Importance Sampling (SIS) routine. Particle counts of 100,000 and 1,000,000 are used. SFPOF estimates are those of individual flights, rather than pooled estimates. Several sequences, each run using different random seed values, should yield similar SFPOF estimates if convergence has been achieved. The variability in these estimates can be used to characterize the simulation error. Convergence of SFPOF estimates for Example CP7 is relatively poor when using individual flight estimates of SFPOF due to dominance of the  $a > a_c$  failure mode. . . . . 80

4.10	Examining convergence for Example CP7 using the bootstrap with 100k particles and $n_{\text{boot}} = 1\text{k}$ . At selected flights during the run of the flight-by-flight and interval versions of the Sequential Importance Sampling (SIS) routine, a bootstrap resampling procedure is used to estimate the sampling distribution of the SFPOF estimate. Confidence bounds are connected by dashed lines for plotting convenience. The interval routine is better converged than the flight-by-flight routine. . . . .	82
4.11	Histogram of bootstrap estimates of SFPOF at the last flight in the service life for Example CP7. 100k particles are used in the flight-by-flight Sequential Importance Sampling (SIS) routine with and $n_{\text{boot}} = 10\text{k}$ . The point estimate of $1.1 \times 10^{-6}$ is near the mode of the histogram. The range of estimates spans over an order of magnitude, indicating that convergence of SFPOF at this flight has not yet been achieved. . . . .	83
4.12	Single Flight Probability Of Failure (SFPOF) for Examples CP4, CP6, CP7 and CP7ext in the Sequential Importance Sampling (SIS) approach using 100k particles and 1k bootstrap samples. Examples CP6 and CP7ext exhibit better convergence than CP4 and CP7 at this sample size. Examples CP4 and CP7 are both dominated by the critical crack failure mode, which makes convergence difficult to achieve for flight-by-flight estimation of SFPOF (see Section 4.7). . . . .	85
4.13	Single Flight Probability Of Failure (SFPOF) for Examples CP4, CP6, CP7 and CP7ext in the Sequential Importance Sampling (SIS) approach using five independent sequences of 1m particles per sequence. There is very little variability between runs, indicating that convergence has been well achieved for all examples. . . . .	86
4.14	Single Flight Probability Of Failure (SFPOF) estimates for Examples CP4, CP6, CP7 and CP7ext using flight-by-flight and interval Sequential Importance Sampling (SIS) routines. The flight-by-flight routine uses 5m particles and each interval routine uses 1m particles. The interval routines partition the service life into intervals of 100 and 500 flights, respectively. The 100 flight interval routine yields SFPOF estimates very similar to those of the flight-by-flight routine for all examples. The 500 flight interval routine yields reasonable results given the large size of the intervals. . . . .	89

- 5.1 Single Flight Probability Of Failure (SFPOF) estimates for Examples CP4, CP6, CP7 and CP7ext using the PRObability Of Fracture (PROF) v3.1 software, Monte Carlo (MC) simulation, and Sequential Importance Sampling (SIS) approaches (with 5m particles for each). The MC estimates provide the benchmark for comparison. Importance sampling is used for the MC estimates prior to the first inspection. The SIS estimates agree very well with the MC estimates. PROF variously underestimates and overestimates SFPOF by up to two orders of magnitude. . . . . 93
- 6.1 Damage Tolerance Analysis (DTA) data for a modified version of Example CP7ext, referred to as the *simple* repair scenario. Type 2 exhibits more severe crack growth and stress intensity. In the Sequential Importance Sampling (SIS) routine, all particles will start as classification  $c = 1$ . Particles will be repaired to classification  $c = 2$  for this simple example. Increased severity is used for this example because the repair Equivalent Initial Flaw Size (EIFS) distribution specified for this problem was more severe than the as-manufactured EIFS distribution, indicating that the repair appropriate for this example yields a component which exhibits increased risk. . . . . 98
- 6.2 Single Flight Probability Of Failure (SFPOF) estimates for modified Example CP7ext; *simple* repair scenario. Estimates are obtained using the explicit MC routine for multiple repair types, the SIS routine for multiple repair types, and the standard SIS routine for the original specification of Example CP7ext (“SIS 1 Type”). The SIS and MC SFPOF estimates are equivalent. When utilizing the more severe classification  $c = 2$  repair (in SIS and MC), SFPOF estimates increase dramatically after the first inspection (the first opportunity for repairs to be made). . . . . 99
- 6.3 Damage Tolerance Analysis (DTA) data for a modified version of Example CP7ext, referred to as the *complex* repair scenario. Classification  $c = 1$  is the as-manufactured component, classification  $c = 2$  is an oversize fastener repair, and classification  $c = 3$  is an installed repair fitting. The behavior of the various repair types is listed in the text. In the Sequential Importance Sampling (SIS) routine, all particles will begin as classification  $c = 1$ . At inspection, the type of repair to be performed for a particle (if a repair occurs) depends on the crack size of that particle at inspection time. . . . . 101

6.4	Single Flight Probability Of Failure (SFPOF) estimates for Example CP7ext; <i>complex</i> repair scenario. The scenario is run using the Sequential Importance Sampling (SIS) routine with 500k particles and the explicit Monte Carlo (MC) routine using 100m trials. SFPOF estimates are very similar later in the service life where MC estimates have converged. . . . .	102
7.1	Damage Tolerance Analysis (DTA) data for expected-usage aircraft A and severe-usage aircraft B. Note these are the same set of DTA data shown in Figure 6.1. . . . .	106
7.2	Single Flight Probability Of Failure (SFPOF) estimates for expected-usage aircraft A and severe-usage aircraft B, using updated usage. Aircraft A, which experienced the expected fleet usage, has very low risk (identical to the prognostic estimates in this case). Aircraft B, on the other hand, has a significantly increased risk. At 2308 flights, the current time, it has been assumed that the usage going forward will be the expected usage (that of aircraft A). This causes a drop in SFPOF estimates going forward for aircraft B, however, the previous severe usage has likely done some damage. In order to remain below the specified SFPOF threshold of $1 \times 10^{-7}$ for the next 2308 flights, an inspection is required at this time. . . . .	108
7.3	Probability Of Detection (POD) curve with and without a Probability of Inspection (POI) parameter. POI causes POD to be factored down uniformly. . . . .	110
7.4	Crack size distribution before and after inspection given that there was no detection. This is obtained via an application of Bayes' rule using the Probability Of Detection (POD) curve to obtain the likelihood of a non-detection given crack length, followed by normalization of the distribution. . . . .	112
7.5	1823A Example 1. The data points represent the $a$ vs. $\hat{a}$ data. A regression analysis is conducted to model the relationship between $a$ and $\hat{a}$ . The detection threshold at $\hat{a} = 238$ , along with the regression model, yields the Probability Of Detection (POD) curve, inlaid at the top of the figure. The POD curve is the probability that, according to the model, a crack of a given length will yield an $\hat{a}$ value above the detection threshold. The probability of a false call (an erroneous detection) is 1%; note the noise density at the bottom left. . . . .	115

7.6	1823A Example 1; crack length distributions at inspection in the Sequential Importance Sampling (SIS) routine. $f(a)$ is the density prior to obtaining an inspection result. Inspection result C (and subsequent Bayes' updating of the density) yields $f(a \hat{a}_C)$ ; likewise for inspection result D. Result D, being a much larger value of $\hat{a}$ , yields an updated crack length distribution which is far more severe than that of result C. . . . .	116
7.7	1823A Example 1; diagnostic Single Flight Probability Of Failure (SFPOF) estimates from the Sequential Importance Sampling SIS routine. The Prognostic result uses the traditional approach to modeling a future scheduled inspection. Result C, being a relatively low value of $\hat{a}$ , suggests that the crack length is likely small and the SFPOF estimates remain low without the need for conducting a repair. Result D, on the other hand, suggests that a relatively large crack exists, therefore a repair is required in order to maintain SFPOF to acceptable levels. . .	118
8.1	Diagram of the typical continuing damage case where two cracks emanate from a single fastener hole. . . . .	122
8.2	Continuing Damage; modified Example CP7 Damage Tolerance Analysis (DTA) data. The hot data are more severe than the cold data. . . . .	128
8.3	Continuing Damage Example CP7 results using the flight-by-flight and interval SIS routines. The estimates of five independent sequences of 200k particles are shown along with the mean estimates. Convergence of the interval routine is excellent. . .	129
8.4	Continuing Damage Example CP7 Single Flight Probability of Failure (SFPOF) estimates using the interval Sequential Importance Sampling (SIS) routine and the explicit Monte Carlo (MC) routine. The SIS routine used 1m particles. The MC routine used 10m trials. The "IS MC" results are those of the importance sampling routine run up to the first inspection (using 100k trials). Also depicted are the SIS results for the single-crack version of CP7 using 100k particles. Agreement between the SIS routine and the MC is excellent. Note that the single-crack model exhibits much higher SFPOF estimates due to the fact that there is no second crack providing additional life. . .	130

- 9.1 Single Flight Probability Of Failure (SFPOF) estimates for CP7ext with no inspections in the service life. The Sequential Importance Sampling (SIS) routine used 100k particles for this run. This result is used to determine the latest time at which an inspection can occur according to the specified SFPOF threshold of  $1 \times 10^{-7}$ , which is breached near flight 6500. . . . . 140
- 9.2 Single Flight Probability Of Failure (SFPOF) estimates for the optimal strategy of modified CP7ext. Results shown utilized the flight-by-flight sequential importance sampling routine using 1m particles. With inspections after 5250 flights and 7250 flights, Single Flight Probability of Failure (SFPOF) is kept below the  $1 \times 10^{-7}$  threshold (reaching a peak value of  $8.3 \times 10^{-8}$ ). . . . . 144

# LIST OF TABLES

3.1	Quantiles of $K_c$ and $K_{\max}$ at the critical crack length $a_c$ for Examples CP7 and CP7ext. For CP7, the 99.9 <sup>th</sup> quantile of $K_{\max}$ is below the 0.1 <sup>th</sup> quantile of $K_c$ , thus failure due to $K_{\max} > K_c$ is highly unlikely even at the largest supplied crack length. The $a > a_c$ failure mode will dominate the problem. The reverse is true for CP7ext. . . . .	35
3.2	Parametric input data for Examples CP4, CP6, CP7 and CP7ext from the PProbability Of Fracture (PROF) v3.0 documentation. . . . .	37
3.3	PROF v3.1 Probability of Crack Detected (PCD) results for Examples CP4, CP6, CP7 and CP7ext [23]. . . . .	40
3.4	Monte Carlo (MC) point estimates and 95% confidence bounds for Single Flight Probability Of Failure (SFPOF) for Examples CP4, CP6, CP7 and CP7ext. The estimates prior to the first inspection (flights 3846 and 4615) are obtained using importance sampling to set the initial parameters, and the estimates prior to the second and third inspections (flights 6923 and 9230) are obtained using standard MC sampling. These bounds can be used to judge the quality of SFPOF estimates from the other approaches. . . . .	48
3.5	Monte Carlo (MC) point estimates and 95% confidence bounds for Probability of Crack Detection (PCD) for Examples CP4, CP6, CP7 and CP7ext. The confidence bounds are obtained using the Wilson score interval. Convergence of PCD estimates using a large number of MC trials is very strong (500m trials were used for CP4 and CP6, and 1b for CP7 and CP7ext). These estimates can be used to judge the quality of PCD estimates from the other approaches. . . . .	49

- 4.1 Sequential Importance Sampling (SIS) example using three particles: initial state. Because the EIFS distribution typically has an exponential shape, the particles with smaller initial crack sizes have higher weights since these are more likely to represent the hidden crack size. . . . . 64
- 4.2 Sequential Importance Sampling (SIS) example using three particles: first flight. The Probability Of Failure (POF) for each particle is first calculated to be used to calculate Single Flight Probability Of Failure (SFPOF) for this flight. Next, the survival probability ( $1-POF$ ) is used to update the importance weights (subsequently normalized) to reflect that failure did not occur; this is done because SFPOF is concerned with the probability that a flight will experience the *first* failure of this component. . . . . 65
- 4.3 Sequential Importance Sampling (SIS) example using three particles: second flight. Particle #3 has reached the critical crack length  $a_c$ , thus Probability Of Failure (POF) for that particle is 100%. Because the survival probability of this particle is zero, its importance weight is reduced to zero following this flight. . . . . 65
- 4.4 Sequential Importance Sampling (SIS) example using three particles: inspection result. The Probability Of Detection (POD) curve is utilized to find the probability that each particle would be found at inspection. The importance weights for a *missed* and *found* version of this particle are set according to  $POD(a)$ . Note there are now six particles. To prevent an exponentially increasing particle count, downsampling can be used to reduce the particle count back to three. . . . . 66
- 4.5 Sequential Importance Sampling (SIS) example using three particles: post-inspection. Particle #3, marked with an asterisk, is a newly generated particle representing the outcome that a repair may have occurred after the inspection. The importance weight of this particle is equal to the Probability of Crack Detection (PCD) calculated for this inspection (note, there would generally be more than one repair particle, so the importance weights would typically sum to PCD). Particles #1 and #2 are sampled from those which were missed at inspection, and the importance weights of these are normalized to a sum of  $1-PCD$ . 67
- 4.6 Probability of Crack Detection PCD estimates for Example CP7 using Sequential Importance Sampling (SIS), comparing the flight-by-flight and interval routines (run in 50 flight intervals). Agreement is excellent at 100k particles for the three inspections. 79

4.7	Probability of Crack Detection PCD estimates for Example CP7 using 5 independent sequences in the flight-by-flight Sequential Importance Sampling (SIS) routine. Convergence of these PCD estimates is strong given the low variability between sequences.	79
4.8	Probability of Crack Detection PCD estimates for Example CP7 using Sequential Importance Sampling (SIS), comparing the flight-by-flight and interval routines. Empirical 95% confidence bounds are obtained using the bootstrap with 100k particles and $n_{\text{boot}} = 1\text{k}$ .	84
4.9	Probability of Crack Detection PCD estimates for Examples CP4, CP6, CP7 and CP7ext using Sequential Importance Sampling (SIS). Empirical 95% confidence bounds are obtained using the bootstrap with 100k particles and $n_{\text{boot}} = 1\text{k}$ . This variability may be unacceptable for some applications, in which case the particle count should be increased.	87
4.10	Probability of Crack Detection (PCD) estimates for Examples CP4, CP6, CP7 and CP7ext from 5 independent sequences of 1m particles. Also shown are the mean and standard errors of the estimates. For PCD one is generally interested in 3 decimal places. According to that level of precision, convergence has been achieved.	88
4.11	Probability of Crack Detected (PCD) estimates for Examples CP4, CP6, CP7 and CP7ext using flight-by-flight and interval Sequential Importance Sampling (SIS) routines. The flight-by-flight routine uses 5m particles and each interval routine uses 1m particles. The interval routines partition the service life into intervals of 100 and 500 flights, respectively. Agreement between the routines is excellent.	90
5.1	Single Flight Probability Of Failure (SFPOF) estimates at several selected flights (during the first interval and just prior to the three scheduled inspections) for Examples CP4, CP6, CP7 and CP7ext. The benchmark Monte Carlo (MC) results are presented as the upper and lower bounds of a 95% confidence interval characterizing the MC error. The Sequential Importance Sampling (SIS) SFPOF estimates fall within (or very near to) the bounds of the MC routine for all examples. The Probability Of Fracture (PROF) v3.1 estimates are outside the MC bounds by two orders of magnitude in either direction for several estimates.	94

5.2	Probability of Crack Detected (PCD) estimates for Examples CP4, CP6, CP7 and CP7ext using Monte Carlo (MC) simulation, Sequential Importance Sampling (SIS), and the PProbability Of Fracture (PROF) v3.1 software. Point estimates are shown for PCD of the MC routine because at three decimal places the 95% confidence bounds shown in Table 3.5d are equivalent. The SIS routine yields PCD estimates nearly identical to those of the benchmark MC routine. PROF, on the other hand, tends to significantly underestimate PCD, particularly for the third inspections. Note the results for Examples CP7 and CP7ext are identical. . . . .	95
6.1	Probability of Crack Detection (PCD) estimates for Example CP7ext; <i>simple</i> repair scenario. The increased crack growth speed after repair leads to larger PCD estimates at the second and third inspections. . . . .	100
6.2	Probability of Crack Detection (PCD) estimates for Example CP7ext; <i>complex</i> repair scenario. The scenario is run using the Sequential Importance Sampling (SIS) routine with 500k particles and the explicit Monte Carlo (MC) routine using 100m trials. The SIS and MC estimates of PCD are nearly identical. . . . .	103
6.3	Cost estimates for Example CP7ext; <i>complex</i> repair scenario. The likelihood of occurrence of each repair type, as estimated by the Sequential Importance Sampling (SIS) routine, is used to predict the costs due to each type of repair at each scheduled inspection. This represents a significant improvement in cost prediction capability over the typical industry approach to Probabilistic Damage Tolerance Analysis (PDTA). . . . .	103
8.1	Continuing Damage Example CP7 PCD estimates from five sequences using flight-by-flight Sequential Importance Sampling (SIS), interval SIS, and explicit Monte Carlo (MC) routines. Each sequence of the SIS routine used 200k particles. Each run of the MC routine used 2m particles. Variability between sequences is low thus convergence is judged to be acceptable. The SIS routines yield PCD estimates similar to those of the MC routine, though the interval routine yields a slight underestimate for the second inspection. . . . .	131

9.1 Cost Estimates for a modified Example CP7ext Through Several Permutations of DI and  $\Delta$ DI Non-Destructive Inspection Intervals. Each run used 500k particles in the interval version (50 flight intervals) of the Sequential Importance Sampling (SIS) routine. Costs are calculated for inspections (Insp), repairs (Rep), false calls (FC), and failures (Fail). Using a Single Flight Probability of Failure (SFPOF) threshold of  $1 \times 10^{-7}$ , the optimal inspection schedule shown here uses  $DI = 6000$  and  $\Delta DI = 2000$  (marked with an asterisk). . . . . 141

9.2 Cost estimates (sum of costs from inspections, repairs, false calls, and failures) and risk estimates (peak values of Single Flight Probability of Failure) for modified Example CP7ext through several permutations of DI and  $\Delta$ DI inspection intervals. Each DI/ $\Delta$ DI pair is run in the interval Sequential Importance Sampling (SIS) routine using 500k particles with 50 flight intervals. Three independent sequences are run for each so that convergence of cost and risk estimates can be examined. The strategy which minimizes costs while maintaining SFPOF below  $1 \times 10^{-7}$  is identified with an asterisk in each batch of 9 runs. Cost estimates for competing strategies are similar in the last batch. If more refinement is desired, this procedure can be continued. . . 143

9.3 Probability of Crack Detection (PCD) estimates for the optimal strategy of modified Example CP7ext. The PCD estimates are used to predict the future repair costs. . . . . 144

9.4 Cost estimates for the optimal strategy of modified Example CP7ext. Costs are calculated for inspections (Insp), repairs (Rep), false calls (FC), and failures (Fail). Note that the total cost predicted using the flight-by-flight routine is \$7130, where the interval routine estimate (using fewer particles) is 7153. The peak SFPOF estimate of the flight-by-flight routine is slightly higher than that of the interval routine, though still below the specified SFPOF threshold of  $1 \times 10^{-7}$ . . . . . 145

# Glossary

**Aircraft Structural Integrity Program (ASIP)** United States Air Force task for an aircraft program to maintain the structural integrity of the airframe and major structural components, beginning with initial design and continuing throughout the service life of the program. 21

**continuing damage** the analysis of locations on the aircraft for which failure involves either multiple locations or multiple cracks. 5, 120

**crack growth** the extension of the length of a crack due to the cyclic application of load. 1, 8

**crack initiation** the period of the life of a structural location during which a crack is forming (or nucleating). measured by the time in flight hours or the number of applied load cycles before a detectable crack appears at the location of interest. 8

**critical crack size** the crack length above which failure is certain. this can represent a point of asymptotic stress intensity, or simply the boundary of a structural feature, such as the distance from a fastener hole to the free edge. 32

**Cumulative Distribution Function (CDF)** for a random variable, the CDF is the probability that the variable is less than a specified value. 30

**cyclic loading** the application of load in which the magnitude increases and decreases repetitively. for example, the repeated pressurization and de-

pressurization of a commercial aircraft fuselage which occurs for each flight, beginning at sea level, ascending to flight altitude, and returning to sea level to complete the flight. 4

**Damage Tolerance Analysis (DTA)** the determination of a structure's ability to sustain defects safely until a repair can be performed. 1, 8, 20, 120

**damage-tolerant** the characteristic that a structure can perform its function in the presence of minor damage, such as small fatigue cracks. 1, 11

**deterioration** a symptom of reduced quality or strength. 1

**diagnostic** the analysis of a problem in which current or recent data is employed to determine the current state; backward-looking. 104

**Equivalent Initial Flaw Size (EIFS)** a representation of the size of a crack, flaw, or defect at manufacture when making the conservative assumption that every structural feature contains an initial crack. for deterministic analysis this is often the minimum detectable size for the applicable NDE/NDI methodology for that structural feature, and for probabilistic analysis it is a probability distribution determined by a combination of laboratory testing, field data, and damage tolerance analysis. 12, 21, 96, 121, 151

**failure** in this work, failure consists of the condition in which a crack grows sufficiently long that the structure is no longer able to withstand loading. 1

**failure rate** the probability of failure during an interval  $t + \Delta t$  divided by the probability that failure will not have occurred prior to time  $t$ . 22

**fatigue** the progressive and localized structural damage that occurs when a material is subjected to cyclic loading. 1

- Flight Hours (FH)** the cumulative number of hours that an aircraft has been in operation. 19
- flight spectrum** a data set representing typical in-flight loads at a specified structural location, often consisting of a sequence of peak and valley loads. 19
- fracture mechanics** the field of study of crack growth and failure due to fatigue cracking. 11
- fracture toughness** a property which describes the ability of a material containing a crack to resist fracture. 13
- hazard function** instantaneous failure rate given survival to the time of interest. mathematically, for a continuous random variable, the hazard function is the PDF of time until first failure divided by the complement of the CDF of time until first failure. 31
- Hidden Markov Model (HMM)** a statistical model in which the Markov process being modeled includes unobserved (hidden) states. 2, 21, 51, 92, 96, 104, 121, 148
- Importance Sampling (IS)** a variance reduction technique using in Monte Carlo simulation to improve convergence speed by utilizing an alternative sampling distribution. 44, 52, 91
- initial crack size** the length of a crack when it forms. formation is in many cases assumed to occur at manufacture. 13
- Linear Elastic Fracture Mechanics (LEFM)** a method of the analysis of fracture which assumes that the material behaves according to certain specified principals, most importantly regarding the determination and use of the fracture toughness property. 13

**load** the overall force to which a structure is subjected in supporting a weight or mass or in resisting externally applied forces. 4

**maintenance** any action taken to maintain structural health, including inspections and repairs. 1

**Monte Carlo (MC)** a technique for solving problems involving random variables in which multiple trial runs, or simulations, are carried out each with a randomly generated outcome for each input random variable. 2, 20, 51, 91, 121, 148

**Non-Destructive Evaluation (NDE)** techniques for determining the state of a structural system which do not introduce damage. 30, 104

**particle filter** a sequential Monte Carlo algorithm for approximating a distribution with a temporal structure; the distribution is represented by a number of samples (referred to as particles in the particle filter literature), which allows for efficient Bayesian updating of the model given observed evidence. 4

**Probabilistic Damage Tolerance Analysis (PDTA)** the probabilistic formulation of a damage tolerance analysis in which one or more of the relevant quantities is represented as a random variable or stochastic process. 1, 11, 20, 51, 91, 96, 109, 121, 133, 148

**Probability Distribution Function (PDF)** the relative probability of any given value for a random variable. 32

**Probability of Crack Detection (PCD)** for a future scheduled inspection, the probability that a crack will be detected in that inspection. 21, 99, 105, 122, 133

**Probability Of Detection (POD)** the probability that a crack will be detected as a function of the attributes of the crack. most often the at-

tribute of interest is the crack length, though additional considerations, such as inspector skill, are possible. 21, 57, 110, 123, 136

**Probability Of Failure (POF)** defined for convenience, POF is the probability of failure for a flight for a single particle in the sequential importance sampling routine. 57

**PRObability Of Fracture (PROF)** a software package maintained by the University of Dayton Research Institute for performing probabilistic damage tolerance analysis. 2

**Probability Of Inspection (POI)** the probability that a scheduled inspection will in fact occur. 31, 110, 134

**prognostic** the analysis of a problem in which the future state is predicted; forward-looking. 6, 104

**R** a free, publicly licensed, and open source data analysis software package. 4

**rogue flaw** a manufacturing defect or other relatively large flaw that exists at the time of manufacture of a structural component. 12

**Sequential Importance Sampling (SIS)** an extension of importance sampling to an evolving process. this is a technique in the broader class of sequential Monte Carlo algorithms. 2, 21, 51, 92, 96, 104, 121, 137, 148

**service life** the total time in which the structure will be utilized. 2

**Single Flight Probability Of Failure (SFPOF)** for a single component and a specified future flight, the probability that a structural failure will occur during the specified flight, given that the structure has survived to that flight and allowing for restorative or preventative maintenance to be performed prior to that flight. 21, 91, 105, 122, 132

**strain** a measure of the deformation of material resulting from applied stress; for a particular direction it is defined as the change in length over the original length. strain is not typically used in high-cycle fatigue analysis. 9

**stress** a measure of the internal forces acting within a deformable body; the dimension of stress is that of pressure, or force per unit area. 9

**stress intensity** the ratio between the peak stress on a stress riser (such as a fastener hole) and the applied stress to the region containing the stress riser. 13

**Time To Crack Initiation (TTCI)** the distribution of the time (in flight hours or cycles) until a crack forms on a material. generally determined through laboratory testing. 13, 27, 151

# Acronyms

Page numbers refer to first use of the acronym in each chapter.

**ASIP** Aircraft Structural Integrity Program. 21

**CDF** Cumulative Distribution Function. 30, 32

**DTA** Damage Tolerance Analysis. 1, 8, 20, 120

**EIFS** Equivalent Initial Flaw Size. 12, 21, 96, 121, 151

**FH** Flight Hours. 19

**HMM** Hidden Markov Model. 2, 21, 51, 92, 96, 104, 121, 148

**IS** Importance Sampling. 44, 52, 91

**LEFM** Linear Elastic Fracture Mechanics. 13

**MC** Monte Carlo. 2, 20, 40, 51, 91, 121, 148

**NDE** Non-Destructive Evaluation. 30, 104

**PCD** Probability of Crack Detection. 21, 37, 99, 105, 122, 133

**PDF** Probability Distribution Function. 32

**PDTA** Probabilistic Damage Tolerance Analysis. 1, 11, 20, 51, 91, 96, 109,  
121, 133, 148

**POD** Probability Of Detection. 21, 57, 110, 123, 136

**POF** Probability Of Failure. 57

**POI** Probability Of Inspection. 31, 110, 134

**PROF** PRobability Of Fracture. 2

**SFPOF** Single Flight Probability Of Failure. 21, 91, 105, 122, 125, 132, 133

**SIS** Sequential Importance Sampling. 2, 21, 51, 92, 96, 104, 121, 137, 148

**TTCI** Time To Crack Initiation. 13, 27, 151

# CHAPTER 1

## INTRODUCTION

### 1.1 Motivation

Deterioration of aerospace structures is a serious safety and economic concern. The gradual process of fatigue cracking can lead to sudden failure of aerospace vehicles. Aerospace structures are often designed to be damage-tolerant so that crack growth proceeds at a reasonably slow rate and inspections can be scheduled at a frequency that prevents cracks from growing to dangerous lengths. The structural engineering discipline of DTA (Damage Tolerance Analysis) is dedicated to the design and analysis of such structures. Although fatigue cracks can be detected with reasonable accuracy, it is generally not feasible to perform detailed structural inspections prior to every flight because of the cost of inspections and the downtime of the aircraft when performing maintenance. For these reasons analysis is required to predict damage accumulation and to develop a structural maintenance strategy which can limit the failure probability of aerospace structures while minimizing unnecessary maintenance.

The current aerospace industry tools available for performing PDTA (Probabilistic Damage Tolerance Analysis) are lacking — for example, the currently available tools may for some problems yield overestimates or underestimates of the failure probability of future flights (see Figure 1.1), cannot realisti-

cally represent the variety of possible future repairs, and do not incorporate observed evidence to update the model during the service life. These limitations, discussed in this work, have contributed to a lack of application of these probabilistic methodologies across the aerospace industry. Conservative, deterministic analysis predominates; such analysis has proven over time to produce safe aircraft, but deterministic analysis has the following negative characteristics:

- it is not possible to quantify the probability of failure,
- an unknown increase in structural mass results from the conservative assumptions, leading to increased fuel expense or reduced payload,
- repair decisions are made without utilizing all available information, such as the results of previous inspections, and
- the likelihood of future repairs is not estimated, leading to sub-optimal maintenance scheduling.

For this problem a modeling methodology is needed which is capable of well-characterizing the fatigue process, of accurately predicting the probabilities of failure of future flights and of repair of future inspections, of updating the model as evidence is observed during the service life, and of finding an acceptably safe maintenance strategy which minimizes unnecessary maintenance. An approach which achieves these goals could significantly improve aircraft structural maintenance.

Several software packages exist for conducting PDTA. A well-known package is PROF (PRObability Of Fracture) [37], which solves the typical version of the PDTA problem (as discussed in Chapter 3). Other proprietary PDTA packages exist, such as RBDMS [55] from The Boeing Company, Recursive Probability Integration (RPI) by Shiao [47], and ProDTA by Liao [31].

In this work it is shown that the fatigue process and the future scheduled inspections (with possible repairs) can be well characterized with a HMM (Hidden Markov Model) [5]. As is described in Chapter 4, the HMM representation can be solved using a particle-based representation of the model state and the

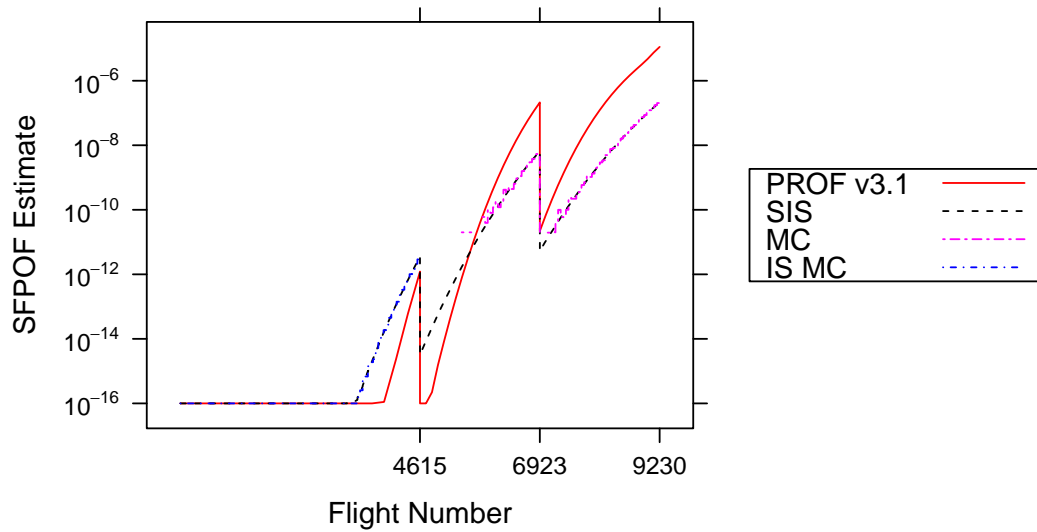


Figure 1.1: Single Flight Probability Of Failure (SFPOF) estimates for an example problem using various approaches. Structural inspections are performed at flights 4615 and 6923 for this example, reducing the SFPOF estimates accordingly. A popular industry tool, PRobability Of Fracture v3.1 (PROF), overestimates and underestimates SFPOF as compared to an explicit Monte Carlo (MC) simulation. Note that importance sampling is used in the MC simulations prior to the first inspection. Sequential Importance Sampling (SIS), the focus of this work, yields SFPOF estimates similar to the benchmark MC estimates.

MC (Monte Carlo) algorithm SIS (Sequential Importance Sampling). This sequential MC approach is a type of particle filter in which the joint distribution of the model state is represented by a number of samples (or “particles”). The flexibility of this approach allows for improvements in PDTA that increase the realism and utility of PDTA.

The selected application for this work is fatigue cracking of metallic structural components. Fatigue is structural damage that occurs due to the cyclic loading of a material, in which the load alternatively increases and decreases. This results in the formation and subsequent growth of cracks. Fatigue failure constitutes at least half of all mechanical failures in general [52]. A comprehensive study of fatigue failures in the United States in 1978 indicated a cost for that year of \$119 billion, or 4% of GDP at the time [41]. Composite materials have been increasingly prevalent on aircraft in recent years; such as on the Boeing 787 aircraft, which had its first flight in 2009 and is 50% composite by weight [1]. Cyclic deterioration of composite materials is a different physical process from that of metals, and the long term behavior of composites is not yet well understood. The vast majority of aircraft structures in operation today are metallic and will remain so for the foreseeable future. This work is applicable in other fields such as marine and civil engineering, which face problems similar to those of the aerospace industry and which also have a rich literature on the subject of structural deterioration. See Straub [53] for an excellent treatment of the deterioration of civil structures, and Madsen et al. [36] for a marine example.

To promote the methods of this work a free, open source software is provided for use in industry and academia, written as an R [40] package called `crackR`. An early version of this software was presented at the 2012 UseR! Conference [21]. R is a free, publicly licensed and open source data analysis software package that has an active community of users who have provided over 4000 user contributed packages to extend its basic functionality. One such package [3], written to accompany the Department of Defense handbook *Nondestructive Evaluation System Reliability Assessment* 1823A [38], provides

statistical methods to develop a model for the crack detection capability of an inspection technology. That software is concerned only with characterizing the quality of an inspection method and does not consider fatigue, failure, or maintenance scheduling.

## 1.2 Original Contributions

The following original contributions are made in this work:

- an explicit MC routine is described which can be used to validate other PDTA approaches,
- an HMM/SIS approach to PDTA is presented which yields results comparable to the explicit MC routine,
- optimization of the maintenance plan is made possible through use of the results of the SIS routine to predict maintenance costs,
- several previously unavailable extensions to the PDTA problem are solved using HMM/SIS, including the modeling of multiple repair types, Bayesian model updating during the service life, and continuing damage,
- a free, publicly licensed and open source PDTA software package for implementing the above concepts on realistic aerospace structures is provided.

## 1.3 Chapter Overview

A presentation of the fundamentals of fatigue analysis for metallic structure is given in Chapter 2. This is by no means comprehensive as this field has a vast literature spanning over a century.

PDTA is introduced in Chapter 3. The typical formulation of the PDTA problem is described in detail. PRobability Of Fracture (PROF) [37], a popular software package with which most PDTA practitioners in the aerospace industry are familiar, is discussed. Example problems from PROF's publicly

available documentation are presented. A new, intuitive and easily defensible MC approach for solving the PDTA problem is described and demonstrated using the PROF example problems. The explicit MC approach is used in this work to judge the quality of the results of other methodologies.

An SIS approach to solving an HMM representation of the traditional PDTA problem of Chapter 2 is presented in Chapter 4. A simplified version of the problem is solved to clarify the approach. The PROF example problems are thoroughly analyzed to demonstrate the SIS approach to PDTA.

The results from the various approaches for the example problems from the PROF documentation are compared in Chapter 5. It is shown that the explicit MC and the HMM/SIS approaches agree well regarding estimates of the probabilities of future failures and repairs, and that PROF does not in general agree with the simulation-based approaches. A plot of the failure probability estimates is shown for one of these examples in Figure 1.1.

An improvement on the treatment of potential future structural repairs is given in Chapter 6. At present, the currently available tools are simplistic regarding the effect of future repairs in that a repair merely resets the crack size and does not reflect that various types of repairs are possible. The type of repair performed can significantly alter the behavior of cracks and should be represented in the PDTA model. The original sampling approaches of this work can allow for multiple repair types, as is shown. By predicting the likelihood of various types of repairs being performed, future repair costs can be more accurately estimated.

Prior to Chapter 7, all analysis in this work is prognostic, or forward-looking. In Chapter 7 it is shown that once aircraft are in service the model can and should be updated to reflect actual usage and other maintenance occurrences, and that the HMM/SIS approach is well-suited to such (diagnostic) updating.

Continuing damage refers to the analysis of locations on the aircraft for which failure involves either multiple locations or multiple cracks. No currently available PDTA tools are capable of realistically solving this problem. Chapter

8 illustrates how the HMM/SIS framework can be used to perform PDTA for the continuing damage problem. An example involving two cracks is presented and solved using both the HMM/SIS and the explicit MC approaches.

Chapter 9 presents a method for predicting the maintenance costs over the life of a structure. Also included is a discussion and demonstration of how an optimal maintenance plan can be determined when there are decisions to be made, such as the timing of inspections. This chapter should be of interest to readers who intend to utilize PDTA to improve cost prediction and cost avoidance for a fleet of aircraft.

The material concludes in Chapter 10 with a reiteration of the original contributions of this work and a discussion of future research opportunities in this area.

# CHAPTER 2

## FATIGUE AND DAMAGE TOLERANCE ANALYSIS

New probabilistic modeling methodologies for the statistical analysis of damage-tolerant aerospace structures are presented in this work. This approach utilizes an existing deterministic DTA (Damage Tolerance Analysis) as input (see Goranson [19] for an excellent discussion of DTA). Note that such an analysis must be performed for each likely failure location, and that in the aerospace industry today a tremendous amount of analytical effort is spent conducting such analyses. This chapter provides background information on the engineering theory of DTA and fatigue cracking in metallic aircraft structures. An introduction to fatigue is given in Section 2.1, followed by additional detail regarding crack initiation and crack growth in Sections 2.2 and 2.3. These sections provide the minimum engineering background necessary to understand the application treated in this work. Finally, Section 2.4 discusses how inspections are traditionally scheduled using DTA.

### 2.1 Introduction to Fatigue

The word “crack” is used in the analysis of structural fatigue to describe any “crack-like flaw”, which may include cracks or other defects such as a void

in the material. In some cases it may be more correct to refer to these as “flaws”. These terms are used interchangeably in this work.

Consider a paper clip as a simple example. It is difficult to snap a paper clip in one motion. However, one can easily break it by bending it back and forth several times. This cyclic loading fatigues the material. Small cracks form in the metal and the strength deteriorates to the point that the same relatively minor load which did not cause failure in a single application leads to failure of the material when applied cyclically. Bending it further in each motion (applying an increased load) will lead to failure more quickly. The applied load results in stress within the material<sup>1</sup>. Stress is typically represented by  $\sigma$ . Note that in this work  $\sigma$  is used for stress rather than for the standard deviation of a Gaussian distribution. Stress is a measure of the internal forces acting within a deformable body. The dimension of stress is that of pressure, or force per unit area; e.g. pounds per square inch (psi) using the United States customary units. The initial stress resulting from the applied load was sufficient to deform the material, but not to cause failure.<sup>2</sup>

Much of the following discussion is derived from Stephens et al. [52], in which an accessible treatment of metal fatigue is given. See also Schijve [46] and Suresh [54]. Fatigue was recognized in the 1850s by Wöhler to be a function of the amplitude of applied stress. Amplitude is the range of stresses between loading and unloading cycles. He showed that larger stress amplitudes,  $S$ , leads to a shorter number of cycles ( $N$ ) to failure. The number of cycles to failure is  $N_f$ . This relation is generally displayed with an  $S$ – $N$  diagram, as is shown in Figure 2.1, adapted from Stephens et al.

Note that in Figure 2.1 the curve does not extend to low stress amplitudes. The minimum stress amplitude plotted is the *fatigue limit*. In theory a part

---

<sup>1</sup>In static structural analysis (involving a single applied load rather than cyclic loading) strain is often used for modeling the behavior of the material; in high-cycle fatigue analysis, as is the case here, stress is typically used.

<sup>2</sup>In engineering analysis, failure must be carefully defined. In this work an abstract aircraft part is considered for which failure is defined mathematically. It is sufficient for discussion purposes to define failure as the condition in which a crack grows sufficiently long that the part in question is no longer able to carry load.

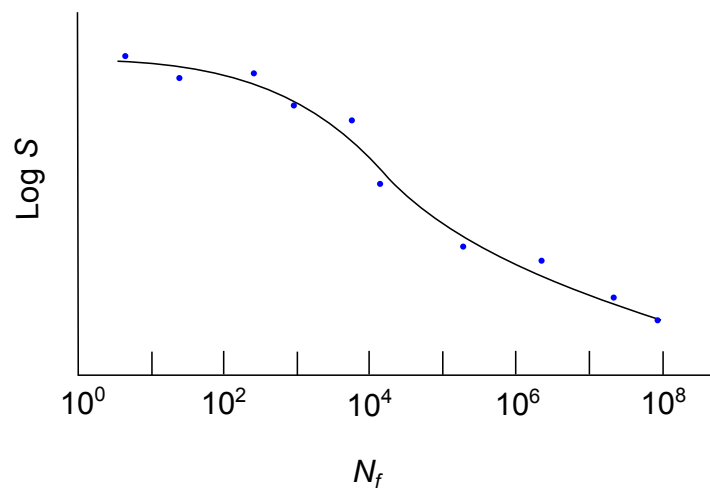


Figure 2.1: Typical  $S$ – $N$  diagram which relates the magnitude of the cyclic stress ( $S$ ) to the number of cycles to failure ( $N$ ). This is a fundamental relationship in fatigue analysis. This is a generic plot of an  $S$ – $N$  diagram, hence units are omitted.

can be designed with an infinite fatigue life by applying cyclic loading with amplitude no larger than the fatigue limit. In practice there is no such thing as infinite life structure, but designing to this criterion will yield an extraordinarily long fatigue life. To achieve this design goal it is generally necessary to increase the thickness of the material, thus increasing the mass and weight of the structure. The *infinite life* design criterion is used for some applications in which the weight of the structure is not a concern, such as railroad tracks. The infinite life criterion is not practical for aerospace applications where removal of unnecessary weight is a primary design goal since heavier structures lead to decreased payload, decreased operating range, or increased fuel costs.

Other design criteria include the *safe life* approach, in which the structure is retired before reaching the fatigue life. This is particularly applicable for unrepairable components and for components which exhibit rapid crack growth due to high cyclic loading frequency, such as helicopter blades and jet engine

turbines.

The modern approach for repairable components in aircraft structures, referred to as damage-tolerant design, involves the field of study known as fracture mechanics to determine whether cracks will grow dangerously large before they can be detected by periodic inspections. In this approach analysts show that cracks will grow slowly and that the structure can function in the presence of relatively small cracks. Structures designed with this approach are the subject of this work. The majority of DTA in the aerospace industry is deterministic, though PDTA (Probabilistic Damage Tolerance Analysis) is an active field of research.

The approach presented in this work provides a means to utilize an existing DTA as input and is less concerned with performing the fatigue analysis itself. Numerous quality software packages exist for performing crack initiation and crack growth analysis, such as NASGRO<sup>3</sup> and AFGROW<sup>4</sup>. The proposed PDTA approach can utilize the results from a generic fatigue analysis, thus allowing for use of the increasingly sophisticated fatigue analysis methodologies that are continually being produced by the engineering community.

## 2.2 Crack Initiation

The study of crack initiation (or crack nucleation) is complex and requires much preliminary engineering knowledge to discuss in detail. In fact there is much that is still not understood about the physics of microscopic crack initiation. The following discussion is at a high level and interested readers should consult Suresh [54] for details and additional references.

The behavior of microscopic cracks is different from that of macroscopic cracks. At the microscopic level flaws can be of a size on the order of several grains of the metal<sup>5</sup>. These microscopic flaws can gradually become more

---

<sup>3</sup>NASGRO, Version 6.2 (September, 2011), from Southwest Research Institute.

<sup>4</sup>AFGROW, Version 5.02 (February, 2014) originally developed by The Air Force Research Laboratory and currently maintained by LexTech, Inc.

<sup>5</sup>Metals generally have a granular structure. Grain sizes can be as small as 0.001", where

severe, can link up with each other, and eventually become what would intuitively be referred to as a crack. The study of crack initiation is concerned with modeling the progression of these microscopic flaws to the end state of a macroscopic crack of a size such that the behavior is that of crack growth and not of crack initiation. Fracture mechanics can indicate the approximate size at which macroscopic crack growth begins to apply.

Crack initiation behavior is highly dependent on various factors, such as the amplitude of applied loading, the material properties, and the quality of the material surface. Crack initiation can often be slowed through surface treatments[14] such as shot peening. Finally, initiation speed can be affected by temperature and other environmental conditions. Sophisticated coupon testing<sup>6</sup> is required to adequately characterize the crack initiation process. A thorough treatment of the statistical design of fatigue experiments is given by R.E. Little[33].

Note that traditional DTA takes a conservative approach. It assumes that a crack has already initiated at the beginning of the life of the structure, and inspections are scheduled according to that assumption. Often the initial size selected is the minimum detectable crack size of the inspection methodology appropriate for the structural feature under consideration. In this way the potential for rapid failure due to a so-called rogue flaw is mitigated. The assumption that an initial flaw exists is also employed in the vast majority of PDTA work. This is made possible through a concept known as EIFS (Equivalent Initial Flaw Size). An attempt is made to describe the initial flaw size as a random variable which when grown according to the laws of macroscopic crack growth, will yield equivalent flaw sizes after initiation. To apply this technique, the selected crack growth model is assumed to apply down to very small crack sizes. In this way one can approximately account for the crack initiation period. That is, the EIFS concept is a means of avoiding

---

the diameter of a human hair is roughly 0.003”.

<sup>6</sup>Coupons are small samples of material which are subjected to a prescribed loading on a testing machine.

the explicit modeling of crack initiation. EIFS is discussed in Section 3.1.3 where the development of an EIFS distribution is described.

When crack initiation has been considered in PDTA, the focus has been on the estimation of the time until the crack reaches a specified macroscopic size. This is often referred to as TTCI (Time To Crack Initiation) [48] [15]. In the future work section of the conclusion in Chapter 10, it is shown how the PDTA approach of this work can accommodate explicit crack initiation modeling by utilizing TTCI instead of EIFS.

## 2.3 Crack Growth

Macroscopic crack growth is a reasonably well-described phenomenon. Fracture mechanics is used to evaluate the strength of structure in the presence of a crack. Most commonly, LEFM (Linear Elastic Fracture Mechanics) is applied to predict crack growth and failure. LEFM does not apply for all situations but it is sufficient to limit the discussion to LEFM here because the use of a more general method, such as elastic-plastic fracture mechanics, will not alter the described approach to PDTA. The important variables to consider in the LEFM approach to crack growth are as follows, each of which is treated below<sup>7</sup>.

- $K$ , the stress intensity factor
- $K_c$ , the fracture toughness
- $\frac{da}{dN}$ , the crack growth rate
- $a_0$ , the initial crack size

### 2.3.1 Stress Intensity Factor, $K$

Stress intensity reflects the well-known fact that the stress in a material spikes locally near features in the geometry such as fastener holes or cutouts

---

<sup>7</sup>Of course, the applied load is also an important factor, but this mainly affects crack growth through its effects on  $K$  and  $\frac{da}{dN}$ .

(holes or empty spaces in the structure). In the case of a crack, the stress intensity at the crack tip (where growth occurs) is crucial. Stress intensity is important because it affects the crack growth rate and the applied stress which causes failure.

The equation which governs the stress intensity at a crack tip is dependent on the geometry of the specimen and the length of the crack. A common reference situation involves a theoretical infinitely large plate subject to a uniform tensile stress<sup>8</sup>. In this case  $K$  is as follows in Equation 2.1, where  $\sigma$  is the applied uniform stress and  $a$  the crack length. For other crack geometries this equation is modified by inserting some number of dimensionless parameters to match experimental or theoretical results. Note that in some cases computational approaches such as finite element analysis are used to determine  $K$ .

$$K = \sigma\sqrt{\pi a/2} \quad (2.1)$$

Often the Normalized Stress Intensity Factor,  $K/\sigma$ , is utilized instead. This representation is a function of only the crack length, thus for a given crack size,  $K/\sigma$  is found with a table lookup. By multiplying the obtained factor by the applied stress  $\sigma$ ,  $K$  is obtained. This is the representation generally utilized in PDTA. For more on this, see Chapter 3.

### 2.3.2 Fracture Toughness, $K_c$

The critical value of  $K$  is referred to as fracture toughness  $K_c$ <sup>9</sup>. This refers to the condition in which crack growth becomes unstable — i.e., rapid.  $K_c$  depends on the material, environment (e.g., temperature), part thickness, and other factors. Fracture toughness is determined through test, and it is a random variable due to the variability inherent in materials. In traditional

---

<sup>8</sup>Tension indicates the part is being “stretched”, with compression representing the opposite condition.

<sup>9</sup> $K_c$  here refers to mode I of the three modes of crack extension ( $K_{c,I}$ ), which is the predominant mode of macroscopic fatigue crack growth [52].

design and analysis,  $K_c$  is assigned a fixed value. In the literature for PDTA, such as Lincoln[32] and Berens[6],  $K_c$  is represented by the normal distribution.

The takeaway for fracture toughness is that when the stress intensity  $K$  reaches  $K_c$ , analytical failure occurs.

### 2.3.3 Crack Growth Rate, $\frac{da}{dN}$

Figure 2.2, adapted from Stephens et al., depicts three examples of crack length versus applied stress cycles for three identical specimens with different cyclic applied stresses where  $S_1 > S_2 > S_3$ . In each case the initial crack length was identical and in each cycle the specimen was unloaded prior to reapplication of load. Note that the crack growth rate  $\frac{da}{dN}$  is the slope at any point of one of the curves, as indicated on the far right of Figure 2.2. The number of cycles to failure,  $N_f$ , is lower for the larger applied stresses, as is the crack length immediately prior to fracture,  $a_c$ .

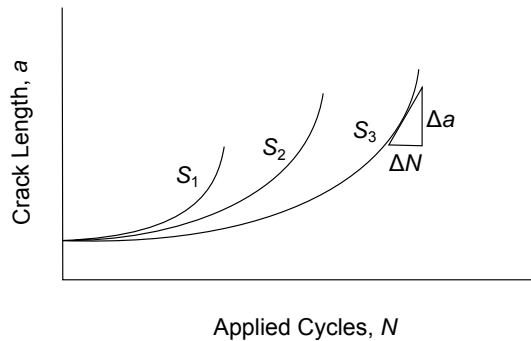


Figure 2.2: Fatigue crack length versus applied loading cycles for three applied stresses, where  $S_1 > S_2 > S_3$ . Crack growth speed  $\left(\frac{\Delta a}{\Delta N}\right)$  is faster for higher applied stress.

The crack growth rate  $\frac{da}{dN}$  is a function of  $\Delta K$ , the applied stress intensity factor amplitude.  $\frac{da}{dN}$  versus  $\Delta K$  is typically drawn on log-log scale and in the majority of cases has a sigmoidal shape that can be divided into three regions as shown in Figure 2.3. At the fracture toughness  $K_c$  unstable growth occurs.

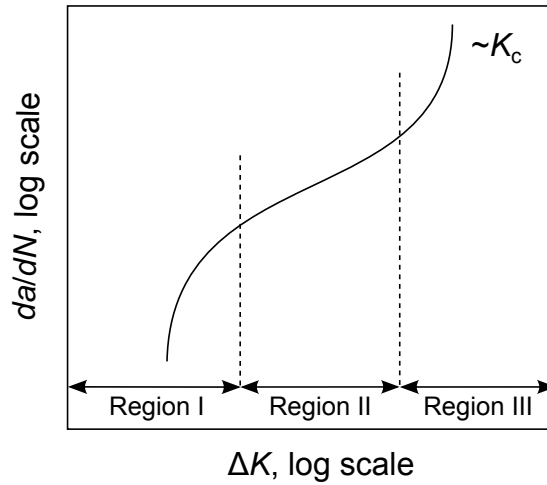


Figure 2.3: Sigmoidal behavior of crack growth rate  $\frac{da}{dN}$  versus  $\Delta K$ , the stress intensity factor range. Region I is the crack initiation region. Region II is approximately linear. Region III, the failure region, shows crack growth rate going asymptotic near the fracture toughness,  $K_c$ .

Note the linearity of Region II, which is also known as the Paris region. The linear relationship corresponds to that of Equation 2.2, first suggested by Paris, Gomez and Anderson[39], where  $C$  and  $m$  are empirically determined parameters for a given situation.

$$\frac{da}{dN} = C[\Delta K]^m \quad (2.2)$$

Note that various other related crack growth equations are utilized in the literature which include other parameters in some way, such as the Forman equation [15]. The use of any such equation yields a deterministic crack growth curve. Because the majority of work in fatigue and fracture mechanics analysis has been devoted to developing such deterministic crack growth models, and existing aircraft programs have already performed such analyses for the potentially risky structural locations, most PDTA approaches utilize a deterministic crack growth curve to represent crack growth. For a discussion of stochastic crack initiation and stochastic crack growth in PDTA, see Chapter 10.

### 2.3.4 Initial Crack Size, $a_0$

In a traditional damage tolerance analysis, the initial crack length utilized is a conventional value for a given situation, often either 0.01 in or 0.05 in<sup>10</sup>. These lengths are generally in Region II of Figure 2.3 so that macro scale crack growth can be utilized. The crack initiation phase of fatigue is therefore skipped and the number of cycles to failure is estimated from this fixed initial crack size. Obviously the selection of initial crack size has a significant effect on the calculated fatigue life when using this simplistic approach.

In PDTA, the initial crack size is a random variable.

## 2.4 Deterministic Damage Tolerance Analysis

In traditional DTA, the initial flaw size is an assumed constant. A simplistic deterministic DTA is presented below for readers unfamiliar with the concept of DTA. In this example the loading is cyclic with fixed peak stress. Suppose Equation 2.1 applies for stress intensity, Paris' Equation 2.2 applies for crack growth, and the various applicable parameters have values as shown below for a typical aluminum structural component.

- Initial flaw size,  $a_0 = 0.05$  in
- Peak applied uniform stress,  $S = 47$  ksi<sup>11</sup>
- One cycle involves stress  $S$  applied in tension and subsequently fully released
- Paris' Law crack growth parameter,  $m = 3$
- Paris' Law crack growth parameter,  $C = 1 \times 10^{-12}$
- Fracture toughness,  $K_c = 50$  ksi  $\sqrt{\text{in}}$

The crack is grown cycle-by-cycle from the initial size  $a_0$  to failure, which occurs when  $K > K_c$ . The result is that the stress intensity  $K$  reaches  $K_c = 50$

---

<sup>10</sup>Often the size is that which is believed to be readily detected by inspection, thus representing an upper limit on the so-called "rogue" crack size that might escape notice at manufacture.

<sup>11</sup>1 ksi = 1000 psi.

at crack length  $a = 0.36$  after roughly  $N_f = 9,700,000$  cycles. See Figure 2.4. If a typical flight includes 1000 such cycles, the predicted life is 9,700 flights (depending on the type of aircraft, this could represent several years or several decades). According to the rule that an inspection be scheduled at one half of this life, this part must be inspected after 4,850 flights occur.

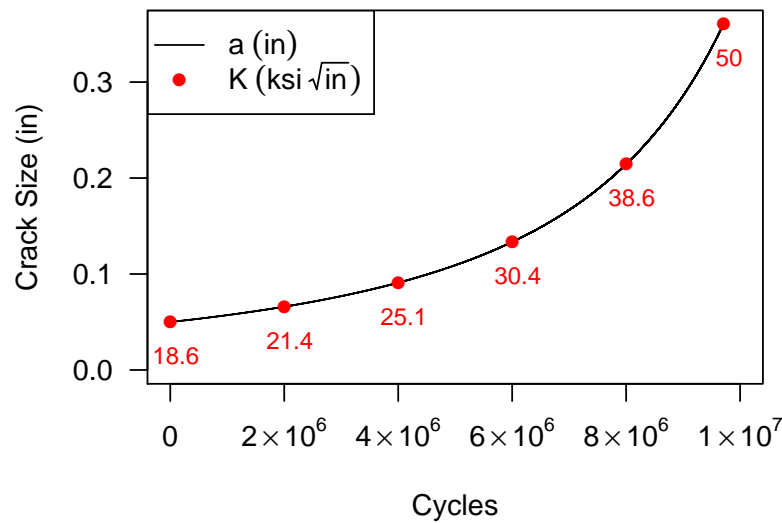


Figure 2.4: Results of the simplistic crack growth example. The time until failure calculated from the conservatively large initial size is used to schedule inspections in the traditional damage tolerance analysis approach.

In this example constant amplitude loading was used. The more realistic situation is variable amplitude loading. With variable amplitude loading there are multiple stress levels to consider and the proportion of the life spent at each stress level must be considered, as well as non-linear effects of load sequencing and other complex phenomena outside the scope of this work.

Load cycles are a simplification of the actual loading on an aircraft part during flight. In a laboratory fatigue test, coupons or parts are cyclically loaded and unloaded at some frequency with either fixed amplitude or vari-

able amplitude loading. On an aircraft, a flight begins on the ground, where the fuselage structure is supported by the landing gear and the wings hang from the fuselage. Once in the air, the entire structure is supported by the wings. This so-called Ground-Air-Ground cycle has a complex relationship with the stresses induced at a specific structural location. In addition, while in the air the loading is continuously changing with each maneuver or gust of wind, and this is subject to random variation. To represent the loading on aircraft structure, a flight spectrum is developed which represents the typical aircraft usage, including both ground and air loads. For a new aircraft such spectra are developed using finite element analysis or other engineering methods. As an existing fleet ages, in-flight loads data is collected from a sample of aircraft and is used to refine the model. In Chapter 7 actual usage is incorporated as observed evidence to update the PDTA model. The flight data is originally a time series of loads at a given location. A spectrum is developed from this by filtering to reduce the spectrum to a sequence of peak and valley pairs (removing the interim noise). Various other filters and engineering methodologies are applied, such as cycle counting [51]. A typical spectrum may contain thousands of such peak/valley pairs. Modern software utilizes the spectrum to perform the crack growth, the details of which are outside the scope of this work.

A spectrum is developed from data covering a certain number of FH (Flight Hours). Flight hours are a common measure of the age of an aircraft. In traditional DTA the flight hours until failure are calculated from a fixed crack size and inspections are typically scheduled at a period one half that time. In much of this work, each individual flight is treated as a discrete event. Often the flight number is used instead of flight hours, where the length of a typical flight in hours is an assumed parameter.

# CHAPTER 3

## PROBABILISTIC DAMAGE TOLERANCE ANALYSIS

Chapter 2 described fatigue damage of metallic aircraft structure and presented a brief overview of the traditional approach to maintenance scheduling using deterministic DTA (Damage Tolerance Analysis). In this chapter PDTA (Probabilistic Damage Tolerance Analysis) is presented. The typical description of the PDTA problem is given in Section 3.1, followed in Section 3.2 by a description of a popular PDTA software tool, PROF, which utilizes the typical problem definition. Examples from the PROF manual are referred to throughout this work, and the definitions of these are given in Section 3.2 along with the PROF results. Finally, an explicit MC (Monte Carlo) approach is presented in Section 3.3 which can obtain defensible results for the typical PDTA problem in a straightforward fashion. The results of the MC approach are used in this work as the baseline for comparison of the results of other PDTA methodologies.

### 3.1 Typical Problem Specification for Probabilistic Damage Tolerance Analysis

PDTA is an active field of research in the aerospace industry. The United States Air Force has specified that a probabilistic risk assessment be performed for aircraft structures; see the ASIP (Aircraft Structural Integrity Program) standard (MIL-STD-1530C) [2]. The goals of such an analysis are to estimate the so-called SFPOF (Single Flight Probability Of Failure) for each flight in the life of the aircraft, as well as PCD (Probability of Crack Detection) for each scheduled inspection (these are discussed in Sections 3.1.1 and 3.1.2, respectively). The typical approach to PDTA involves the following guidelines. Extensions to this are treated in later chapters, however, the first goal of this work is to show that an HMM (Hidden Markov Model)/SIS (Sequential Importance Sampling) approach is capable of solving the typical PDTA problem.

- A flaw exists at time zero, the size of which is a random variable known as EIFS (Equivalent Initial Flaw Size)
- Fracture toughness  $K_c$  is a random variable
- Crack growth is a deterministic function of elapsed flight hours
- Normalized stress intensity  $K/\sigma$  is a deterministic function of crack length  $a$
- Maximum applied stress per flight  $\sigma_{\max}$  is a random variable, independent from flight-to-flight
- $a$ ,  $K_c$ , and  $\sigma_{\max}$  are mutually independent
- Crack detection capability is a function of crack length at inspection, specified by a POD (Probability Of Detection) curve
- Subsequent inspections are independent

Several of these items are self-explanatory or have been discussed at length in the preceding chapters. The EIFS concept is detailed in Section 3.1.3. The max stress per flight distribution is described in Section 3.1.4. Finally,

the POD curve, the method for characterizing the detection capability of an inspection methodology, is described in Section 3.1.5.

### 3.1.1 Single Flight Probability Of Failure

The SFPOF concept is central to PDTA. The Joint Service Specification Guide for Aircraft Structures [28], from the United States Department of Defense, requires that a structural risk assessment be performed on a component-by-component basis and suggests limits on SFPOF between  $1 \times 10^{-7}$  to  $1 \times 10^{-5}$  for *each* component (where the limit depends on the criticality of the structure or type of damage). Note that a system-level risk assessment is not required for aircraft structures according to the current specifications. A definition for SFPOF is not defined in that document, though there is a general agreement within the research community [9] [29] [30] as to what it is intended to measure<sup>1</sup>. Consider the following verbal definition of SFPOF:

**Definition 1** *For a single component, Single Flight Probability of Failure (SFPOF) is, for a specified future flight, the probability that a structural failure will occur during the specified flight, given that the structure has survived to that flight and allowing for restorative or preventative maintenance to be performed prior to that flight.*

The key is that SFPOF is the probability that the flight of interest fails *given* survival of the prior flights; that is, SFPOF is a conditional probability. SFPOF is related to the concept of a failure rate [26]. If the reliability function  $R(t) = 1 - F(t)$  is the complement of the cumulative distribution of time until first failure, the failure rate is

$$\lambda(t) = \frac{R(t) - R(t + \Delta t)}{\Delta t \times R(t)}. \quad (3.1)$$

---

<sup>1</sup>See also Freudenthal [16] for an interpretation of the conditional failure probability of structures.

The failure rate can take on values greater than one and is therefore not a probability. SFPOF is, on the other hand, explicitly defined to represent a probability.

Suppose  $t$  is the flight of interest and  $\phi_i$  represents failure of flight  $i$ , which can be either TRUE or FALSE. For simplicity in the below  $\phi_i$  represents failure of flight  $i$  and  $\bar{\phi}_i$  represents survival of flight  $i$ . The event in which all flights leading up to flight  $t$  survive *and* the flight of interest fails is

$$\bar{\phi}_1 \cap \bar{\phi}_2 \cap \cdots \cap \bar{\phi}_{t-1} \cap \phi_t,$$

the probability of which can be written

$$\Pr(\bar{\phi}_1, \bar{\phi}_2, \cdots, \bar{\phi}_{t-1}, \phi_t).$$

This is not SFPOF as it has been defined here, rather, SFPOF is the probability that the flight of interest fails *given* survival of the prior flights. Noting that survival or failure of subsequent flights is not independent, we have

$$\Pr(\bar{\phi}_1, \bar{\phi}_2, \cdots, \bar{\phi}_{t-1}, \phi_t) = \Pr(\bar{\phi}_1, \bar{\phi}_2, \cdots, \bar{\phi}_{t-1}) \Pr(\phi_t | \bar{\phi}_1, \bar{\phi}_2, \cdots, \bar{\phi}_{t-1}).$$

SFPOF is the second factor in the above equation. The following equation is utilized in Section 3.3 in the explicit MC routine to perform the benchmark SFPOF estimation for this work:

$$\text{SFPOF}_t = \Pr(\phi_t | \bar{\phi}_1, \bar{\phi}_2, \cdots, \bar{\phi}_{t-1}) = \frac{\Pr(\bar{\phi}_1, \bar{\phi}_2, \cdots, \bar{\phi}_{t-1}, \phi_t)}{\Pr(\bar{\phi}_1, \bar{\phi}_2, \cdots, \bar{\phi}_{t-1})}. \quad (3.2)$$

The typical PDTA problem utilizes a deterministic crack growth analysis as input. Because of this most approaches to PDTA involve two failure conditions<sup>2</sup>. In this case SFPOF is the probability that either of the following conditions occur in the PDTA analysis on a specified flight given that neither has previously occurred.

---

<sup>2</sup>Another possible failure condition is *net section yielding*, which is not discussed in this work.

1.  $K > K_c$ 
  - Stress intensity  $K$  exceeds fracture toughness  $K_c$
  - The maximum stress intensity of the flight is the value of interest, so often  $K_{\max}$  is written
2.  $a > a_c$ 
  - Crack length  $a$  exceeds critical crack length  $a_c$
  - Often the less preferable failure mode, since failure in the PDTA due to this event may indicate the deterministic damage tolerance analysis provided as input was incomplete (discussed further in Section 3.2.2)
  - This failure mode is generally included as a necessity, since the deterministic crack growth table must have an end point

### 3.1.2 Probability of Crack Detection

At time zero the crack length is described by the EIFS distribution (see Section 3.1.3). The representation of the EIFS distribution (e.g., samples or quantiles) is grown through time according to the specified crack growth model. At the time of the first inspection there is a representation of the crack size distribution which can be used to predict the outcome of the inspection. As described in Section 3.1.5 the inspection capability is characterized by a POD curve. This curve represents the best fit POD model from a test program designed to identify the detection capability of an inspection method. The specifics of how the POD curve is used to determine PCD depend on how the crack size distribution is represented in the model. In general if  $f(a)$  is the density of the crack size distribution at inspection time and  $\text{POD}(a)$  is a deterministic function yielding the probability of detecting a crack of length  $a$ , PCD for the inspection is an expected value represented by

$$\text{PCD} = \mathbb{E}(\text{POD}(a)) = \int_0^{\infty} \text{POD}(a) f(a) da. \quad (3.3)$$

### 3.1.3 Equivalent Initial Flaw Size

In the majority of the PDTA literature a simplifying assumption is made that a crack exists at time zero. This assumption requires a concept known as EIFS [15]. Example applications of the EIFS concept to PDTA can be found in Lincoln [32] and Berens [6]. The “equivalent” component of the name indicates that the initial crack sizes are not actually physical lengths, but rather are the initial crack sizes that *would have been* if the crack growth portion of the fatigue life were extrapolated to very small crack sizes (see Section 2.3 for a discussion of crack growth and fatigue life). When EIFS is used in PDTA, crack initiation is not modeled. Ideally the crack sizes obtained after growing the EIFS distribution through time will be equivalent to the crack sizes which would be obtained if crack initiation and crack growth were both explicitly modeled.

The following is adapted from the technical report *Fastener Hole Quality* [15]. EIFS is determined through a combination of fatigue test data and crack growth analysis. When fitting an EIFS distribution through test, some number of pristine specimens  $n$  are cyclically loaded until failure occurs for each specimen. The load sequence for each specimen is known and the initiation and growth of the crack are tracked, ultimately leading to failure after  $N_f$  cycles. Each specimen will exhibit a unique path to failure. The fastest-growing crack is typically used to fit a deterministic crack growth model, and the obtained model is referred to as a “master” curve. See Figure 3.1.

Note the master curve is assumed to apply down to very small crack sizes even though the linear-elastic macroscopic crack growth model may be inappropriate at these tiny crack lengths (see Chapter 2). Once the analytical representation of the master curve is obtained, the model is used to find for each specimen the initial crack size  $a_0$  which *would* lead to failure in  $N_f$  cycles if the model were true. Finally, a probability distribution is fit to the  $n$  calculated values of  $a_0$  to obtain the EIFS distribution.

Suppose a crack is assumed to reach macroscopic size at a length of  $a_{\text{init}}$ .

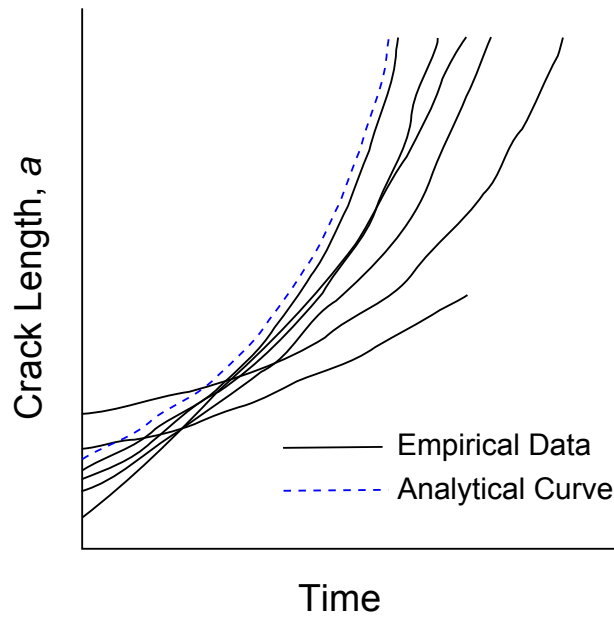


Figure 3.1: Example analytical crack growth curve conservatively fit to the most extreme specimen from empirical data acquired through fatigue testing. The Equivalent Initial Flaw Size (EIFS) distribution is fit using the analytical “master” curve.

The graphic in Figure 3.2, adapted from the *Durability Methods Development* technical report by Shinozuka [48], illustrates the situation. The test program yields a distribution of the time until a specimen will have initiated (reached length  $a_{init}$ ), known as the TTCI (Time To Crack Initiation) distribution. The EIFS distribution is shown on the y-axis. Growing the EIFS distribution according to the master curve will yield an equivalent TTCI distribution.

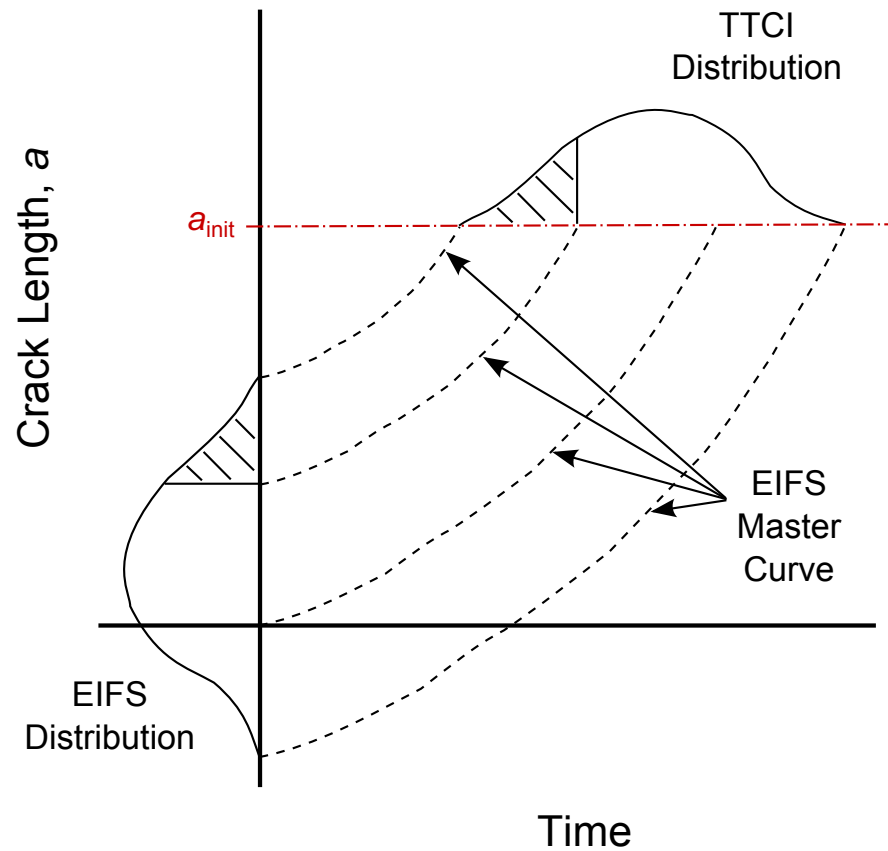


Figure 3.2: Master curve relating an Equivalent Initial Flaw Size (EIFS) distribution to a Time To Crack Initiation (TTCI) distribution. The crack is said to have initiated at length  $a_{init}$ . The EIFS distribution is typically used in probabilistic damage tolerance analysis instead of the TTCI distribution.

Figure 3.2 makes it clear that negative values for initial crack size may be

obtained when using this approach. If the analyst intends to fit distribution with positive support to these data (such as the exponential or two-parameter Weibull), then negative values are not allowed. Shinozuka recommends using a truncated distribution if negative support is not desired, though he also notes that negative EIFS is not necessarily an issue because the EIFS concept is not intended to suggest that these initial sizes are physically meaningful. The EIFS distributions for the example problems provided in the documentation of the PROF software have positive support.

The approach used to fit the master curve should be coherent with the approach used to obtain the crack growth curve for use in PDTA. In theory the EIFS distribution should be fit for each application and applied load, but in practice it is treated as a material property. Liu and Mahadevan[35] and Xiang et al. [58] attempt to derive a version of EIFS that is a material property through asymptotic methods (e.g. using infinite fatigue life). In this work, we assume the EIFS distribution and the crack growth analysis were obtained in a coherent fashion.

In summary, EIFS is a useful construct which allows for PDTA to be conducted without modeling the crack initiation phase of fatigue. Because crack size is such an influential factor in fatigue cracking, the EIFS distribution is one of the dominant input parameters to PDTA. The focus in this work is on the traditional PDTA problem involving the use of EIFS as the initial crack size since this approach has been deemed acceptable by the airworthiness authority of the United States Air Force to meet the standards of ASIP [2]. However, in Chapter 10 a possible approach to performing PDTA utilizing both crack initiation and crack growth is described in hopes of motivating further research in this area.

### 3.1.4 Maximum Applied Stress Per Flight

The maximum applied stress per flight –  $\sigma_{\max}$  – describes the peak loading applied during a flight to the region of the failure location. See Figure 3.3 for

a depiction of the loading at a fastener hole in the presence of a fatigue crack of length  $a$ . In the figure the part is in tension (i.e., it is being “stretched”).

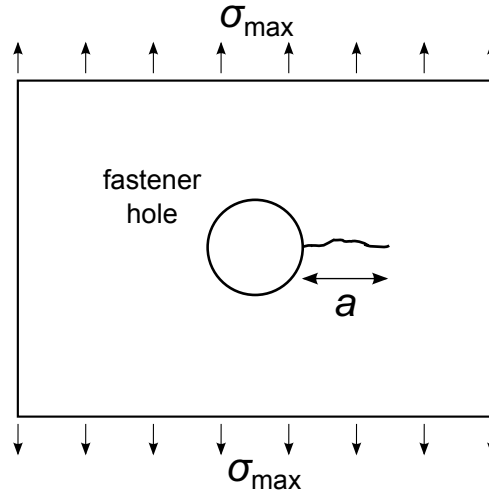


Figure 3.3: The maximum applied stress per flight  $\sigma_{\max}$  is the peak stress applied during a single flight to the region containing the failure location. In this case, the failure location is a crack of length  $a$  at a fastener hole.

As described in Chapter 2 the loading on an aircraft component is described by a flight spectrum. The spectrum details the tensile and compressive stresses which expect to be encountered by the component. If the original flight test data used to specify the flight spectrum is available, this should be used to specify a distribution for the max stress per flight. Often the original test data will not be available and the spectrum must be used to approximate the distribution of  $\sigma_{\max}$ .

In PDTA the length of the crack at any given time determines the normalized stress intensity  $K/\sigma$  local to the crack tip. If  $\sigma_{\max}$  is a known constant,  $K_{\max} = \sigma_{\max} \times K/\sigma$ . If  $\sigma_{\max}$  is a probability distribution, the distribution of  $K_{\max}$  can be found through variable transformation, an example of which is given in Chapter 4, Section 4.3.1 in which  $\sigma_{\max}$  follows the Gumbel distribution. The Gumbel distribution is commonly utilized to represent  $\sigma_{\max}$ <sup>3</sup>.

<sup>3</sup>The Gumbel distribution is often used for max stress per flight, though other related distributions may be more appropriate for some cases, such as the generalized extreme value

The Gumbel can be derived as the maximum (or minimum) from a number of samples taken from various probability distributions [20]. One can fit the max stress distribution by sampling a number of stresses from the spectrum which correspond to the duration of one flight and recording the max stress encountered. This would then be repeated many times to obtain many sample values of max stress per flight, from which a distribution family can be selected and the appropriate parameters fit.

For the purposes of this work it is assumed that  $\sigma_{\max}$  has a specified distribution.

### 3.1.5 Probability of Detection Curve

This section presents the modeling methodology recommended by the Department of Defense handbook 1823A [38] for characterizing the detection capability of NDE (Non-Destructive Evaluation)<sup>4</sup>. This handbook, titled *Non-destructive Evaluation System Reliability Assessment*, provides an R software package[3] for developing a POD curve from NDE test data.

There are various types of NDE, including visual inspection and technology-assisted methods such as eddy current, ultrasonic, and dye penetrant inspections. Thorough discussion of the physics and application of many such techniques are given in Hellier [27] and Shull [50].

The POD curve is a non-decreasing function of the crack length (larger cracks are more likely to be found) so is generally written  $\text{POD}(a)$ . Also,  $0 \leq \text{POD}(a) \leq 1$ . The functional form of a CDF (Cumulative Distribution Function) has these characteristics and is often used. The literature regularly utilizes the log-normal CDF and occasionally the exponential CDF. The function as a log-normal CDF is shown in Equation 3.4, in which  $\mu$  and  $\sigma$  are the mean and standard deviation in the log space and  $\Phi(\cdot)$  indicates the CDF of a standard normal random variable.

---

distribution.

<sup>4</sup>Another common terminology is *Non-Destructive Inspection*, or NDI.

$$\text{POD}(a) = \Phi \left( \frac{\ln(a) - \mu}{\sigma} \right) \quad (3.4)$$

It is always possible that an inspection will indicate the presence of a crack even though there is no crack present; i.e., a false call (or false positive or false alarm). This is mainly a cost consideration, though Straub [53] has suggested that the probability of a false indication be incorporated in the POD curve for analysis purposes. In this case, the POD curve does not intersect the origin but instead has some positive probability of a crack detection when the crack length is zero. Use of such a curve would cause a repair of some kind in the analysis, which may be the case in some realistic applications; for example, if the crack is too small to see with the naked eye but regulations require a repair occur if a crack finding is indicated by the inspection system. The examples in this work utilize a POD curve which intersects the origin.

A POD curve may also incorporate the probability that the inspection will occur as scheduled. This is the so-called POI (Probability Of Inspection) parameter, which is discussed in Section 7.2.1.

## 3.2 PROF Software

PRobability Of Fracture [37], or PROF, was produced and is maintained by the University of Dayton Research Institute. PROF v3.1 was released in 2011. The methods of this software are described in Section 3.2.1, and example problems from its publicly available documentation are given in Section 3.2.2.

### 3.2.1 PROF Software Methodology

The current version of PROF estimates SFPOF as a hazard function [26]. The hazard function is a relation from survival analysis and reliability analysis which represents the instantaneous failure rate (see Equation 3.1). The formulation is

$$h(t) = \frac{f(t)}{1 - F(t)} \quad (3.5)$$

where  $f(t)$  and  $F(t)$  are the PDF (Probability Distribution Function) and CDF of the distribution of the time  $t$  until first failure, respectively.

The hazard rate is not a probability (e.g., it can take on values greater than one). According to its name, the SFPOF measure is clearly intended to represent a probability. The hazard rate is convenient to use to estimate SFPOF because it often yields similar estimates and it can be calculated without the need for explicit survival conditioning. Note that in Chapter 5 it is shown that estimates using the hazard rate (obtained with the PROF software), while often similar, can differ significantly from the conditional probability interpretation of SFPOF presented in Equation 3.9. The PROF formulation calculates the hazard rate for two fracture scenarios and sums these. The two scenarios are: 1) slow crack growth to  $a_c$ , the critical crack size, and 2) sudden fracture due to a large load which causes failure before the crack has reached size  $a_c$ . PROF refers to the hazard rates from these two components as  $h_1(t)$  and  $h_2(t)$ , respectively. The PROF methodology is described at a high level below. For more information, see the PROF v3.0 documentation [37].

PROF utilizes a deterministic crack growth curve. Such a curve necessarily has an endpoint crack size, and this crack size is  $a_c$ <sup>5</sup>. This can be interpreted as the crack size at which an infinitesimal load will cause failure. PROF maintains a crack size distribution  $f_t(a)$  which describes the length of the crack at  $t$  FH. Prior to an inspection having been performed, this is the EIFS distribution “grown” to the time of interest using the deterministic crack growth curve. The complications caused by scheduled inspections and possible repairs is treated later in this section.

For the first failure condition in which the crack grows to size  $a_c$ , PROF utilizes the current crack size distribution and the crack growth table to obtain a distribution for the time until  $a_c$  is reached, represented in the documentation by  $ft(t)$  and  $Ft(t)$  (PDF and CDF, respectively). The corresponding hazard rate  $h_1(t)$  is then calculated from these using Equation 3.5. Note that

---

<sup>5</sup>PROF will in some cases specify a smaller critical length known as  $a_{\text{haz}}$ .  $a_c$  is used here for consistency within this work.

any portion of the crack size distribution which has previously grown beyond  $a_c$  is ignored in the calculation of SFPOF in PROF. Given that failure did not previously occur, with proper survival conditioning the probability mass beyond  $a_c$  should be zero, indicating that it is impossible that these crack sizes represent the truth. Because PROF does not perform an explicit conditioning on survival of previous flights, there is probability mass beyond  $a_c$ , which PROF elects to ignore.

For the second failure condition, the maximum stress per flight (see Section 3.1.4) can cause fracture toughness to be exceeded. PROF represents the max stress as the exceedance probability distribution function for the maximum stress per flight as represented by  $\hat{H}(\sigma) = 1 - H(\sigma)$  which gives the probability of exceeding a given stress  $\sigma$  during a single flight (where  $H(\cdot)$  is the CDF of the max stress per flight distribution). The formulation for the hazard rate of the second failure condition is shown in Equation 3.6, where  $g(K_c)$  is the fracture toughness distribution and  $\sigma_c(a, K_c)$  is the stress which leads to failure for a fixed crack size and fracture toughness.

$$\text{POF} = \int_0^{a_c} f(a) \int_0^\infty g(K_c) \hat{H}[\sigma_c(a, K_c)] dK_c da \quad (3.6)$$

PROF performs the failure calculation at selected flights and proceeds through the life of the aircraft. When the time of a scheduled inspection arrives, the crack size distribution before inspection,  $f_{\text{before}}(a)$ , is used to calculate PCD using Equation 3.7 using numerical integration.

$$\text{PCD} = \int_0^\infty \text{POD}(a) f_{\text{before}}(a) da \quad (3.7)$$

It is assumed that when a crack is detected the crack will immediately be repaired and the repaired flaw size is governed by an EIFS distribution appropriate for this structure and the type of repair under consideration. At each quantile of  $f_{\text{before}}(a)$ , the density is reduced by  $\text{POD}(a)$  and the total proportion of the crack size distribution which is detected is PCD. The crack size distribution after the inspection is shown in Equation 3.8 below where

$f_{\text{after}}(a)$  is the PDF of the crack size distribution after repair and  $f_{\text{R}}(a)$  is the PDF of the EIFS distribution for the repair.

$$f_{\text{after}}(a) = \text{PCD} \times f_{\text{R}}(a) + [1 - \text{POD}(a)] \times f_{\text{before}}(a) \quad (3.8)$$

### 3.2.2 PROF Example Problems

Examples from the publicly available PROF documentation are described in this section. Note that minor adjustments to these were made including: the crack growth and normalized stress intensity tables are truncated to end at a common crack length, the number of similar locations is reduced to one, and the probability of inspection parameter is set to 100%. There are three example problems in the documentation: CP4, CP6, and CP7.

Two versions of Example CP7 are used in this work. When this problem is run in PROF v3.1, the following warning is issued: “Better results may be obtained under some circumstances by extending the geometry curve out to 2.425 K/sigma.”. Example CP7 tends to fail because of breaching the critical crack length, or  $a > a_c$ . In the explicit MC routine for Example CP7 shown later in this chapter, all 1 billion trials fail because of  $a > a_c$ . The damage tolerance analysis input table for CP7 ends at a crack length of 0.518” (this is  $a_c$ ) where  $K/\sigma = 1.671$ . The crack length  $a_c$  has an associated  $K_{\text{max}}$  distribution, the 0.999 quantile of which is at 67.75 ksi $\sqrt{\text{in}}$ . The 0.001 quantile of the  $K_c$  distribution is at 70.18 ksi $\sqrt{\text{in}}$ , thus failure due to  $K_{\text{max}} > K_c$  is highly unlikely even at the very end of the input data.

If these data were extended out to  $a_c = 2.595$ ” (where  $K/\sigma = 5.9146$ ), the 0.001 quantile of  $K_{\text{max}}$  at the new  $a_c$  falls at 191.98, which is well above the 0.999 quantile of  $K_c$  at 95.82. The extended version of the problem (referred to in this work as Example CP7ext) virtually guarantees failure due to  $K_{\text{max}} > K_c$  and not  $a > a_c$ . In the explicit MC routine for CP7ext, all 1 billion trials fail because of  $K > K_c$ . These problems will be compared to highlight the impact of the differing failure modes. See Table 3.1.

There are therefore four example problems considered: CP4, CP6, CP7,

Table 3.1: Quantiles of  $K_c$  and  $K_{\max}$  at the critical crack length  $a_c$  for Examples CP7 and CP7ext. For CP7, the 99.9<sup>th</sup> quantile of  $K_{\max}$  is below the 0.1<sup>th</sup> quantile of  $K_c$ , thus failure due to  $K_{\max} > K_c$  is highly unlikely even at the largest supplied crack length. The  $a > a_c$  failure mode will dominate the problem. The reverse is true for CP7ext.

Variable	Quantile	
	0.001	0.999
$K_c$ (CP7 and CP7ext)	70.18	95.82
$K_{\max}$ at $a_c$ (CP7)	54.22	67.75
$K_{\max}$ at $a_c$ (CP7ext)	191.98	239.87

and CP7ext. The crack growth and  $K/\sigma$  curves are shown in Figures 3.4 and 3.5, respectively.

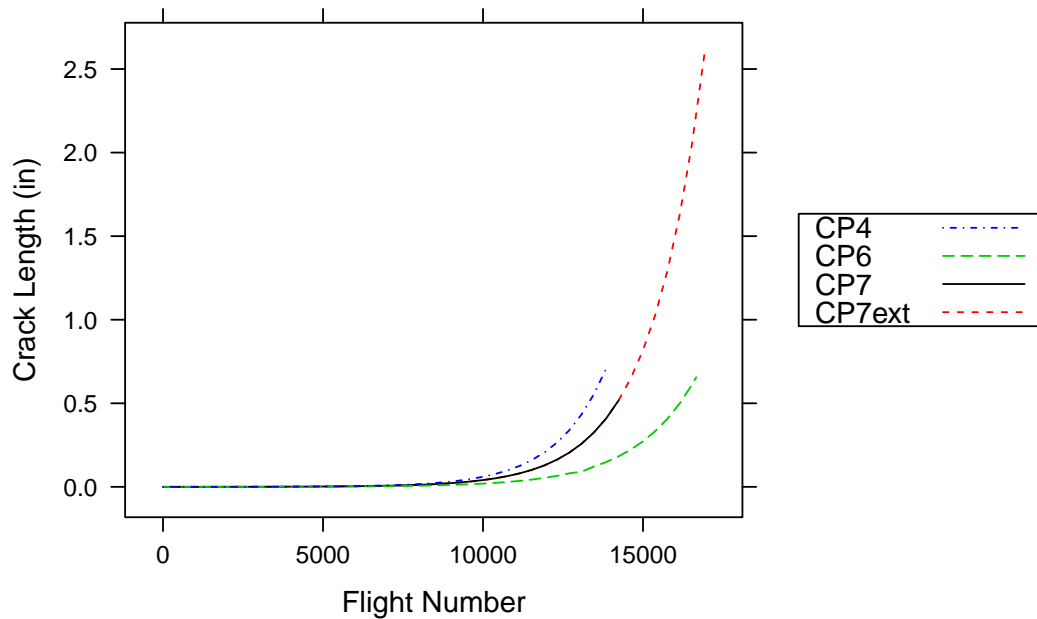


Figure 3.4: Crack growth curves for Examples CP4, CP6, CP7 and CP7ext from the PProbability Of Fracture (PROF) v3.0 documentation. CP7ext contains input data at far larger crack sizes than do the other examples.

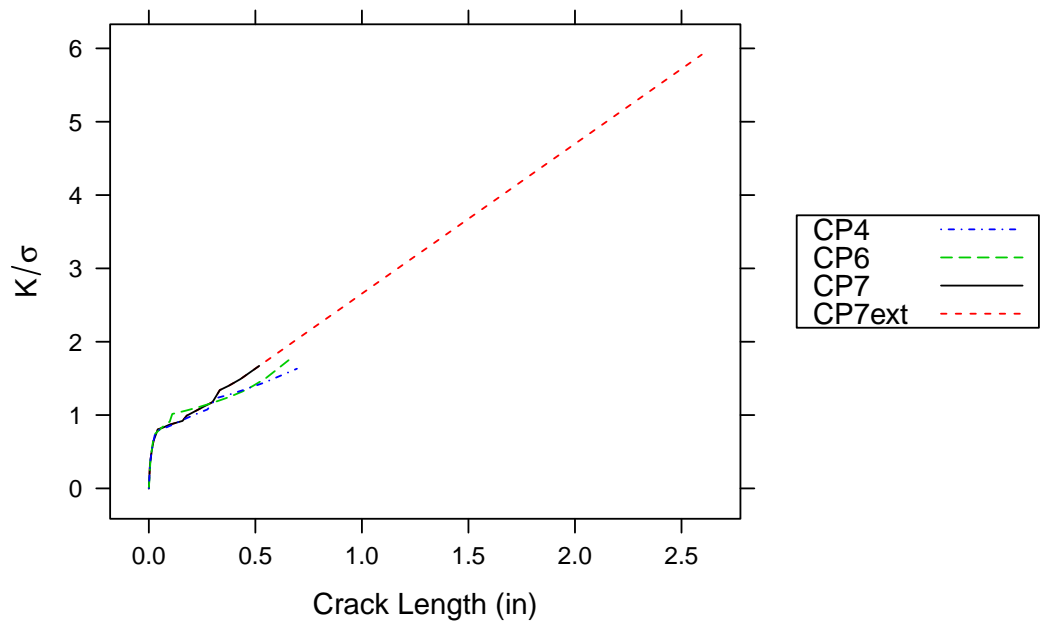


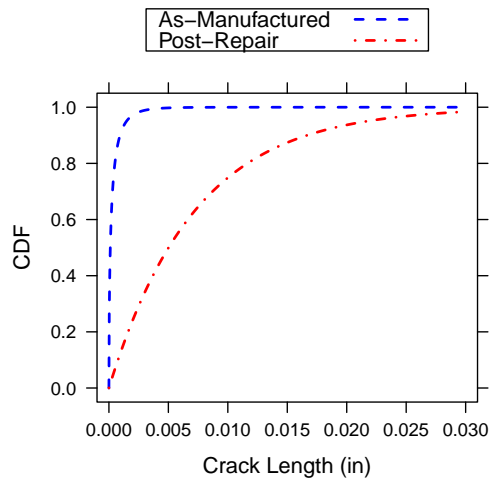
Figure 3.5:  $K/\sigma$  curves for Examples CP4, CP6, CP7 and CP7ext from the PProbability Of Fracture (PROF) v3.0 documentation. CP7ext contains input data at far larger crack sizes than do the other examples.

Table 3.2: Parametric input data for Examples CP4, CP6, CP7 and CP7ext from the PProbability Of Fracture (PROF) v3.0 documentation.

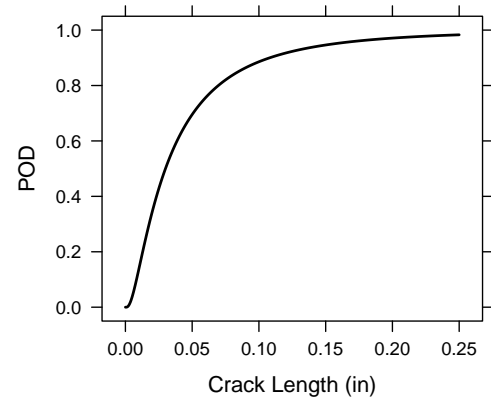
Category	Parameter	CP4	CP6	CP7/CP7ext
Initial Crack Length	Weibull Scale	0.0000417	0.0001534	0.000219
Initial Crack Length	Weibull Shape	0.45	0.5	0.575
Repair Crack Length	Weibull Scale	0.0072382	0.0072382	0.0072382
Repair Crack Length	Weibull Shape	1	1	1
Max Stress Distribution	Gumbel Scale	0.832	0.708	0.916
Max Stress Distribution	Gumbel Location	31.079	26.461	34.229
Fracture Toughness	Kc Mean	83	52.7	83
Fracture Toughness	Kc Std. Dev.	4.15	2.635	4.15
POD Parameters	Median	0.03	0.035	0.03
POD Parameters	Slope	1	1	1
POD Parameters	Minimum Detectable Size	0	0	0
POD Parameters	POI	1	1	1
Inspection Times	Interval #1 (FH)	6000	6000	6000
Inspection Times	Interval #2 (FH)	3000	3000	3000
Inspection Times	Interval #3 (FH)	3000	3000	3000
Aircraft Parameters	Similar Locations	1	1	1
Aircraft Parameters	Reserved For Future Use	0	0	0
Aircraft Parameters	Hours Per Flight	1.3	1.3	1.3

Plots of several input parameters for Example CP7 are given here. The as-manufactured EIFS distribution for this example differs from the EIFS distribution following a repair. The Weibull-distributed CDFs for these are shown in Figure 3.6, along with the POD curve (Log-normal CDF), fracture toughness distribution (normally distributed), and maximum stress per flight distribution (Gumbel distributed). Details of the PROF input parameters for CP4, CP6, CP7, and CP7ext are in Table 3.2, along with the naming conventions PROF itself uses. Note that the four examples use a common post-repair EIFS distribution.

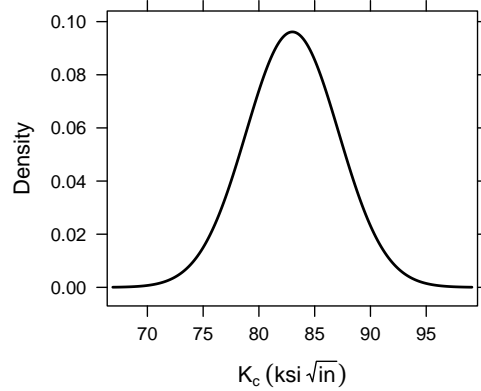
PROF itself is a GUI-driven software package written for Microsoft Windows. SFPOF results are obtained as a table with default output at 20 equally spaced intervals within each inspection interval. PCD results are also tabulated. See Figure 3.7 for SFPOF results for the examples using PROF v3.1. Note that the future scheduled inspections reduce the estimate of SFPOF for the subsequent flights since it is likely any relatively large crack (which has not yet caused a part failure) will be detected and repaired at any scheduled



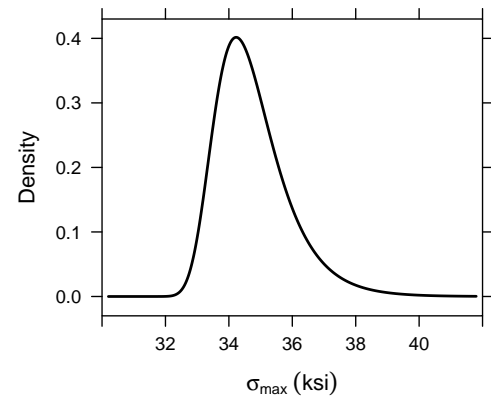
(a) Equivalent Initial Flaw Size



(b) Probability of Detection



(c) Fracture Toughness



(d) Max Stress Per Flight

Figure 3.6: Various input data for PROF Example CP7. The distribution family and parameters for each are given in Table 3.2.

inspections.

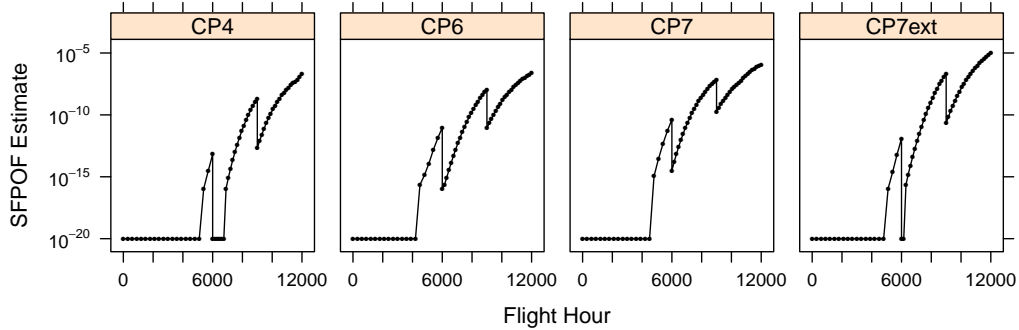


Figure 3.7: PProbability Of Fracture (PROF) v3.1 Single Flight Probability Of Failure (SFPOF) estimates for Examples CP4, CP6, CP7 and CP7ext [23]. By default, PROF estimates SFPOF at 20 equally spaced points in each inspection interval, contributing to the jagged appearance prior to the first inspection at 6000 flight hours. Note that unlike the results of the other approaches used in this work, this plot uses flight hours instead of flight numbers.

Note that PROF's estimates of SFPOF late in the life of the aircraft are higher for CP7ext than for CP7, which is unexpected. The crack growth and  $K/\sigma$  curves were extended to a larger  $a_c$  for CP7ext, which suggests that failure should occur comparatively later. Intuitively, because the DTA data has not been prematurely truncated (leading to earlier failure), this *should* result in decreased estimates of SFPOF. Extending the DTA data in this way results in *increased* SFPOF estimates in PROF. The cause of this behavior may be due to the way PROF treats cracks which have previously reached the critical crack length  $a_c$ . PROF ignores this portion of the crack size distribution when calculating SFPOF. Given failure has not previously occurred, these crack sizes are known to be impossible. Given the definition of SFPOF as a probability of failure conditional on survival to the flight of interest, PROF *should* be performing a Bayes' update of the crack size distribution given survival to the flight of interest. In that case, the support of the crack size distribution

Table 3.3: PROF v3.1 Probability of Crack Detected (PCD) results for Examples CP4, CP6, CP7 and CP7ext [23].

Insp	CP4	CP6	CP7	CP7ext
1	0.021	0.040	0.068	0.068
2	0.110	0.124	0.220	0.220
3	0.339	0.262	0.426	0.426

beyond  $a_c$  would contain no probability mass (unlike the situation in PROF). When the DTA data is extended (as in Example CP7ext), PROF no longer ignores these possible crack sizes, and the SFPOF estimates increase. Given the closed-source nature of PROF, this assessment is speculative. In contrast, the Monte Carlo and the Sequential Importance Sampling estimates of SFPOF (discussed later in this work) are reduced for CP7ext when compared to CP7, as expected (see Figure 5.1).

PCD results for each example are given in Table 3.3.

### 3.3 Explicit Monte Carlo Approach

As part of this work an explicit MC routine [25] was created which can estimate SFPOF and PCD for the problem described in Section 3.1. For a survey of MC methods in various fields, see Liu [34]. The routine itself is described in Section 3.3.1. The estimation of SFPOF and PCD using the results of the MC routine is presented in Section 3.3.2. A method for increasing the efficiency of the routine in the absence of scheduled inspections is described in Section 3.3.3. Results of Examples CP4, CP6, CP7 and CP7ext using the MC routine are presented in Section 3.3.4.

#### 3.3.1 Analysis Routine

Recall from Equation 3.9, SFPOF is the probability that the component fails during the flight of interest *given* survival of the component in all prior flights. The most direct way to calculate SFPOF is to repeatedly simulate the

life cycle flight-by-flight, only moving on to the next flight if the current flight survives. When failure occurs in a given simulation trial, the trial is stopped, thus all failures occur after survival of the prior flights. In this approach  $n$  trials are utilized, each of which represents the complete life cycle for a single component. In each trial the necessary variables are generated directly from their respective probability distributions and the entire life cycle is simulated flight-by-flight until a failure is observed. The two failure conditions discussed in Section 3.1.1 are used: 1)  $K > K_c$  and 2)  $a > a_c$ .

For example, three trials (out of typically many millions) could proceed as follows:

1. flight 1 survives, flight 2 survives,  $\dots$ , flight 6544 survives, flight 6545 fails
2. flight 1 survives, flight 2 survives,  $\dots$ , flight 5212 survives, flight 5213 fails
3. flight 1 survives, flight 2 survives,  $\dots$ , flight 7104 survives, flight 7105 fails

The routine is depicted in Figure 3.8. First, fracture toughness  $K_c$  and initial crack length  $a_0$  are independently generated from their respective distributions. Next, the crack length is grown from flight-to-flight and a value of max stress per flight  $\sigma_{\max}$  is generated for each flight. This continues until either failure condition is met or a scheduled inspection occurs. In this approach the crack length at the time of inspection for a given trial is known and  $\text{POD}(a)$  is used to find the probability that a crack is detected and repaired at this time. A Bernoulli random variable is generated to determine if a detection occurs. If the crack is found, a repair is assumed to occur and the crack length is reset by generating a new size from the repair EIFS distribution. If not detected, the routine continues.

The above routine is run  $n$  times to obtain  $n$  sample values for the flight of first failure, as well as the outcome for the scheduled inspections which occurred before failure of each trial.

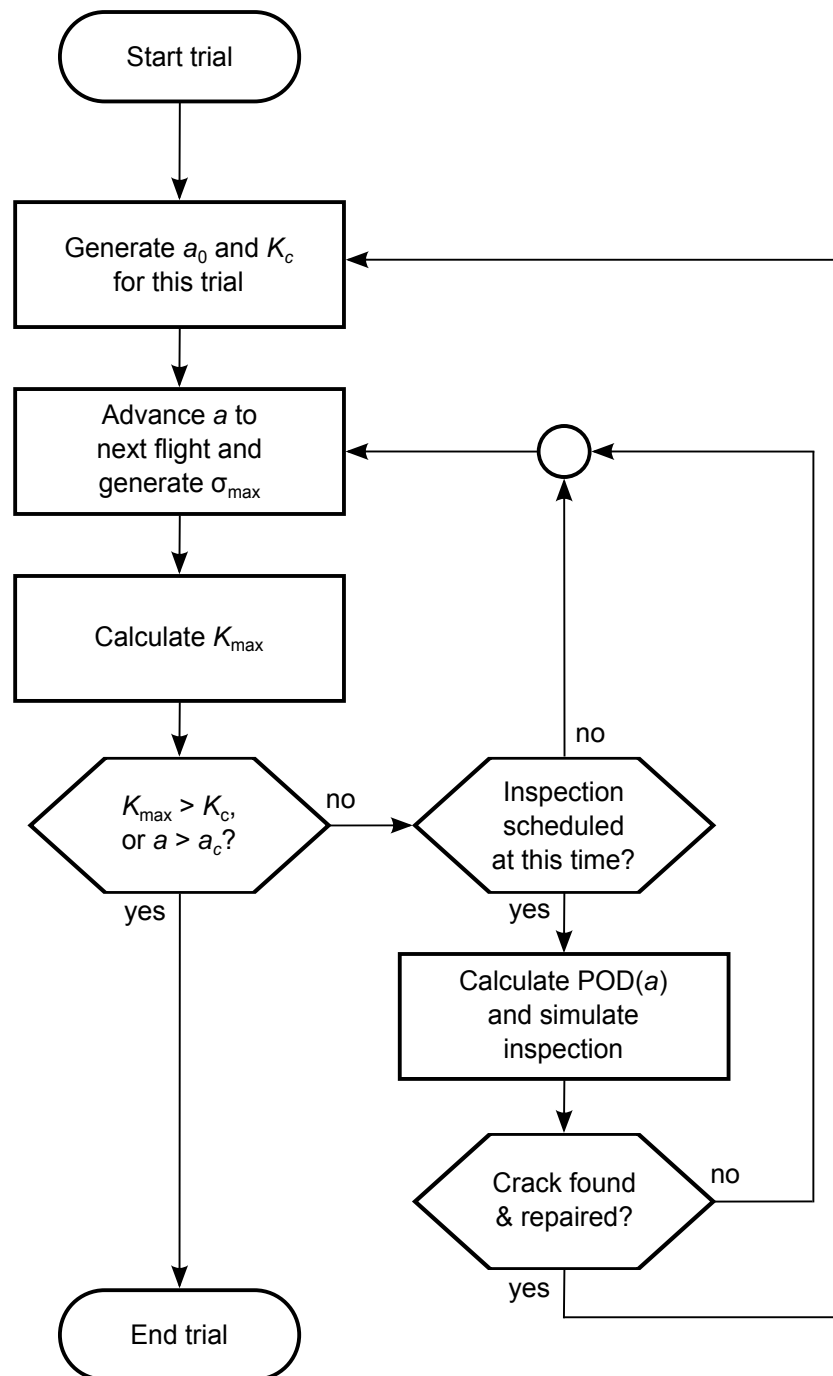


Figure 3.8: Flow chart of an explicit Monte Carlo (MC) routine for a single trial, representing the complete life of the aircraft for one structural location on a single aircraft. This routine can also be used with importance sampling in the absence of scheduled inspections; see Section 3.3.3.

### 3.3.2 SFPOF and PCD Estimation for the Monte Carlo Routine

SFPOF can be directly estimated for any selected flight given there were a sufficient number of trials of the MC routine to yield at least one failure at the flight of interest. Suppose there are  $n$  trials,  $t$  is the flight of interest,  $\gamma_i$  is the first flight to failure for trial  $i$ , and  $I(\cdot)$  is an indicator function that is equal to 1 when the statement is TRUE, 0 otherwise. SFPOF is the proportion of trials which first fail on flight  $t$  divided by the proportion that survive to flight  $t$ , or

$$\text{SFPOF}_t \approx \frac{\frac{1}{n} \sum_{i=1}^n I(\gamma_i = t)}{\frac{1}{n} \sum_{i=1}^n I(\gamma_i \geq t)} = \frac{\sum_{i=1}^n I(\gamma_i = t)}{\sum_{i=1}^n I(\gamma_i \geq t)}. \quad (3.9)$$

An estimate of the MC error for the estimate of SFPOF at a particular flight can be obtained by recognizing that the failure of a given flight is a binomial probability. The point estimate of that probability is given in equation 3.9. The number of binomial trials corresponding to that estimate is the number of trials of the MC routine which survived to the flight of interest. The Wilson score interval[57] is used because it performs well with success probabilities near zero or one (as is the case here).

For each scheduled inspection PCD is calculated as follows. Suppose the inspection of interest is scheduled to occur prior to flight  $t$ , and that  $\psi_i$  is TRUE for trial  $i$  if a repair occurred at this inspection in the MC routine. Note that if for trial  $i$  the component failed prior to flight  $t$ ,  $\psi_i$  is FALSE. PCD is the proportion of repairs performed at this inspection among trials which survived to flight  $t$ , or

$$\text{PCD}_t \approx \frac{\sum_{i=1}^n I(\psi_i)}{\sum_{i=1}^n I(\gamma_i \geq t)} . \quad (3.10)$$

The MC error of PCD is estimated similarly to that of SFPOF using the Wilson score interval.

The explicit MC routine is slow to converge when calculating SFPOF on a flight-by-flight basis. With 1 billion samples, an estimate of SFPOF below around  $1 \times 10^{-9}$  (1 failure in 1 billion trials, ignoring the denominator of Equation 3.9) cannot be obtained, and estimates should not be considered reliable below perhaps  $1 \times 10^{-8}$  (where 10 failures occurred in 1 billion trials). To speed convergence, failures of nearby flights can be pooled by partitioning all flights into a number of flight intervals. To estimate SFPOF in this way, Equation 3.9 is used where  $t$  represents an interval of flights rather than individual flights. The resulting estimates are then divided by the number of flights in each interval to obtain the failure probabilities which correspond to single flights. Examples are given in Section 3.3.4.

If the flight intervals are relatively short, the approximation is reasonable since SFPOF tends to increase gradually. Whether the flight-by-flight or interval version of the SFPOF calculation is utilized, there must be a failure at a particular flight/interval in order to obtain an estimate of SFPOF. In general, the SFPOF estimates will show significant scatter until SFPOF estimates are larger and failures in the MC routine are more common.

### 3.3.3 Importance Sampling Modification

The estimates of SFPOF when utilizing the MC routine are slow to converge because the failure of a particular future flight is a rare event. The actual initial crack size distribution  $f(a_0)$  generally has the majority of its density at very small crack lengths and failure occurs later if the initial crack size  $a_0$  is small. IS (Importance Sampling) [44] can be used when there are no

inspections so that convergence of  $SFPOF_t$  is achieved with far fewer samples. Importance sampling is discussed in Section 4.2. The method involves utilizing an alternative sampling distribution  $g(a_0)$  for the initial crack length so that initial cracks tend to be larger and failure will occur more quickly in general. The importance weight  $w_i$  for trial  $i$  is the ratio of the densities of the actual and sampling distributions at the initial crack length for that trial, or  $w_i = f(a_0)/g(a_0)$ . In this case, the MC SFPOF point estimate is as follows:

$$SFPOF_t \approx \frac{\frac{1}{n} \sum_{i=1}^n I(\gamma_i = t) w_i}{\frac{1}{n} \sum_{i=1}^n I(\gamma_i \geq t) w_i} = \frac{\sum_{i=1}^n I(\gamma_i = t) w_i}{\sum_{i=1}^n I(\gamma_i \geq t) w_i}. \quad (3.11)$$

Confidence bounds for SFPOF estimates from the IS routine can be characterized by utilizing Efron's bootstrap technique. In this approach, the data obtained from the MC routine are re-sampled with replacement  $n_{boot}$  times (including the importance weights) and Equation 3.11 is utilized for each re-sampled data set to obtain  $n_{boot}$  estimates of  $SFPOF_t$ . The 2.5<sup>th</sup> and 97.5<sup>th</sup> quantiles of the resulting estimates are taken as the approximate 95% CI estimate.

Like the explicit MC routine, estimates of SFPOF can be obtained for intervals of flights rather than for individual flights. Due to the efficiency of the IS routine, this is not necessary from the point-of-view of convergence. Pooling SFPOF into interval estimates can make for SFPOF plots which are easier to read (see Figure 3.10).

### 3.3.4 Monte Carlo Results for CP4, CP6, CP7 and CP7ext

The MC routine produced in this work was coded in both R and in Fortran 90. The routines are equivalent, but the Fortran routine is faster due to the nature of the software. The MC examples of this chapter are run using the Fortran routine to obtain a large number of samples in a reasonable time. The Fortran routine was run on a standard Windows machine using 1 billion trials

for Examples CP7 and CP7ext, with a total runtime of about 600 hours (8 instances of 125 million samples were run, each taking 75 hours to complete). Examples CP4 and CP6 were each run using 500 million trials.

The flight-by-flight point estimates of SFPOF from the MC routine are shown in Figure 3.9 for Examples CP4, CP6, CP7 and CP7ext. Also shown in the figure are interval estimates acquired by partitioning all flights into 50 flight intervals.

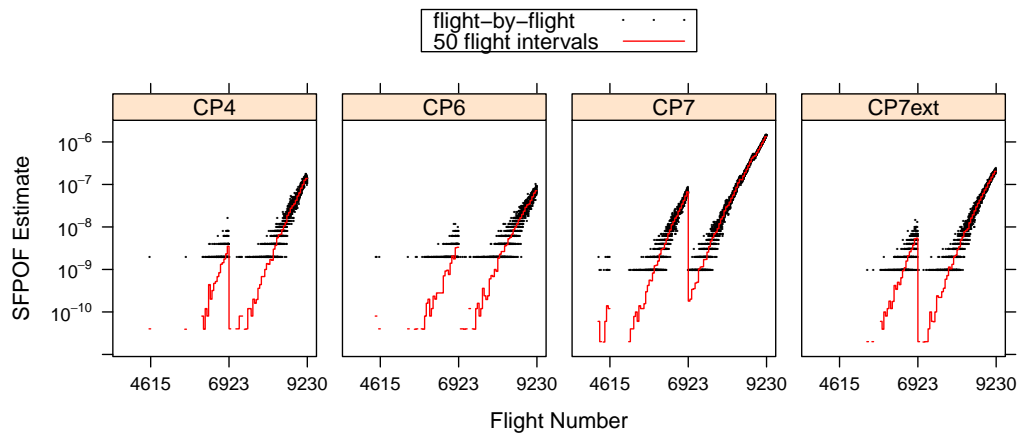


Figure 3.9: Explicit Monte Carlo (MC) Routine, Single Flight Probability Of Failure (SFPOF) flight-by-flight and interval estimates for Examples CP4, CP6, CP7 and CP7ext. Examples CP4 and CP6 use a sample size of 500 million, and Examples CP7 and CP7ext each use 1 billion samples. The SFPOF point estimate for each flight is shown as a dot. Interval estimates are acquired by partitioning all flights into 50 flight intervals and pooling the results, improving convergence. The methods of Section 3.3.2 can be used to estimate the MC error in SFPOF estimates for the flights of interest.

Note that in the flight-by-flight point estimates of SFPOF, bands appear to form that extend from left to right. With 1 billion samples the lowest such band occurs near  $1 \times 10^{-9}$ , indicating those flights which had a single failure in the run. The next band appears at  $2 \times 10^{-9}$  for flights where two failures occurred, and so on.

As discussed in Section 3.3.3, an IS run using the MC routine can provide quality estimates at low levels of SFPOF, though this approach cannot include scheduled inspections. Running the importance sampling version of the MC routine does not require alteration of the code; rather the sampling distribution for EIFS is altered and the results are post-processed accordingly to maintain unbiasedness in the SFPOF estimates. For these examples, the sampling distribution selected is Exponential(rate= 6) since this includes far more large initial cracks and has the same support as the Weibull EIFS distribution. Flight-by-flight and interval estimates of SFPOF from the IS MC routine are in Figure 3.10. Note that SFPOF estimates below  $1 \times 10^{-16}$  have been set to  $1 \times 10^{-16}$ .

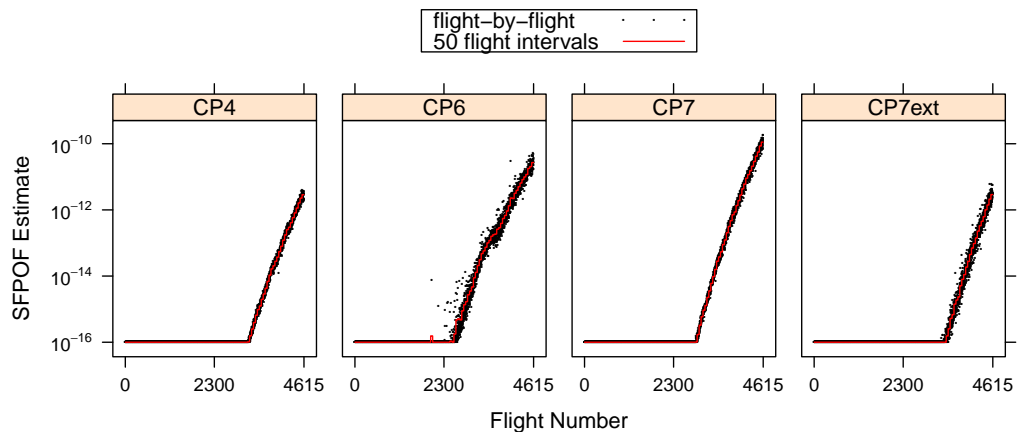


Figure 3.10: Importance Sampling (IS) Monte Carlo (MC) Single Flight Probability Of Failure (SFPOF) flight-by-flight and interval estimates for Examples CP4, CP6, CP7 and CP7ext. For the interval estimates all flights are partitioned into 50 flight intervals. Each example is run until the first scheduled inspection. SFPOF estimates have converged well at small failure probabilities, in contrast to the MC results of Figure 3.9. The methods of Section 3.3.3 can be used to characterize the MC error in these estimates.

The error in the SFPOF estimates of the explicit MC routine can be estimated by calculating 95% confidence interval bounds at selected flights, ob-

tained using the Wilson score interval for obtaining binomial confidence bounds (see Section 3.3.2). The MC error of the IS MC can be estimated using Efron's bootstrap. These confidence intervals are shown below in Table 3.4 for several selected flights, including one flight during the first inspection interval and the flights just prior to the three scheduled inspections. Note the confidence bounds prior to the first inspection (flights 3846 and 4615) are obtained using the importance sampling to set the initial crack length, and the bounds prior to the second and third inspections (flights 6923 and 9230) are obtained using standard Monte Carlo sampling. Also note these results correspond to the flight-by-flight SFPOF estimates as opposed to the interval estimates.

Table 3.4: Monte Carlo (MC) point estimates and 95% confidence bounds for Single Flight Probability Of Failure (SFPOF) for Examples CP4, CP6, CP7 and CP7ext. The estimates prior to the first inspection (flights 3846 and 4615) are obtained using importance sampling to set the initial parameters, and the estimates prior to the second and third inspections (flights 6923 and 9230) are obtained using standard MC sampling. These bounds can be used to judge the quality of SFPOF estimates from the other approaches.

(a) Example CP4				(b) Example CP6			
Flight	PointEst	Lower	Upper	Flight	PointEst	Lower	Upper
3846	$2.52 \times 10^{-14}$	$1.32 \times 10^{-14}$	$5.01 \times 10^{-14}$	3846	$4.64 \times 10^{-13}$	$2.03 \times 10^{-13}$	$8.56 \times 10^{-13}$
4615	$2.20 \times 10^{-12}$	$9.59 \times 10^{-13}$	$4.78 \times 10^{-12}$	4615	$2.76 \times 10^{-11}$	$1.12 \times 10^{-11}$	$4.92 \times 10^{-11}$
6923	$2.00 \times 10^{-09}$	$1.03 \times 10^{-10}$	$1.13 \times 10^{-08}$	6923	$4.00 \times 10^{-09}$	$1.10 \times 10^{-09}$	$1.46 \times 10^{-08}$
9230	$1.36 \times 10^{-07}$	$1.07 \times 10^{-07}$	$1.72 \times 10^{-07}$	9230	$6.20 \times 10^{-08}$	$4.37 \times 10^{-08}$	$8.80 \times 10^{-08}$

(c) Example CP7				(d) Example CP7ext			
Flight	PointEst	Lower	Upper	Flight	PointEst	Lower	Upper
3846	$8.27 \times 10^{-13}$	$5.40 \times 10^{-13}$	$1.20 \times 10^{-12}$	3846	$9.48 \times 10^{-15}$	$4.69 \times 10^{-15}$	$1.58 \times 10^{-14}$
4615	$7.40 \times 10^{-11}$	$3.26 \times 10^{-11}$	$1.27 \times 10^{-10}$	4615	$2.95 \times 10^{-12}$	$1.36 \times 10^{-12}$	$5.04 \times 10^{-12}$
6923	$6.50 \times 10^{-08}$	$5.10 \times 10^{-08}$	$8.28 \times 10^{-08}$	6923	$8.00 \times 10^{-09}$	$4.05 \times 10^{-09}$	$1.58 \times 10^{-08}$
9230	$1.46 \times 10^{-06}$	$1.38 \times 10^{-06}$	$1.53 \times 10^{-06}$	9230	$2.19 \times 10^{-07}$	$1.92 \times 10^{-07}$	$2.50 \times 10^{-07}$

PCD estimates from the MC routine for each example are shown in Table 3.5d. These include the lower and upper bounds of 95% confidence confidence intervals obtained using the Wilson score interval.

Table 3.5: Monte Carlo (MC) point estimates and 95% confidence bounds for Probability of Crack Detection (PCD) for Examples CP4, CP6, CP7 and CP7ext. The confidence bounds are obtained using the Wilson score interval. Convergence of PCD estimates using a large number of MC trials is very strong (500m trials were used for CP4 and CP6, and 1b for CP7 and CP7ext). These estimates can be used to judge the quality of PCD estimates from the other approaches.

(a) Example CP4				(b) Example CP6			
Insp	PointEst	Lower	Upper	Insp	PointEst	Lower	Upper
1	0.02259	0.02258	0.02260	1	0.03307	0.03305	0.03309
2	0.17409	0.17406	0.17413	2	0.11481	0.11478	0.11484
3	0.59167	0.59162	0.59171	3	0.30080	0.30076	0.30084

(c) Example CP7				(d) Example CP7ext			
Insp	PointEst	Lower	Upper	Insp	PointEst	Lower	Upper
1	0.07002	0.07001	0.07004	1	0.07001	0.07000	0.07003
2	0.24125	0.24122	0.24127	2	0.24124	0.24122	0.24127
3	0.52586	0.52583	0.52589	3	0.52603	0.52600	0.52606

The MC routine can also provide insight as to whether each trial failed due to the  $a > a_c$  or  $K > K_c$  failure mode. CP4 and CP7 fail nearly 100% of the time because of the  $a > a_c$  mode. CP7ext fails exclusively because of  $K > K_c$ . CP6 is split roughly equally between the two modes.

# CHAPTER 4

## HIDDEN MARKOV MODEL / SEQUENTIAL IMPORTANCE SAMPLING APPROACH TO PROBABILISTIC DAMAGE TOLERANCE ANALYSIS

In Chapter 3 the typical PDTA (Probabilistic Damage Tolerance Analysis) problem was presented along with the descriptions of a popular software package and an explicit MC (Monte Carlo) approach. The MC routine is excellent for providing a straightforward solution to the PDTA problem, with the drawback that it is a relatively inefficient routine. In this chapter a novel approach to PDTA is described which utilizes SIS (Sequential Importance Sampling) to solve a HMM (Hidden Markov Model) representation of the problem. This approach provides results comparable to those of the explicit MC with much shorter runtime. In Chapter 5, the various approaches to PDTA will be compared and discussed, and in later chapters the flexibility of the HMM/SIS approach is demonstrated through several extensions to the typical PDTA problem.

HMM is described in Section 4.1. IS (Importance Sampling) and SIS are described in Sections 4.2 and 4.3, respectively. Section 4.3.1 gives an overview of the PDTA model using SIS. A simplified example is presented in Section 4.4 using only three particles to represent the model state. The SIS approach is shown graphically in Section 4.5 through a series of plots of the model state. The simulation naturally proceeds on a flight-by-flight basis, though it is possible to proceed instead in intervals of several flights. Using the interval approach instead of the flight-by-flight approach increases the speed of the routine but reduces the fidelity of the results. The interval version of the SIS model is presented in Section 4.6. Convergence of the SFPOF and PCD estimates in the SIS model is discussed in Section 4.7. The analyses of several example problems are presented in detail in Section 4.8.

## 4.1 Hidden Markov Model (HMM)

Consider a Markovian, nonlinear, non-Gaussian state-space model as described in Doucet et al. [13]. The unobserved, or hidden, states are modeled as a discrete-time Markov process  $\{\mathbf{X}_t\}_{t \geq 0}$  such that

$$\mathbf{X}_0 \sim \mu(\mathbf{x}_0) \text{ and } \mathbf{X}_t | (\mathbf{X}_{t-1} = \mathbf{x}_{t-1}) \sim f(\mathbf{x}_t | \mathbf{x}_{t-1}) \quad (4.1)$$

where  $t$  is the discrete-time index,  $\mu(\cdot)$  is a probability density function and  $f(\mathbf{x}' | \mathbf{x})$  is the probability density associated with moving from  $\mathbf{x}$  to  $\mathbf{x}'$ . The goal is to estimate the model state  $\{\mathbf{X}_t\}_{t \geq 0}$ , which cannot be directly observed.  $\{\mathbf{Y}_t\}_{t \geq 1}$  can be observed. It is assumed that given  $\{\mathbf{X}_t\}_{t \geq 0}$  the observations  $\{\mathbf{Y}_t\}_{t \geq 1}$  are statistically independent with marginal densities

$$\mathbf{Y}_t | (\mathbf{X}_t = \mathbf{x}_t) \sim h(\mathbf{y}_t | \mathbf{x}_t). \quad (4.2)$$

Equations (4.1) and (4.2) define a Bayesian model where at each time point (4.1) represents the prior distribution and (4.2) represents the likelihood of the observed evidence. The joint posterior distribution at any time point  $t$  is given

by Bayes' rule:

$$p(\mathbf{x}_t | \mathbf{y}_{1:t}) = \frac{p(\mathbf{x}_t)p(\mathbf{y}_{1:t}|\mathbf{x}_t)}{p(\mathbf{y}_{1:t})}. \quad (4.3)$$

For a general introduction to Bayesian analysis, see Gelman et al. [17]. Note that in (4.3) in the literature each  $\mathbf{x}_t$  is sometimes written  $\mathbf{x}_{0:t}$ . The former is used here to clarify that this is a first-order Markov process and that the state prior to time index  $t$  is no longer relevant.

A hidden Markov model (HMM) is described by (4.1) and (4.2). The aim is to estimate recursively in time the joint posterior distribution of the model state given the observed evidence. For the majority of non-linear, non-Gaussian models the distributions in (4.3) cannot be computed in closed-form. Numerical methods are thus required.

## 4.2 Importance Sampling (IS)

In this section a brief overview of IS is presented. Interested readers should consult Robert and Casella [44] for a thorough discussion of IS.

In traditional MC sampling, the expectation of a random variable is calculated by generating a number of samples from the variable of interest. Let  $x_1, x_2, \dots, x_n$  be  $n$  independent and identically distributed (iid) draws from a distribution with density  $f(x)$ . Note that  $X$  can be vector-valued, but is presented here as univariate for the sake of simplicity. The expectation of  $X$  is approximated by

$$\mathbb{E}(X) \approx \frac{1}{n} \sum_{i=1}^n x_i.$$

In many cases a simulation can be made more efficient if there is increased sampling in some particular region. This is accomplished by utilizing a *sampling distribution*  $g(x)$  instead of the actual distribution  $f(x)$ , where the sampling distribution is selected such that the supports are the same ( $f(x)$  and  $g(x)$  are capable of generating the same values) and that the density of  $g(x)$  is heavier than that of  $f(x)$  in the region of interest. If  $\hat{x}_1, \hat{x}_2, \dots, \hat{x}_n$  is an iid

sample of size  $n$  from a distribution with density  $g(x)$ . The *weighting function* is defined as

$$w(x) = \frac{f(x)}{g(x)}.$$

In this case, the (unbiased) expectation of  $X$  is approximated by

$$\mathbb{E}(X) \approx \frac{1}{n} \sum_{i=1}^n \frac{f(\hat{x}_i)}{g(\hat{x}_i)} \hat{x}_i.$$

### 4.3 Sequential Importance Sampling (SIS)

SIS is a sequential MC algorithm based on importance sampling. See Doucet et al. [12] or Arulampalam et al. [4] for a tutorial on sequential MC methods. The SIS method involves a *particle*-based representation of the model state. The posterior density at time  $t$ ,  $p(x_t|y_{1:t})$ , is approximated by a finite set of  $n$  weighted particles. The weights are normalized so that  $\sum_i^n w_t^{(i)} = 1$ , where  $w_t^{(i)}$  is the weight of particle  $i$  at time  $t$ . The approximation can be written

$$p(\mathbf{x}_t|\mathbf{y}_{1:t}) \approx \sum_{i=1}^n w_t^{(i)} \delta_{\mathbf{x}_t^{(i)}}(\mathbf{x}_t) \quad (4.4)$$

where  $\delta_{\mathbf{a}}(\mathbf{x})$  is the Dirac delta function concentrated at  $\mathbf{a}$  [43].

Each particle is in effect a *possible* value(s) for the model state. The normalized importance weight can be thought of as the relative likelihood that this particle represents the underlying truth. The collection of particles can be used to estimate any property of  $p(\mathbf{x}_t|\mathbf{y}_{1:t})$ . If the aim is to estimate  $\mathbb{E}(f_t(\mathbf{x}_t))$ , the expectation of some arbitrary function  $f$  of the model state at time  $t$ , a Monte Carlo estimate is

$$\mathbb{E}(f_t(\mathbf{x}_t)) \approx \sum_{i=1}^n f_t(\mathbf{x}_t^{(i)}) w_t^{(i)}. \quad (4.5)$$

For the properties of this estimator, see Doucet et al.

To use (4.5) for recursive estimation, a method is required for updating the importance weights when time advances and a new observation  $\mathbf{y}_{t+1}$  arrives.

If the prior distribution for  $\mathbf{X}$  is adopted as the importance distribution (a standard case), the importance weights satisfy [12]

$$w_t^{(i)} \propto w_{t-1}^{(i)} p(\mathbf{y}_t^{(i)} | \mathbf{x}_t^{(i)}). \quad (4.6)$$

The particle weights are updated using (4.6), then after re-normalization represent the posterior.

The fatigue process considered in this work can be described by (4.1) and (4.2). The state after flight  $t$  is  $\mathbf{X}_t$ , consisting of crack lengths, a static parameter (fracture toughness, see Section 3.1), and the normalized importance weights. Crack growth in the standard PDTA analysis is deterministic and monotonically increasing. Because the transition distribution from flight-to-flight is deterministic, (4.6) holds. The  $\mathbf{y}_t$  observed is *survival* of flight  $t$ .

Note that this is prognostic; one does not actually wait until flights successfully occur in reality to move onto the next flight in the simulation. The sequential *observation* of survival of each flight can be thought of as an *assertion* made because our target estimand is a failure probability conditioned on the survival of all previous time steps. The *observation* terminology is that of HMM/SIS.

Because the model has been (recursively) conditioned on survival of flights 0 through  $t - 1$ , the calculated probability of failure of flight  $t$  is *SFPOF by definition*. Thus estimation of the probability of failure using (4.5) provides both the SFPOF estimate for the next flight as well as the likelihood of survival of the next flight (the complement of SFPOF) to be used to update the model according to (4.6). Details of the probability of failure calculation are given in Section 4.3.1.

Suppose an inspection will occur in the future after flight  $t$  and that as a result a repair may immediately occur. This possible future repair can be modeled in a fashion similar to Equation (4.2) as

$$\mathbf{X}_{t'} | (\mathbf{X}_t = \mathbf{x}_t) \sim f(\mathbf{x}_{t'} | \mathbf{x}_t), \quad (4.7)$$

where the model state after flight  $t$  is  $\mathbf{X}_t$  and the state after inspection and

before flight  $t + 1$  is  $\mathbf{X}_t$ .

In SIS the initial state may be obtained either by directly sampling from the relevant probability distributions, or through IS. There are three distributions from which one must be able to sample in order to utilize SIS. First, one must be able to generate the initial state with  $\mu(\mathbf{x}_0)$ , which usually presents few problems since a convenient  $\mu(\mathbf{x}_0)$  can be selected. Next, the transition distribution,  $f(\mathbf{x}_t|\mathbf{x}_{t-1})$ , is needed which defines how the state evolves from one discrete time point to the next. The transition distribution is often stochastic in SIS, but it may be deterministic. Finally, one must be able to calculate the observation likelihood with  $h(\mathbf{y}_t|\mathbf{x}_t)$ , the distribution of the observable variable(s) at time  $t$  given the state at time  $t$ .

### 4.3.1 Probability of Failure or Detection for a Single Particle

Recall, for a given flight the variables of interest are the crack length,  $a$ , fracture toughness,  $K_c$ , maximum applied stress per flight,  $\sigma_{\max}$ , and the normalized stress intensity,  $K/\sigma$ , which is a deterministic function of crack length. Note it is assumed that the extent of crack growth during a single flight is negligible (i.e., the crack size at the beginning of each flight is utilized to calculate the probability of failure given the crack is that length). For a flight in which  $a$  and  $K_c$  are known (as is the case in the calculation for a given particle), and  $\sigma_{\max}$  follows the Gumbel distribution, the probability of failure of that flight is easily obtained as shown below.

As in the explicit MC routine there are two failure modes:  $K > K_c$  and  $a > a_c$ . For a particle, if  $a_c$  will be breached during the flight of interest (this is known with certainty when utilizing deterministic crack growth), the probability of failure of this particle for that flight is 100%. Otherwise failure occurs with probability  $\Pr(K_{\max} > K_c|a, K_c)$ . To calculate this the distribution of  $K_{\max}$  is needed. With crack size  $a$  known,  $K/\sigma$  (constant) is found using the geometry table. The distribution of  $\sigma_{\max}$  can be found via variable

transformation since  $K_{\max} = \sigma_{\max} \times K/\sigma$ . For example, suppose the max stress per flight distribution is specified as Gumbel( $\mu, \beta$ ), with  $\mu$  and  $\beta$  fixed parameters. The distribution of  $K_{\max}$  is obtained as follows. For simplicity of notation,  $X = \sigma_{\max}$ ,  $Y = K_{\max}$ , and  $p = K/\sigma$ .

$$\begin{aligned}
X &\sim \text{Gumbel}(\mu, \beta) \\
f_X(x) &= \frac{1}{\beta} \exp\left(-\frac{x-\mu}{\beta} - e\left(-\frac{x-\mu}{\beta}\right)\right) \\
g(x) &= px \\
g^{-1}(y) &= \frac{y}{p} \\
\frac{d}{dy}g^{-1}(y) &= \frac{1}{p} \\
f_X(y) &= \frac{d}{dy}g^{-1}(y) \cdot f_X(g^{-1}(y)) \\
f_Y(y) &= \frac{1}{p} \cdot \frac{1}{\beta} \exp\left(-\frac{y/p-\mu}{\beta} - e\left(-\frac{y/p-\mu}{\beta}\right)\right) \\
&= \frac{1}{p\beta} \exp\left(-\frac{y-p\mu}{p\beta} - e\left(-\frac{y-p\mu}{p\beta}\right)\right) \\
Y &\sim \text{Gumbel}(p\mu, p\beta) \\
K_{\max} &\sim \text{Gumbel}\left(\frac{K}{\sigma}\mu, \frac{K}{\sigma}\beta\right)
\end{aligned}$$

With max stress per flight given as Gumbel( $\mu, \beta$ ), the distribution of  $K_{\max}$  is conveniently specified as a Gumbel distribution with known parameters. Note, because the Gumbel distribution is overwhelmingly utilized in the literature to represent max stress per flight, the current version of the software for performing PDTA using SIS (described in Chapter 10) utilizes the Gumbel distribution for  $\sigma_{\max}$ . If another common distribution is desired, a variable transformation such as that shown above should be performed to obtain a convenient representation of the distribution of  $K_{\max}$ . To determine  $\Pr(K_{\max} > K_c)$ , one need only plug in the constant values of  $\mu$ ,  $\beta$ , and  $K/\sigma$  to determine the CDF of  $K_{\max}$ , and subsequently evaluate the reliability function (1-CDF) of  $K_{\max}$  at the constant value of  $K_c$ . This is done individually for each particle as if the values of  $a$  and  $K_c$  for that particle are the truth. In the remainder of this chapter, the estimate of the failure probability for a single particle is referred to as POF (Probability Of Failure).

The POD (Probability Of Detection) curve gives the probability of finding

a crack given its size, so PCD for particle  $i$  is simply  $\text{POD}(a^{(i)})$ .

As mentioned above, once POF and  $\text{POD}(a)$  have been calculated for each particle, the MC estimate is obtained using Equation 4.5. This will be made clear through a simple example utilizing three particles in Section 4.4. Before doing so several additional items are considered: calculating the initial state, updating the weights to reflect survival, and updating the state as a consequence of reaching a future scheduled inspection.

### 4.3.2 Calculating the Initial State

It is possible to use the actual joint distribution  $f_{A,K_c}(a, k_c)$  to set the initial state. For most PDTA problems this is inefficient because SFPOF estimates are dominated by the right tail of EIFS and because of this a great many particles will be required to obtain a quality estimate of SFPOF. This inefficiency is similar to that of the explicit MC routine. Importance sampling is thus used to determine the initial state and increase the speed of convergence, particularly for flights early in the service life and those soon after inspections. To do so, a joint sampling distribution  $g_{A,K_c}(a, k_c)$  is required from which to generate the initial values of  $a$  and  $K_c$ , as well as  $f_{A,K_c}(a, k_c)$  which is used to determine the initial weights.  $f_{A,K_c}(a, k_c)$  is easy to obtain because  $a$  and  $K_c$  are independent since  $f_{A,K_c}(a, k_c) = f_A(a)f_{K_c}(k_c)$ .  $K_c$  is typically normally distributed and  $a$  is often Weibull distributed<sup>1</sup>. For  $K_c$ , sampling directly from the actual distribution is acceptable. For  $a$  it is beneficial for convergence speed to skew the sampling towards larger crack sizes. The sampling distribution is therefore  $g_{A,K_c}(a, k_c) = g_A(a)f_{K_c}(k_c)$ .

For example, the actual distribution and a possible sampling distribution for crack length  $a$  for Example CP7 from the PROF documentation (see Section 3.2.2 for details) are shown below with the  $x$ -axis on the log scale for plotting convenience. The actual distribution is Weibull with scale 0.000219

---

<sup>1</sup>Occasionally EIFS is log-normal or exponential; it is usually (though not necessarily) a distribution with positive support that favors smaller values. See Section 3.1.3.

and shape 0.575. The sampling distribution is also Weibull with shape 0.575, though the scale has been increased 100-fold to 0.0219. The increased scale parameter yields a distribution with the same support but which yields larger crack lengths more frequently.

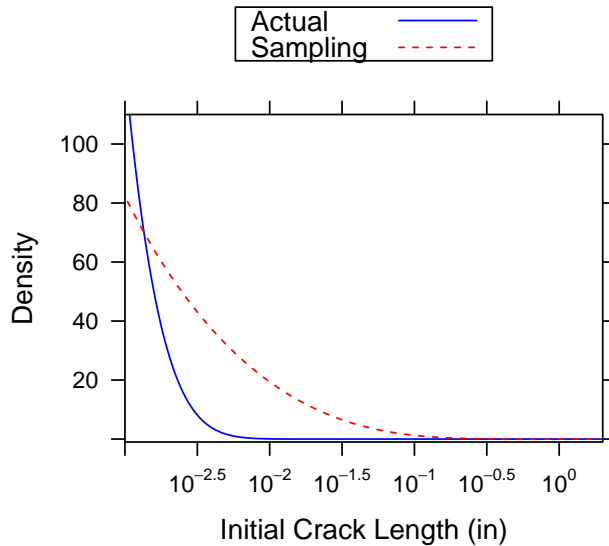


Figure 4.1: Example actual and sampling Equivalent Initial Flaw Size (EIFS) distributions for Example CP7. The actual distribution is Weibull with scale 0.000219 and shape 0.575. The sampling distribution is also Weibull with shape 0.575, though the scale has been increased 100-fold to 0.0219. The increased scale parameter yields a distribution with the same support but which yields larger crack lengths more frequently. Larger initial crack sizes in the Sequential Importance Sampling (SIS) routine lead to more likely failure for these particles, contributing to improved convergence speed.

The sampling distributions for the examples in this work were selected through trial-and-error. It may be that convergence can be improved by using a more rigorous approach to tailoring the joint sampling distribution to each particular PDTA problem, or possibly by using an adaptive sampling procedure.

### 4.3.3 Updating the Weights to Reflect Survival

For the first flight in the service life, POF is calculated for each particle. Before moving onto flight  $t = 2$ , it is observed that a failure did not occur during flight  $t = 1$ . Equation 4.6 is used for this purpose.

The likelihood is simply  $1 - \text{POF}$  for each particle when the evidence is that  $y = \text{TRUE}$  (survival). By taking the element-wise product on the right hand side of the equation, the particle weights are adjusted to represent the relative likelihoods after observing survival. Finally, normalization is required so that  $\sum_{i=1}^n w^{(i)} = 1$ .

### 4.3.4 Scheduled Inspections

At inspection time, PCD must be estimated. For an individual particle of length  $a_t$  just prior to inspection, the probability of detection is  $\text{POD}(a_t)$ . Like SFPOF, PCD is simply a weighted average over the particles, or

$$\text{PCD} = \sum_{i=1}^n \text{POD} \left( a_t^{(i)} \right) w_t^{(i)}, \quad (4.8)$$

where  $a_t^{(i)}$  and  $w_t^{(i)}$  are the crack length and weight of particle  $i$  just prior to the inspection (after flight  $t$ ).

It is assumed that when a crack is found it will be immediately repaired<sup>2</sup>. In PDTA, the outcome of this future inspection can be predicted using Equation 4.8. The model state after this inspection must reflect that a repair may or may not have occurred. That is, the outcome of the future inspection is a hidden random variable as described by Equation 4.7.

The transition from before the inspection at time index  $t$  to after the inspection at time index  $t'$  must now occur. Assume for simplicity that if there is a single type of repair which is performed when the crack is found. The sampling distribution for the transition distribution at an inspection has not yet been specified. If effect, it must be decided which particles should be

---

<sup>2</sup>In some aircraft programs the repair will be delayed for a period of time for convenience; this possibility is not considered in this work.

repaired and which should be missed. There are many possibilities for this. The most obvious is to use the prior distribution as the sampling distribution, where particle  $i$  is repaired with probability  $\text{POD}(a_t^{(i)})$ . With this sampling distribution larger particles are far more likely to get repaired. The result will be that after the repair nearly all of the particles will be very small, and there will be very few particles after inspection for which failure is likely. This will lead to poor estimates of SFPOF until the particles can eventually grow back to the region where failure is more likely. Thus, while perfectly valid, this approach is poor. Note that if this approach is used, the expected value of the total weight of the repaired particles will be PCD, and the total weight of the “missed” particles will be  $1 - \text{PCD}$ .

The approach taken in this work, which maintains ample representation of the entire sample space after inspection, is to select particles for repair at random. The importance weights of the missed and repaired particles are then *separately* normalized to  $1 - \text{PCD}$  and PCD, respectively. In this way, because the total weight of the repaired particles is PCD, the state is forced to reflect that there is a PCD% chance a repair occurred. This can be generalized to any number of different types of repairs or inspection outcomes.

To perform this procedure, a number of particles to repair ( $n_r$ ) and a number of particles to miss ( $n_m$ ) must first be selected. Note this procedure maintains the particle count at  $n$  (which is not necessary). To encourage the particles in each set to have weights on a similar order of magnitude, the proportion of particles assigned to each category can be set roughly equal to the total weight of that set. That is, set  $n_r \approx n \times \text{PCD}$  and  $n_m = n - n_r$ . In this case if a repair is more likely, the repair case will be represented by more particles (and vice versa). This is particularly helpful if repair is either very unlikely or very likely.

Note that particles with zero weight ( $a \geq a_c$ ) should not be selected for inclusion in the  $n_m$  missed particles because they are useless for estimation. If the number of particles with positive weights  $n^+$  is less than  $n_m$ , then  $n_r$  should be increased to  $n - n^+$  to avoid keeping useless particles. The  $n_m$  particles to

be missed are selected without replacement from the  $n^+$  particles with positive weights. Equation 4.6 is used to update the weights of these missed particles according to the likelihood that each particle would be missed at inspection. Finally, the weights of these  $n_m$  particles are then normalized to  $1 - \text{PCD}$ .

In this application the repaired particles can be generated without regard to the state prior to repair because the repaired crack length is independent of the crack length prior to repair (see Section 3.1).  $n_r$  new particles are therefore generated from the appropriate crack length and fracture toughness distributions for the repair, importance weights are initialized in the usual way, and finally the weights of the  $n_r$  repaired particles are normalized to sum to PCD.

A simple example of this procedure for a case containing  $n = 3$  particles is given in Section 4.4. In Section 4.8 it is shown by example that the procedures outlined in this section yield SFPOF and PCD estimates equivalent to those of the explicit MC routine.

In Chapter 6, the typical PDTA problem is extended so that multiple types of repairs are possible.

### 4.3.5 SIS Routine Flow Chart

A flow chart describing the explicit MC routine was shown in Figure 3.8. A similar chart describing the SIS routine is given in Figure 4.2. In the MC routine, each trial is an independent realization of what occurs at a structural location over the service life for a simulated aircraft. Each trial of the MC routine yields a single value of the first flight to failure. In contrast, the SIS routine simultaneously simulates many possible realizations while repeatedly updating the importance weights for each particle.

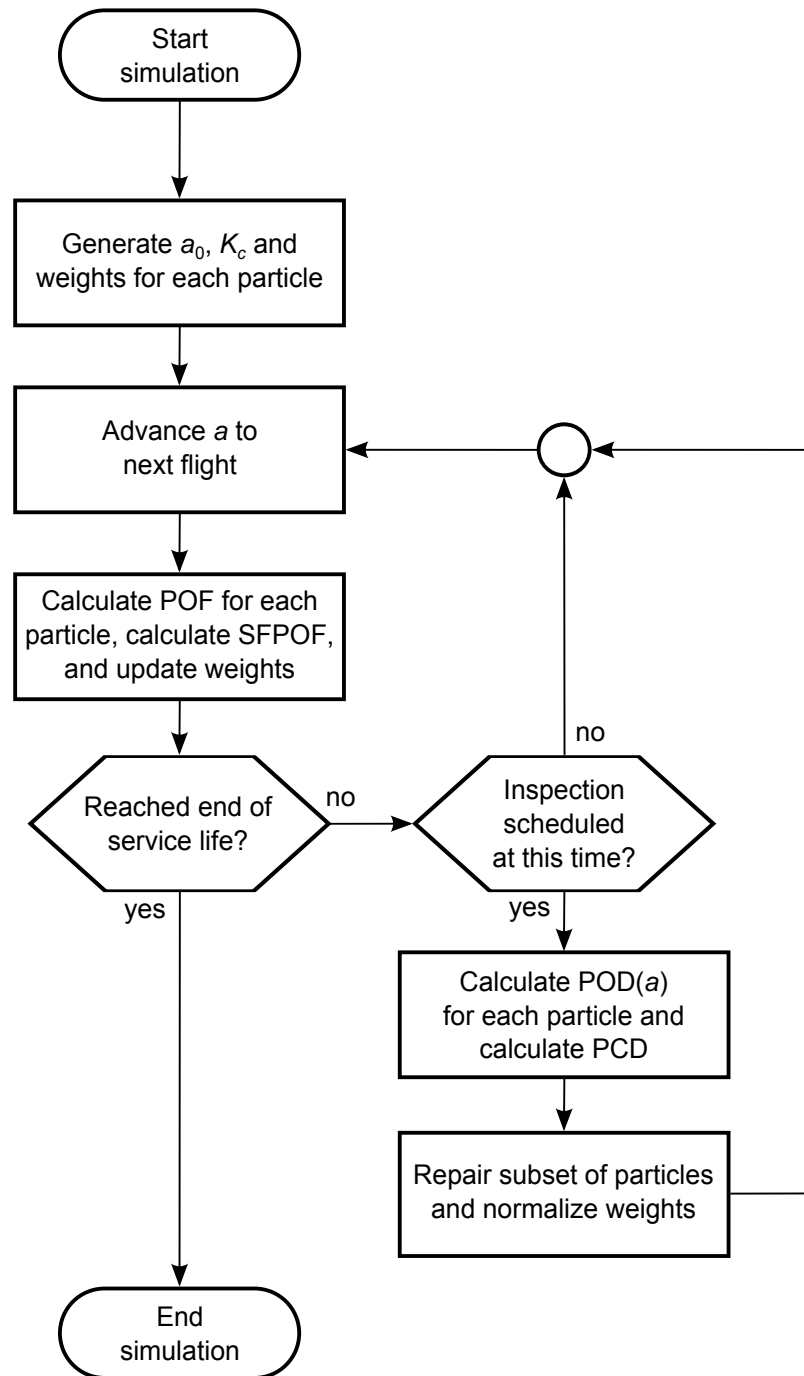


Figure 4.2: Flow chart of the Sequential Importance Sampling (SIS) routine using many simultaneous simulations.

Table 4.1: Sequential Importance Sampling (SIS) example using three particles: initial state. Because the EIFS distribution typically has an exponential shape, the particles with smaller initial crack sizes have higher weights since these are more likely to represent the hidden crack size.

Particle	$a_0(\text{in})$	$K_c(\text{ksi}\sqrt{\text{in}})$	$w$
1	0.005	42	0.80
2	0.022	35	0.19
3	0.560	40	0.01

## 4.4 Three Particle Example Problem

The above concepts are further illustrated via a simple numerical example with  $n = 3$  particles. These numbers are artificial and selected to demonstrate the key concepts. Suppose that the critical crack size  $a_c$  will be reached during the 2<sup>nd</sup> flight by the 3<sup>rd</sup> particle. Importance sampling is used to set the initial state and the initial weights  $w$  are obtained in the usual way for importance sampling. Table 4.1 displays the initial state. Note that  $a_1 < a_2 < a_3$ , and as such  $w_1 > w_2 > w_3$ . This is due to the shape of the EIFS distribution in which smaller initial cracks are more likely to occur.

The  $K/\sigma$  table is used to obtain the constant value of  $K/\sigma$  for each particle, and this is used along with  $K_c$  and the distribution of  $\sigma_{\max}$  to find POF for each particle. SFPOF for the first flight is found by taking a weighted average of the estimates of POF:  $\text{SFPOF}_1 = 0.80(0) + 0.19(0.01) + 0.01(0.30) = 4.9 \times 10^{-3}$ . After SFPOF is calculated, the survival update is performed to reflect that a failure did not occur in flight 1 for any of the particles. The updated weights are found with  $w \times (1 - \text{POF})$ . Finally, the particle weights are normalized so  $\sum_{i=1}^n w^{(i)} = 1$ . See Table 4.2.

The routine now considers the second flight, the data for which is shown in Table 4.3. The cracks each grew for one flight and as a result the associated  $K/\sigma$  values increase and the calculated POF for each particle is also increased. Recall it was specified that particle #3 will grow to exceed  $a_c$  during this flight,

Table 4.2: Sequential Importance Sampling (SIS) example using three particles: first flight. The Probability Of Failure (POF) for each particle is first calculated to be used to calculate Single Flight Probability Of Failure (SFPOF) for this flight. Next, the survival probability ( $1-\text{POF}$ ) is used to update the importance weights (subsequently normalized) to reflect that failure did not occur; this is done because SFPOF is concerned with the probability that a flight will experience the *first* failure of this component.

Particle	$w$	$a(\text{in})$	POF	$1-\text{POF}$	$w(\text{update})$	$w(\text{norm})$
1	0.80	0.005	0.0%	100.0%	0.8000	0.80394
2	0.19	0.022	1.0%	99.0%	0.1881	0.18903
3	0.01	0.560	30.0%	70.0%	0.0070	0.00703

Table 4.3: Sequential Importance Sampling (SIS) example using three particles: second flight. Particle #3 has reached the critical crack length  $a_c$ , thus Probability Of Failure (POF) for that particle is 100%. Because the survival probability of this particle is zero, its importance weight is reduced to zero following this flight.

Particle	$w$	$a(\text{in})$	POF	$1-\text{POF}$	$w(\text{update})$	$w(\text{norm})$
1	0.80394	0.006	0%	100%	0.80394	0.81273
2	0.18903	0.024	2%	98%	0.18525	0.18727
3	0.00703	$a_c$	100%	0%	0.00000	0.00000

which results in  $\text{POF} = 100\%$  for that particle.  $\text{SFPOF}_2 = 0.80394(0) + 0.18903(0.02) + 0.00703(1) = 1.08 \times 10^{-2}$ . The weights are then updated to reflect survival of this flight as before. Note that the weight for particle #3 is reduced to zero reflecting the fact that since failure did not occur during flight 2, and deterministic crack growth is assumed, it is not possible that particle #3 represents the truth.

For this simple example, the critical crack failure mode has some influence because there is some weight on particle #3 when  $a_c$  is breached. In a well-specified problem, when the  $K_{\max} > K_c$  failure mode is dominant, POF should be high before  $a_c$  is breached in which case the repeated Bayesian updating of

Table 4.4: Sequential Importance Sampling (SIS) example using three particles: inspection result. The Probability Of Detection (POD) curve is utilized to find the probability that each particle would be found at inspection. The importance weights for a *missed* and *found* version of this particle are set according to  $\text{POD}(a)$ . Note there are now six particles. To prevent an exponentially increasing particle count, downsampling can be used to reduce the particle count back to three.

Particle	$a(\text{in})$	$w$	$\text{POD}(a)$	$w(\text{miss})$	$w(\text{find})$
1	0.008	0.81273	0.2%	0.81110	0.00163
2	0.027	0.18727	52.3%	0.08933	0.09794
3	$a_c$	0.00000	100.0%	0.00000	0.00000

the particle weights will reduce  $w$  to near zero before reaching  $a_c$ . This is the ideal situation since the critical crack length is usually not physically meaningful. The  $a > a_c$  failure mode is also less than ideal regarding convergence (more on this in Section 4.7). Consider the extreme case where the  $K_{\max} > K_c$  failure mode has no influence and failure only occurs because of  $a_c$ . In this case POF will be zero for every flight prior to reaching  $a_c$ . In other words, a particle will only contribute to the SFPOF estimate on the flight where  $a_c$  is breached. Thus to have quality SFPOF estimates at every flight in the service life, one would need enough particles that several will reach  $a_c$  at every flight. Contrast this with a  $K_{\max} > K_c$  dominated problem, where any relatively large crack particle contributes to the SFPOF estimate and estimates will as a result converge more quickly.

This example concludes with an inspection. Table 4.4 gives the crack sizes after the third flight, the weights after updating for survival,  $\text{POD}(a)$  for these particles, and the weights of each particle if that particle were missed or found at inspection.

PCD for this inspection is, like SFPOF, a weighted average (using the weights prior to inspection).  $\text{PCD} = 0.81273(0.002) + 0.18727(0.523) + 0 = 0.09957$ . To maintain  $n = 3$  particles, 2 particles are selected at random

Table 4.5: Sequential Importance Sampling (SIS) example using three particles: post-inspection. Particle #3, marked with an asterisk, is a newly generated particle representing the outcome that a repair may have occurred after the inspection. The importance weight of this particle is equal to the Probability of Crack Detection (PCD) calculated for this inspection (note, there would generally be more than one repair particle, so the importance weights would typically sum to PCD). Particles #1 and #2 are sampled from those which were missed at inspection, and the importance weights of these are normalized to a sum of  $1 - \text{PCD}$ .

Particle	$a(\text{in})$	$K_c(\text{ksiin})$	$w$
1	0.008	42	0.81110
2	0.027	35	0.08933
3	*0.006	*37	0.09957

without replacement to represent the non-detection event, and 1 particle will be newly generated to represent a repair. It is not sensible to retain particle #3, since the weight of this particle is zero and it will no longer contribute to the SFPOF or PCD estimates. Suppose particles #1 and #2 are retained, and that the third particle is a repaired particle. This is shown in Table 4.5. The sum of the weights of the repaired particles must be equal to PCD to reflect the fact that there is a 0.09957 probability that the underlying truth at this point is that a repair has been performed. In this case there is only one repaired particle, so the weight of particle #3 is 0.09957. Similarly, the weights of the missed particles must sum to  $1 - \text{PCD}$  so the weights of particles #1 and #2 are normalized to a sum of  $1 - \text{PCD}$ . The values marked with an asterisk are newly drawn from the repair flaw size distribution and the fracture toughness distribution, respectively.

The example just shown demonstrates the method, which in practice would continue throughout the service life of interest and would utilize thousands or millions of particles.

## 4.5 Graphical Depiction of the SIS Approach

The SIS routine begins with generation of the initial state. This can be visualized with a plot. Figure 4.3 shows the initial state for CP7ext using 1000 particles. The plot is truncated on the left to make the plot easier to read. In the figure the dot sizes represent the particle weights, and the location of each particle indicates the values of  $a$  and  $K_c$  for that particle. The larger initial cracks have a lower weight due to the exponential shape of the initial flaw size distribution. The contour lines show the probability of failure for a single particle corresponding to  $\Pr(K_{\max} > K_c)$  as a function of  $a$  and  $K_c$ . The indication at 0.518" is the critical crack length  $a_c$  in the unmodified Example CP7. Note that failure due to  $K_{\max} > K_c$  is still very unlikely at this crack size. Lastly, the rug on the top and right indicates the marginal location of each particle.

As time passes, the particles experience crack growth and move to the right, eventually approaching the critical crack length (for CP7ext this is the limit of the  $x$ -axis in Figure 4.3). In Figure 4.4, the state is shown for 100 particles and these advance in crack length over 500 flights. Note the arrows appear to be all the same length; crack growth for Example CP7ext is an exponential function, so with the  $x$ -axis on the log scale the growth appears to be uniform even though the larger cracks are growing at a much faster rate. Also note that the fracture toughness  $K_c$  has not changed for any particle.

The SIS routine proceeds by growing the cracks and updating the weights at each flight until reaching a scheduled inspection. In addition, SFPOF estimates are calculated at a selected interval of flights. At inspection time, some particles will be detected and repaired ( $a$ ,  $K_c$  and  $w$  are reset accordingly). PCD is estimated at each inspection as the probability that a crack was found. Plots of the states before and after a scheduled inspection at flight 4615 are shown in Figures 4.5a and 4.5b, respectively, using 1000 particles. Note that before inspection, there are a number of particles which have reached the critical crack size  $a_c$  and have weight  $w = 0$ . At inspection, all of these particles are

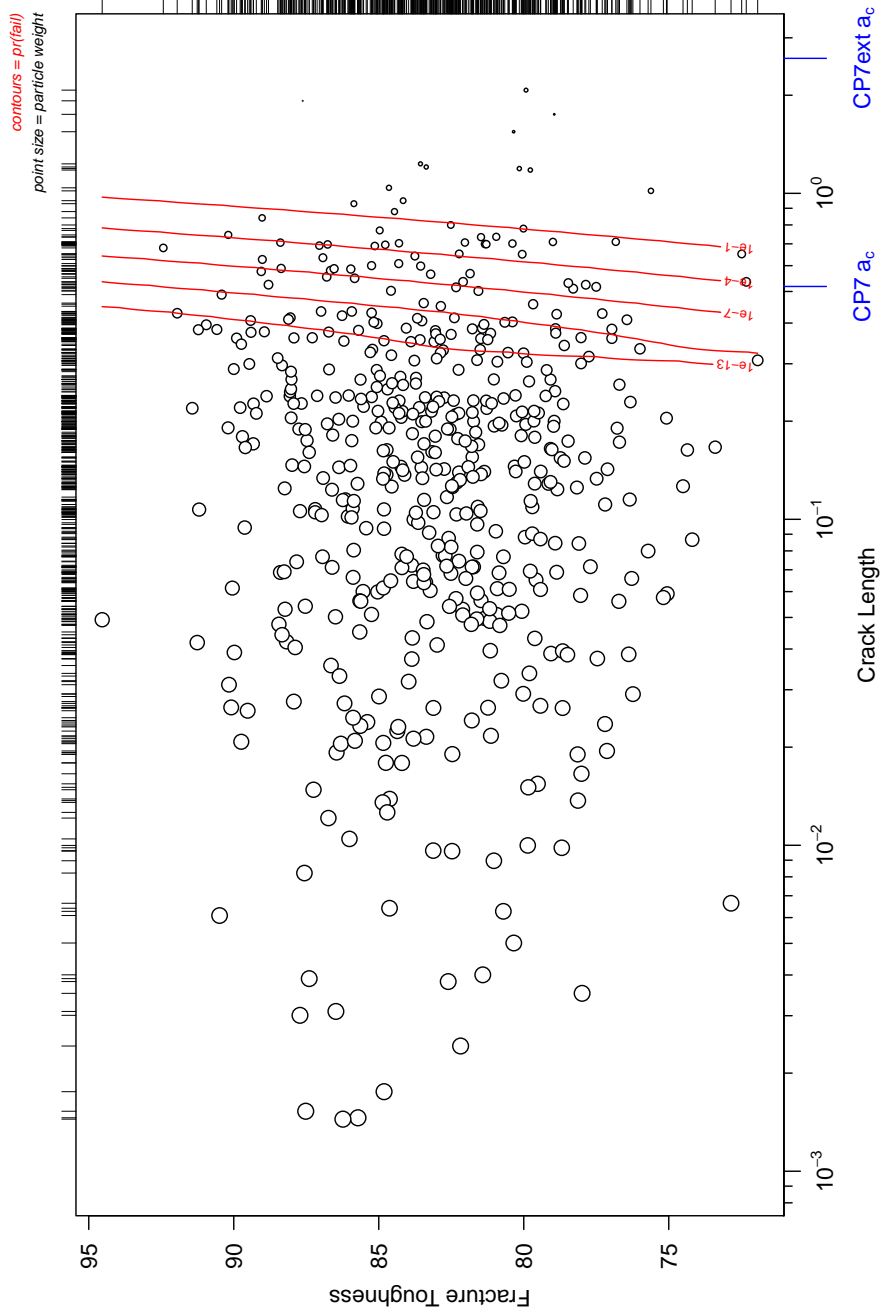


Figure 4.3: Possible Sequential Importance Sampling (SIS) initial state for Example CP7ext with 1000 particles.

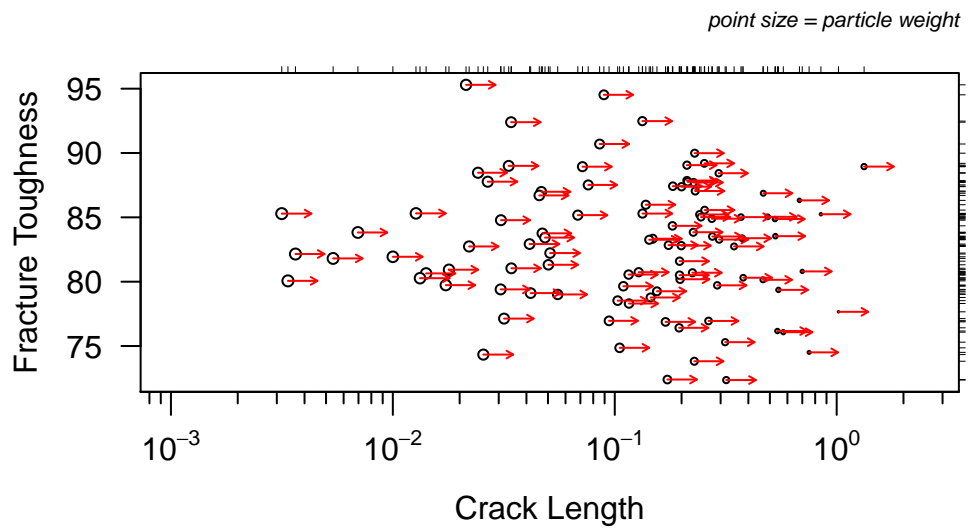


Figure 4.4: Changing state over 500 flights for Example CP7ext using 100 particles in the Sequential Importance Sampling (SIS) approach. Note the arrows appear to be all the same length; crack growth for Example CP7ext is an exponential function, so with the  $x$ -axis on the log scale the growth appears to be uniform even though the larger cracks are growing at a much faster rate. Also note that the fracture toughness  $K_c$  has not changed for any particle.

removed, along with a randomly selected set of particles which were found at inspection. This procedure of crack growth followed by inspection is repeated for all inspection intervals in the specified life.

## 4.6 Interval Version of the SIS PDTA Routine

The SIS routine described in Section 4.3.1 proceeds flight-by-flight, updating the particle weights after each flight. This is ideal since each flight is a discrete event. An approximate approach involves a calculation which proceeds through the service life one *interval* of flights at-a-time instead. In this case, the algorithm would need to calculate the probability of surviving the interval for each particle, and the weight update can be performed at the end of each interval of flights.

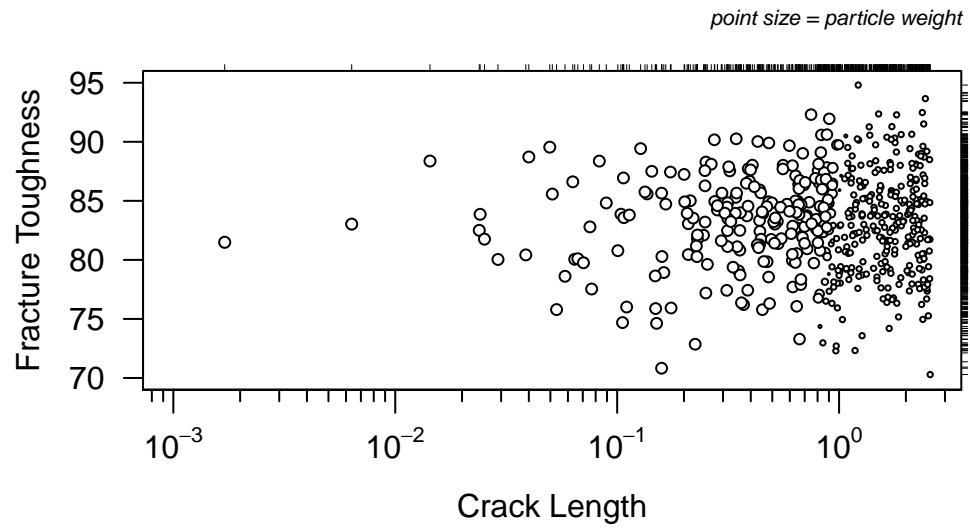
Suppose an interval consisting of  $m$  flights is under consideration and the goal is to calculate the probability of survival for the interval for a single particle. Let  $S_{\text{int}}$  be a Boolean random variable indicating survival of the interval, and for convenience let  $p_{\text{int}} = \Pr(S_{\text{int}} = \text{T})$  (where  $\text{T}=\text{TRUE}$ ). In the flight-by-flight routine the probability of survival of each flight given survival of all previous flights is sequentially obtained. Let  $S_t$  indicate survival of flight  $t$  and  $p_t = \Pr(S_t = \text{T})$ . In the case of the standard algorithm,

$$p_{\text{int}} = \Pr(S_1 = \text{T}) \times \Pr(S_2 = \text{T}|S_1 = \text{T}) \times \dots \times \Pr(S_m = \text{T}|S_1 = \text{T}, \dots, S_{m-1} = \text{T}).$$

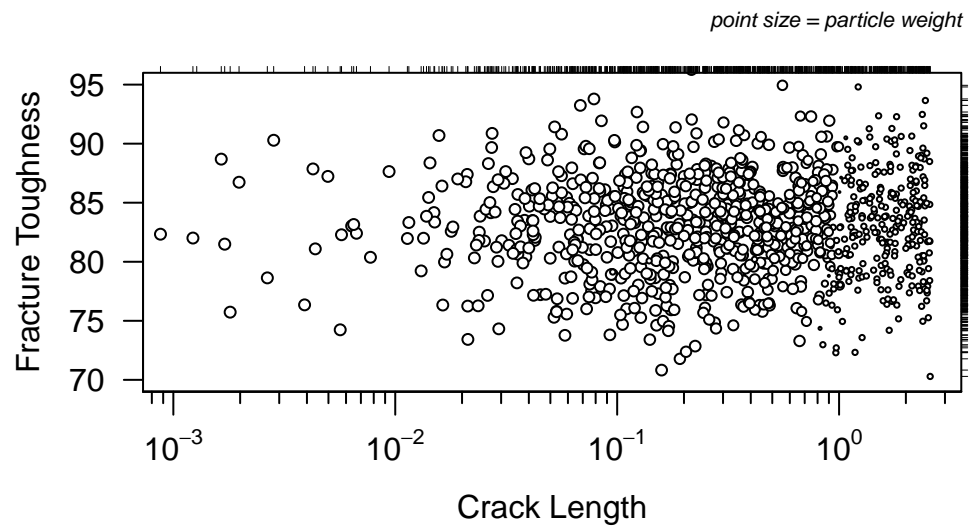
In the interval routine an approximation to the above involves estimating a representative survival probability for each flight in the interval; let this be  $p^*$ . Once  $p^*$  is obtained, the survival probability for the interval,  $p_{\text{int}}$ , is estimated by

$$p_{\text{int}} = (p^*)^m.$$

Recall, there are two ways a particle can fail:  $K > K_c$ , or  $a > a_c$ . The probability of failure due to each is separately estimated for the interval. For an interval of flights in the SIS routine,  $\Pr(K > K_c)$  increases gradually for each flight in the interval.  $\Pr(a > a_c)$ , on the other hand, is zero for all but at



(a) Before Inspection



(b) After Inspection

Figure 4.5: State for Example CP7ext before and after inspection using 1000 particles in the Sequential Importance Sampling (SIS) approach. Note the particles which had reached the critical crack length  $a_c$  are discarded.

most one flight in the interval (since the critical crack size is either breached during a flight, or it is not). With a short interval of flights, it is reasonable to assume that failure due to breach of  $a_c$  is roughly equal among flights in the interval. Thus the probability of failure due to  $a > a_c$  is set to

$$\Pr(a > a_c) = 1/m$$

for any particles which breach  $a_c$  during the interval. That is, the survival probability (according to  $a > a_c$ ) is 100% for particles which do not breach  $a_c$ , or  $(m - 1)/m$  for particles which do breach  $a_c$ .

For  $K > K_c$  failure, the probability of survival  $\Pr(K_{\max} < K_c)$  is estimated using a modification of Simpson's Rule. First, the crack length  $a$  for the particle is found for the first, middle, and last flights of the interval; call these  $a_{\text{frst}}$ ,  $a_{\text{mddl}}$ , and  $a_{\text{last}}$ . The usual approach to calculating  $\Pr(K_{\max} < K_c)$  is used for the three representative flights to obtain  $p_{\text{frst}}$ ,  $p_{\text{mddl}}$ , and  $p_{\text{last}}$ , the probabilities of survival for the first, middle, and last flights, respectively. The quadratic approximation follows. Note this is modified from Simpson's Rule to yield the average value rather than the area under the curve. The survival probability estimate for a typical flight in the interval is

$$\Pr(K_{\max} < K_c) = \frac{1}{6} (p_{\text{frst}} + 4p_{\text{mddl}} + p_{\text{last}}).$$

Finally, the failure probabilities from the two failure modes are combined. By assuming failure will occur because of only one of the modes (preventing the probability of failure estimate from exceeding unity) they are combined with

$$1 - p^* = \Pr(a > a_c) + \Pr(K_{\max} > K_c) - \Pr(a > a_c) \times \Pr(K_{\max} > K_c).$$

Note that in this approach, failure due to  $a > a_c$  for any flight in the interval is used to estimate SFPOF. In the flight-by-flight routine, if a particle fails because of  $a > a_c$  when  $\Pr(K_{\max} > K_c)$  is negligible, that particle contributes to estimation of SFPOF in only one flight. In this case, when a problem is dominated by the  $a > a_c$  failure mode, SFPOF estimates in the flight-by-flight

routine converge slowly, requiring many particles. The interval routine, on the other hand, can converge far more quickly because of the pooling of failures of flights within an interval. This is discussed further in Section 4.7.

## 4.7 Convergence of the SIS Routine

In SIS, as in all MC approaches, the sampling error will reduce as more samples are taken. There is a trade-off between the runtime and the MC error. Also, as described in the previous section, for some problems convergence of SFPOF estimates can be improved using interval estimation rather than flight-by-flight estimation. A general discussion of convergence of the SIS PDTA routine is given in this section. Two general purpose methods to assessing convergence for sequential Monte Carlo are described as well; these are running independent sequences (Section 4.7.1), and bootstrap re-sampling (Section 4.7.2). For a discussion of approaches to monitoring convergence for iterative simulations, see Brooks and Gelman [8].

In practice the purpose of performing a PDTA analysis is to maintain a specified level of safety while minimizing unnecessary maintenance costs. Thus the SFPOF estimates at every flight are not as important as the *peak* value of SFPOF obtained in the service life. Also, it is desired that the total maintenance costs from inspections, repairs, and failures be accurate. In Chapter 9 the methods for estimating maintenance costs are provided, and in practice it is recommended that the cost estimates and peak SFPOF estimates of the SIS routine be considered when judging convergence of the SIS routine. This section focuses on the overall convergence of SFPOF and PCD estimates only.

Consider first the flight-by-flight version of the SIS routine. In this, SFPOF is separately estimated for each flight, and the importance weights are updated after every flight. This will yield the most accurate SFPOF and PCD estimates once a sufficient number of samples are obtained. In some cases, particularly when the critical crack failure mode dominates a problem, convergence of SFPOF can be slow in the flight-by-flight routine. Consider Figure 4.6, which

depicts the SFPOF estimates for Examples CP7 and CP7ext using various particle counts. Because SFPOF is estimated for many flights, and the crack growth curve is generally a smooth function, SFPOF estimates which have converged should appear relatively smooth over the service life (except for at scheduled inspections where the SFPOF estimates decrease sharply). SFPOF estimates for CP7ext converge using far fewer particles than CP7. This is due to the fact that CP7 is dominated by the  $a > a_c$  failure mode and CP7ext is dominated by the  $K > K_c$  failure mode. In the explicit MC routine discussed in Chapter 3, 100% of trials of CP7 fail due to  $a > a_c$ , and 100% of trials of CP7ext fail due to  $K > K_c$ .

Due to its poor convergence, CP7 is the focus of the remainder of this section. Because CP7 fails due to  $a > a_c$ , each particle contributes to the estimation of SFPOF at only a single flight: the flight in which  $a_c$  is breached. The SFPOF estimates are choppy as a result. By assuming SFPOF is equal for relatively short intervals of flights, SFPOF estimates from the flight-by-flight routine can be pooled to speed convergence. See Figure 4.7. Note that this approach is a modification of the results of the flight-by-flight routine, not an alteration of the routine itself.

An approximate approach which performs the SIS simulation by proceeding several flights at-a-time is described in Section 4.6. As with the pooling of results of the flight-by-flight routine, this can obtain converged SFPOF estimates using fewer particles. In addition, because there are fewer calculations involved when proceeding several flights at-a-time, the run time can be drastically reduced. The results of this approach will be approximate overall, where the results when pooling nearby estimates of the flight-by-flight routine are approximate only within each pooled interval. SFPOF estimates resulting from the pooled flight-by-flight and the interval routines are shown in Figure 4.8, using 50 flight intervals for each. Note the flight-by-flight routine makes its calculations at every flight, and the interval routine makes its calculations at every interval. In the approach described in Section 4.6, estimates are made at the first, middle, and end flights in the interval. Thus when advancing

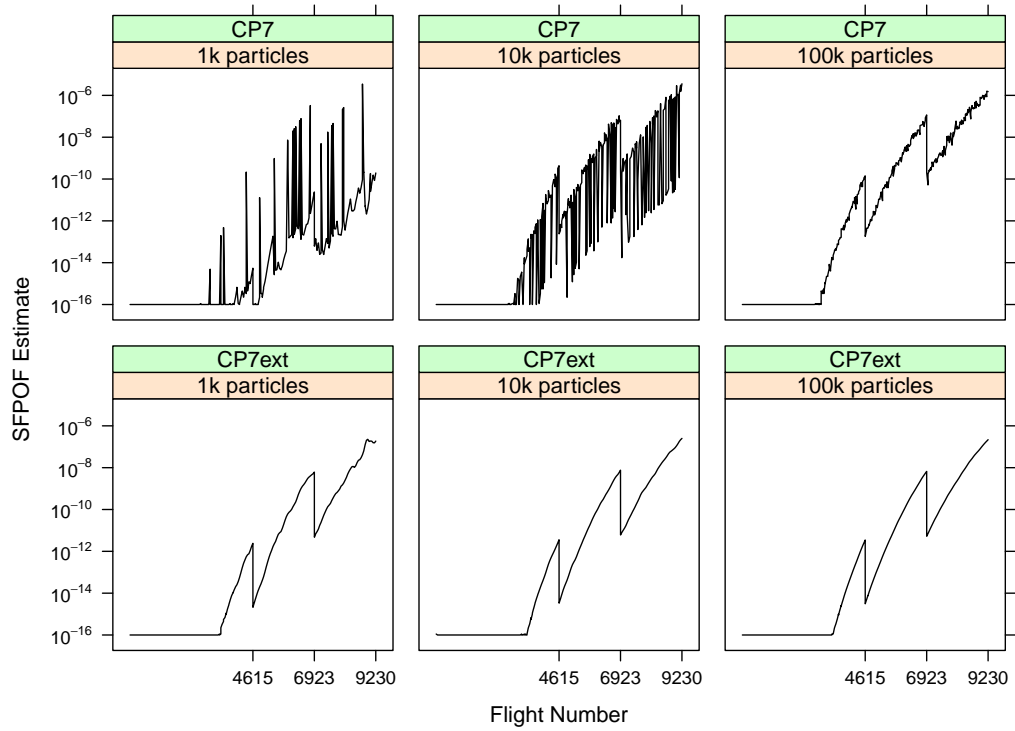


Figure 4.6: Single Flight Probability Of Failure (SFPOF) estimates for Examples CP7 and CP7ext using the flight-by-flight Sequential Importance Sampling (SIS) routine. Because SFPOF is estimated for many flights, and the crack growth curve is generally a smooth function, SFPOF estimates should appear relatively smooth over the service life (except for at scheduled inspections where the SFPOF estimates decrease sharply). SFPOF estimates for CP7ext converge using far fewer particles than CP7. This is due to the fact that CP7 is dominated by the  $a > a_c$  failure mode and CP7ext is dominated by the  $K > K_c$  failure mode.

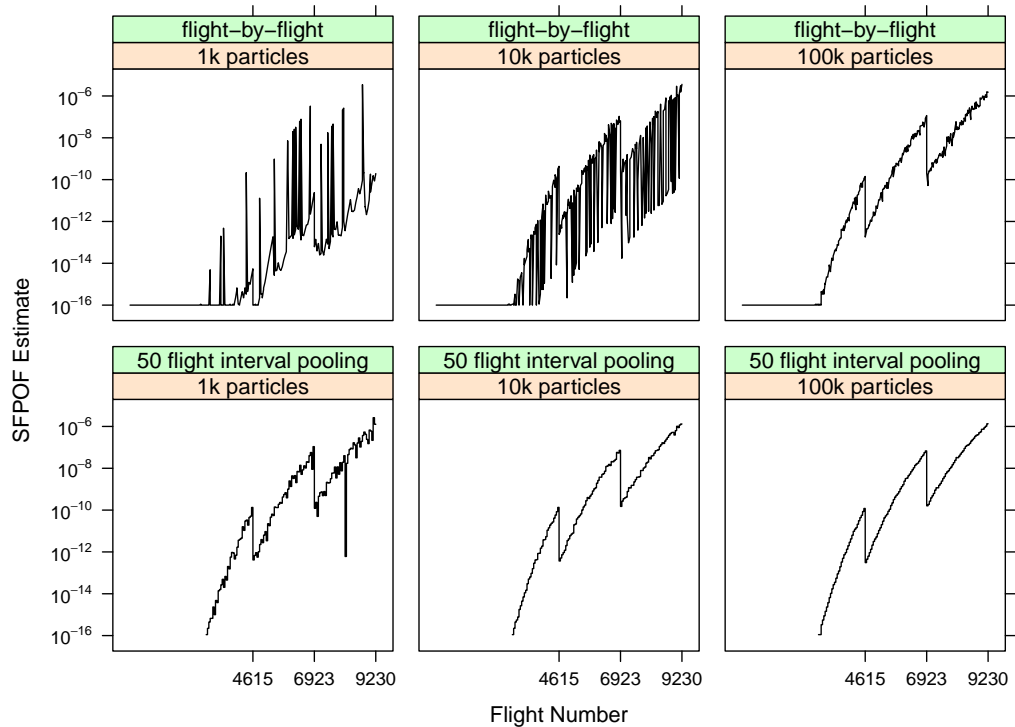


Figure 4.7: Single Flight Probability Of Failure (SFPOF) estimates for Examples CP7 using the flight-by-flight Sequential Importance Sampling (SIS) routine. CP7 is dominated by the  $a > a_c$  failure mode and convergence is slow using flight-by-flight estimates of SFPOF. By pooling results in 50 flight intervals, convergence is improved.

50 flights at-a-time, the flight-by-flight approach will take roughly 50/3 times longer to run.

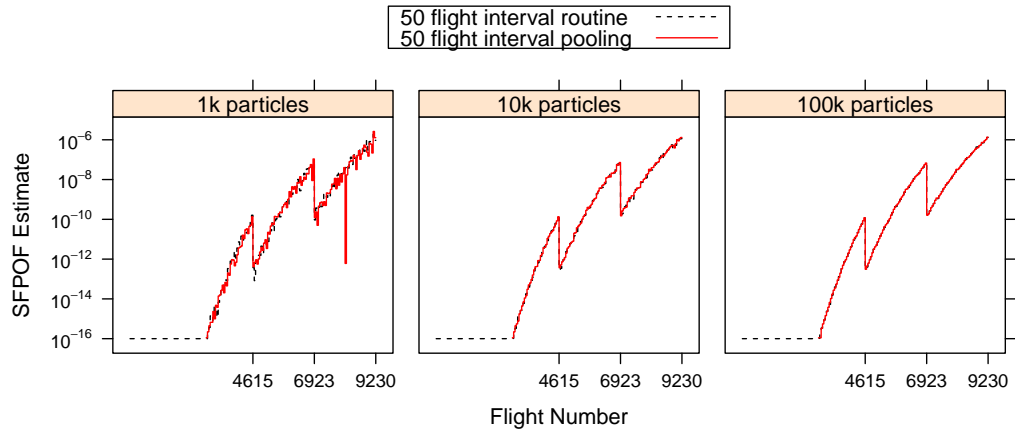


Figure 4.8: Single Flight Probability Of Failure (SFPOF) estimates for Example CP7 using Sequential Importance Sampling (SIS), comparing the flight-by-flight and interval routines. Flight-by-flight results are pooled at 50 flight intervals, and the interval routine proceeds 50 flights at-a-time. Similar SFPOF results can be obtained by proceeding several flights-at-a-time rather than flight-by-flight, requiring fewer calculations to do so. For larger intervals, runtime is further reduced though increasingly approximate.

Table 4.6 shows the PCD estimates for CP7 from the flight-by-flight and interval routines for the runs shown in this section.

In practice an analyst may run the SIS routine and observe the SFPOF and PCD estimates. Next, the particle count can be increased. If the results are comparable to the previous run, convergence may have been achieved. This informal approach to assessing convergence may suffice, but the MC error is in no way quantified when taking this approach.

#### 4.7.1 Running Independent Sequences

A more rigorous approach to estimating the level of convergence involves running the routine repeatedly with different random seed values and compar-

Table 4.6: Probability of Crack Detection PCD estimates for Example CP7 using Sequential Importance Sampling (SIS), comparing the flight-by-flight and interval routines (run in 50 flight intervals). Agreement is excellent at 100k particles for the three inspections.

(a) Flight-by-Flight Routine				(b) Interval Routine			
Insp	1k	10k	100k	Insp	1k	10k	100k
1	0.066	0.072	0.070	1	0.073	0.072	0.070
2	0.219	0.241	0.240	2	0.245	0.242	0.241
3	0.525	0.520	0.525	3	0.537	0.526	0.524

ing the estimates from the runs. Consider Figure 4.9 below, where Example CP7 is run in 5 independent SIS sequences with 100k and 1m particles in each run, respectively. Convergence appears to be well achieved at 1m particles per sequence due to the low variability between sequences.

PCD estimates of the 5 independent sequences are given in Table 4.7.

Table 4.7: Probability of Crack Detection PCD estimates for Example CP7 using 5 independent sequences in the flight-by-flight Sequential Importance Sampling (SIS) routine. Convergence of these PCD estimates is strong given the low variability between sequences.

(a) 100k Particles per Sequence						
Insp	Seq 1	Seq 2	Seq 3	Seq 4	Seq 5	
1	0.070	0.070	0.071	0.069	0.071	
2	0.242	0.241	0.243	0.241	0.242	
3	0.527	0.527	0.526	0.527	0.526	

(b) 1m Particles per Sequence						
Insp	Seq 1	Seq 2	Seq 3	Seq 4	Seq 5	
1	0.070	0.070	0.070	0.070	0.070	
2	0.241	0.241	0.241	0.242	0.242	
3	0.526	0.526	0.525	0.527	0.526	

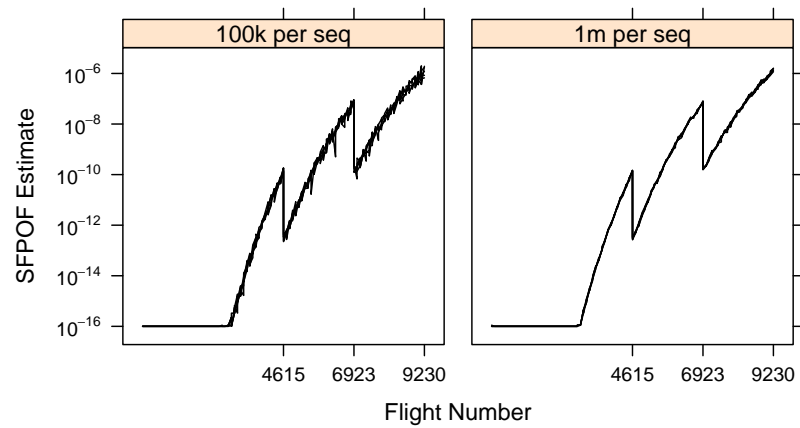


Figure 4.9: Examining convergence for Example CP7 using five sequences run in parallel in the flight-by-flight Sequential Importance Sampling (SIS) routine. Particle counts of 100,000 and 1,000,000 are used. SFPOF estimates are those of individual flights, rather than pooled estimates. Several sequences, each run using different random seed values, should yield similar SFPOF estimates if convergence has been achieved. The variability in these estimates can be used to characterize the simulation error. Convergence of SFPOF estimates for Example CP7 is relatively poor when using individual flight estimates of SFPOF due to dominance of the  $a > a_c$  failure mode.

When running independent sequences one would use the average of the sequences as the point estimate and characterize the variability using the individual estimates. For example, one could run more such sequences and obtain empirical confidence bounds for SFPOF or PCD by taking the appropriate quantiles as the bounds. Such an approach would provide a quantitative assessment of the MC error in the estimates. This approach can be time consuming.

### 4.7.2 Bootstrap Re-sampling

A useful approach to judging the convergence of a single sampling sequence involves Efron's bootstrap. The complete state of the model at the flight of interest must be known to use this method, so it is best performed as a secondary task during the SIS run. Suppose an SIS run utilizes  $n$  particles. The point estimate of SFPOF for a particular flight or PCD for a scheduled inspection is calculated in the usual way. At that time in the calculation a new data set can be created by re-sampling  $n$  particles with replacement from the set (where the pairings of  $a$ ,  $K_c$ , and  $w$  are preserved). This is done  $n_{\text{boot}}$  times and for each set SFPOF or PCD is calculated (after normalizing the weights). The  $n_{\text{boot}}$  estimates are an approximation of the sampling distribution and a bootstrap confidence interval may be reported. In addition to Efron's paper, see Robert and Casella [44] [45] for examples of the bootstrap applied in a Monte Carlo setting.

The results of flight-by-flight and interval runs of Example CP7 using 100k particles are shown in Figure 4.10. A point estimate of SFPOF is obtained at 100 flight intervals for this run, and at each estimation time a bootstrap re-sampling procedure is also performed. In the figure, 1000 bootstrap re-samples of the state are used (each sampling 100k particles with replacement) and the 2.5<sup>th</sup> and 97.5<sup>th</sup> quantiles of the SFPOF estimates are displayed. Note there are hundreds of individual bootstrap confidence intervals connected by dashed lines for plotting convenience. As discussed earlier in this section, for Example

CP7 convergence is relatively poor for the flight-by-flight routine. For several calculations the confidence interval dips considerably, which is an indication that there are not enough particles breaching the critical crack size for that particular flight. The convergence is much faster for the approximate interval routine which uses all of the critical crack size breaches of the interval when estimating SFPOF. Note in Figure 4.10 the bootstrap interval tends to track the point estimate, which is generally the case since the bootstrap is based on a single run of the SIS routine. Thus the bootstrap is not quite so powerful at assessing convergence as the multiple independent sequences approach, though it is often the faster approach. For the examples in the remainder of this work, the multiple independent sequences approach is used to judge convergence.

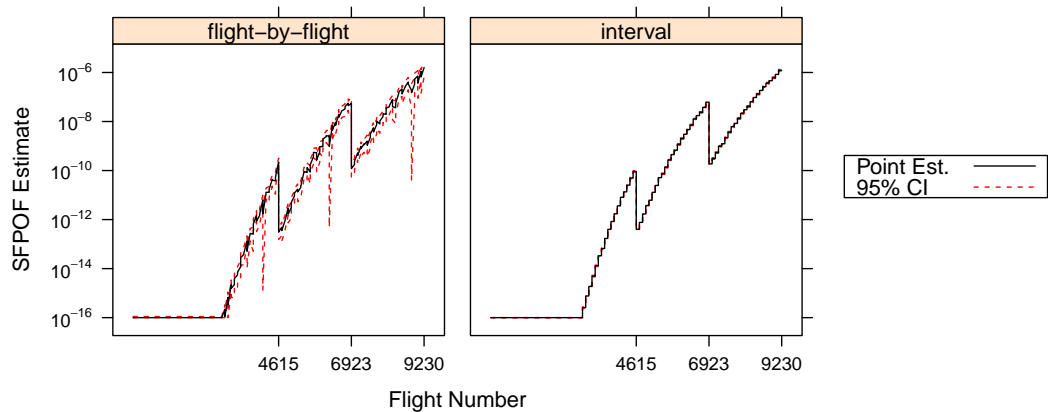


Figure 4.10: Examining convergence for Example CP7 using the bootstrap with 100k particles and  $n_{\text{boot}} = 1\text{k}$ . At selected flights during the run of the flight-by-flight and interval versions of the Sequential Importance Sampling (SIS) routine, a bootstrap resampling procedure is used to estimate the sampling distribution of the SFPOF estimate. Confidence bounds are connected by dashed lines for plotting convenience. The interval routine is better converged than the flight-by-flight routine.

A histogram of bootstrap estimates can provide insight regarding the sampling distribution. This is done for the last flight in the service life in Figure

4.11, using 10,000 bootstrap estimates from the flight-by-flight SIS routine.

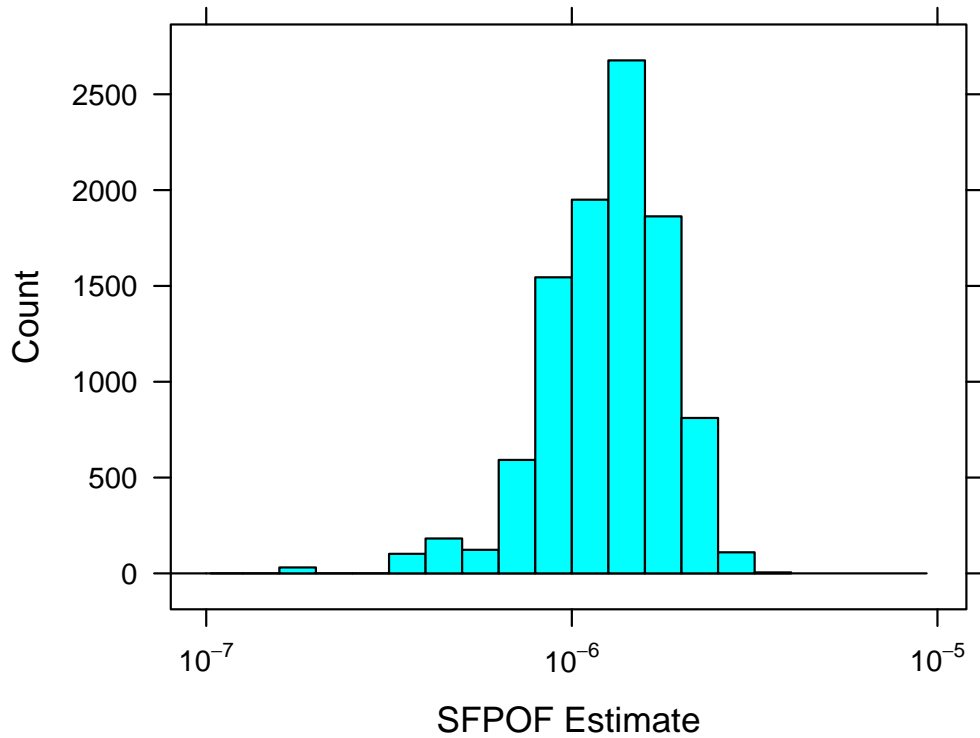


Figure 4.11: Histogram of bootstrap estimates of SFPOF at the last flight in the service life for Example CP7. 100k particles are used in the flight-by-flight Sequential Importance Sampling (SIS) routine with  $n_{\text{boot}} = 10\text{k}$ . The point estimate of  $1.1 \times 10^{-6}$  is near the mode of the histogram. The range of estimates spans over an order of magnitude, indicating that convergence of SFPOF at this flight has not yet been achieved.

Point estimates and upper and lower confidence bounds for PCD are shown in Table 4.8.

Table 4.8: Probability of Crack Detection PCD estimates for Example CP7 using Sequential Importance Sampling (SIS), comparing the flight-by-flight and interval routines. Empirical 95% confidence bounds are obtained using the bootstrap with 100k particles and  $n_{\text{boot}} = 1\text{k}$ .

(a) Flight-by-Flight Routine				(b) Interval Routine			
Insp	PointEst	Lower	Upper	Insp	PointEst	Lower	Upper
1	0.070	0.070	0.071	1	0.070	0.069	0.071
2	0.241	0.238	0.245	2	0.242	0.239	0.245
3	0.526	0.517	0.534	3	0.521	0.512	0.530

## 4.8 SIS Results for Examples CP4, CP6, CP7 and CP7ext

The SIS routine is written using the statistical computing language R [40] and is published as part of a software package called `crackR` [22] (along with the explicit MC routine). See Chapter 10 for information regarding the use of the software and how to obtain it. The time required to run the routine depends on the number of particles utilized. For example, using 100k samples the routine completes in about 12 minutes (using a standard Windows machine). The SFPOF estimates for CP7ext actually converge at around 10k particles and this takes about one minute.

Convergence of the SFPOF estimates in the SIS routine can be assessed using the methods of Section 4.7. These methods are used to determine how many particles are required for each example to obtain quality estimates of SFPOF. First, each example is run using 100k particles, requesting SFPOF estimates every 50 flights. During these runs 1k bootstrap samples are taken at each estimate of SFPOF; see Figure 4.12. Examples CP6 and CP7ext exhibit better convergence than CP4 and CP7 at this sample size.

Next, five independent sequences are run using 1m particles in each sequence (see Figure 4.13). There is very little variability between runs when

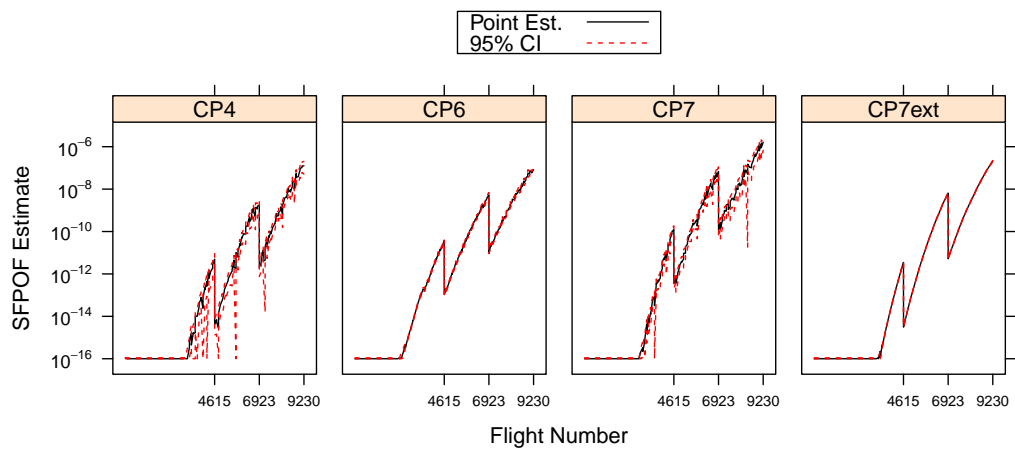


Figure 4.12: Single Flight Probability Of Failure (SFPOF) for Examples CP4, CP6, CP7 and CP7ext in the Sequential Importance Sampling (SIS) approach using 100k particles and 1k bootstrap samples. Examples CP6 and CP7ext exhibit better convergence than CP4 and CP7 at this sample size. Examples CP4 and CP7 are both dominated by the critical crack failure mode, which makes convergence difficult to achieve for flight-by-flight estimation of SFPOF (see Section 4.7).

using 1m particles per sequence, indicating that convergence of SFPOF has been well achieved for all examples.

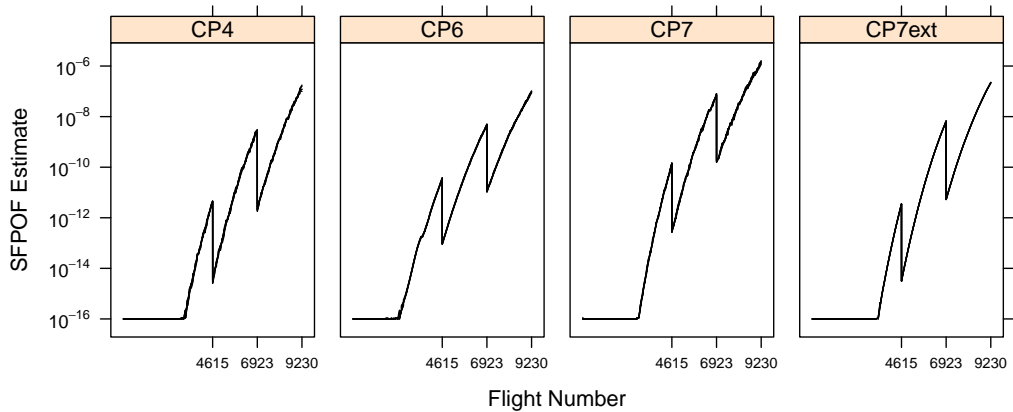


Figure 4.13: Single Flight Probability Of Failure (SFPOF) for Examples CP4, CP6, CP7 and CP7ext in the Sequential Importance Sampling (SIS) approach using five independent sequences of 1m particles per sequence. There is very little variability between runs, indicating that convergence has been well achieved for all examples.

Convergence of PCD can be similarly characterized. Table 4.9 gives empirical 95% confidence bounds for PCD resulting from  $n_{\text{boot}} = 1\text{k}$  bootstrap estimates taken at each inspection in the SIS run using 100k particles. The estimates from five sequences run in parallel, each using 1m particles, are given in Table 4.10. Also given are the mean and standard error of each estimate. For PCD one is generally interested in 3 decimal places. According to that level of precision, convergence of PCD estimates has generally been achieved for the four example problems.

Lastly the results of the flight-by-flight SIS routine are compared to those of the interval SIS routine. The flight-by-flight routine gives the ideal results since it correctly represents the life as a sequence of individual flights. The interval routine can yield reasonable results in less time, making it useful for preliminary or exploratory analysis. The flight-by-flight results using 5m

Table 4.9: Probability of Crack Detection PCD estimates for Examples CP4, CP6, CP7 and CP7ext using Sequential Importance Sampling (SIS). Empirical 95% confidence bounds are obtained using the bootstrap with 100k particles and  $n_{\text{boot}} = 1\text{k}$ . This variability may be unacceptable for some applications, in which case the particle count should be increased.

(a) Example CP4					(b) Example CP6				
	Flight	PointEst	Lower	Upper		Flight	PointEst	Lower	Upper
1	4615	0.023	0.022	0.023	1	4615	0.035	0.034	0.036
2	6923	0.175	0.173	0.177	2	6923	0.119	0.115	0.123
3	9231	0.589	0.582	0.597	3	9231	0.306	0.284	0.328

(c) Example CP7					(d) Example CP7ext				
	Flight	PointEst	Lower	Upper		Flight	PointEst	Lower	Upper
1	4615	0.070	0.070	0.071	1	4615	0.070	0.070	0.071
2	6923	0.244	0.241	0.247	2	6923	0.244	0.239	0.248
3	9231	0.527	0.519	0.536	3	9231	0.523	0.513	0.534

particles (by combining the five sequences of Figure 4.13) represent the most accurate SIS results in this work and are used to represent the SIS routine. The interval routine is run twice with 1m particles, partitioning the service life in 100 and 500 flight intervals, respectively. SFPOF plots for these approaches are shown in Figure 4.14. The 100 flight interval routine yields SFPOF estimates very similar to those of the flight-by-flight routine for all examples. The 500 flight interval routine yields reasonable results given the large size of the intervals.

PCD estimates for the flight-by-flight and interval runs are given in Table 4.11. Agreement between the routines is excellent.

Table 4.10: Probability of Crack Detection (PCD) estimates for Examples CP4, CP6, CP7 and CP7ext from 5 independent sequences of 1m particles. Also shown are the mean and standard errors of the estimates. For PCD one is generally interested in 3 decimal places. According to that level of precision, convergence has been achieved.

(a) Example CP4				(b) Example CP6			
Seq	Insp 1	Insp 2	Insp 3	Seq	Insp 1	Insp 2	Insp 3
1	0.0226	0.1739	0.5924	1	0.0320	0.1114	0.2961
2	0.0226	0.1738	0.5915	2	0.0343	0.1187	0.3068
3	0.0226	0.1745	0.5918	3	0.0322	0.1117	0.2961
4	0.0225	0.1740	0.5919	4	0.0340	0.1178	0.3052
5	0.0226	0.1744	0.5914	5	0.0347	0.1194	0.3064
Mean	0.0226	0.1741	0.5918	Mean	0.0334	0.1158	0.3021
St Err	0.0000	0.0001	0.0002	St Err	0.0006	0.0018	0.0025

(c) Example CP7				(d) Example CP7ext			
Seq	Insp 1	Insp 2	Insp 3	Seq	Insp 1	Insp 2	Insp 3
1	0.0698	0.2408	0.5263	1	0.0701	0.2418	0.5254
2	0.0701	0.2410	0.5258	2	0.0697	0.2397	0.5250
3	0.0702	0.2412	0.5250	3	0.0702	0.2415	0.5256
4	0.0704	0.2422	0.5267	4	0.0702	0.2411	0.5265
5	0.0702	0.2421	0.5260	5	0.0701	0.2416	0.5256
Mean	0.0701	0.2415	0.5260	Mean	0.0701	0.2411	0.5256
St Err	0.0001	0.0003	0.0003	St Err	0.0001	0.0004	0.0002

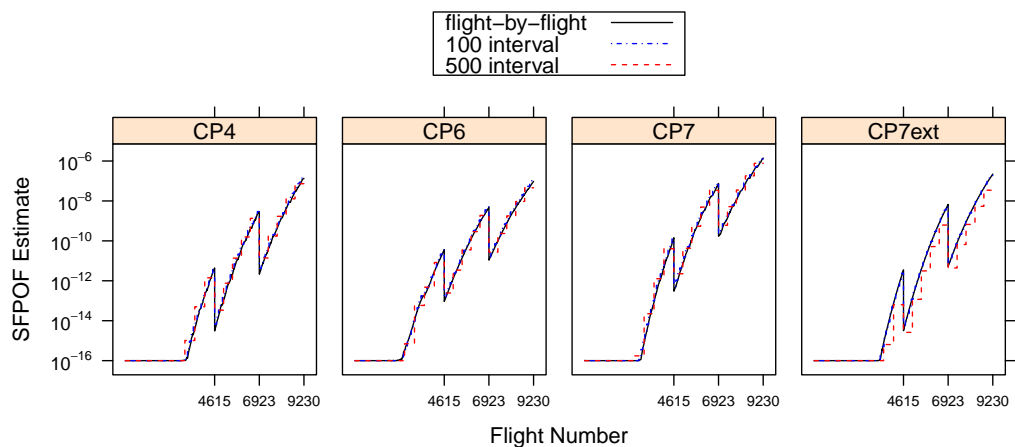


Figure 4.14: Single Flight Probability Of Failure (SFPOF) estimates for Examples CP4, CP6, CP7 and CP7ext using flight-by-flight and interval Sequential Importance Sampling (SIS) routines. The flight-by-flight routine uses 5m particles and each interval routine uses 1m particles. The interval routines partition the service life into intervals of 100 and 500 flights, respectively. The 100 flight interval routine yields SFPOF estimates very similar to those of the flight-by-flight routine for all examples. The 500 flight interval routine yields reasonable results given the large size of the intervals.

Table 4.11: Probability of Crack Detected (PCD) estimates for Examples CP4, CP6, CP7 and CP7ext using flight-by-flight and interval Sequential Importance Sampling (SIS) routines. The flight-by-flight routine uses 5m particles and each interval routine uses 1m particles. The interval routines partition the service life into intervals of 100 and 500 flights, respectively. Agreement between the routines is excellent.

(a) Example CP4				(b) Example CP6			
Insp	FBF	100 Int	500 Int	Insp	FBF	100 Int	500 Int
1	0.023	0.022	0.023	1	0.033	0.034	0.031
2	0.174	0.174	0.174	2	0.116	0.116	0.110
3	0.592	0.592	0.593	3	0.302	0.303	0.294

(c) Example CP7				(d) Example CP7ext			
Insp	FBF	100 Int	500 Int	Insp	FBF	100 Int	500 Int
1	0.070	0.070	0.070	1	0.070	0.070	0.070
2	0.241	0.241	0.241	2	0.241	0.242	0.241
3	0.526	0.526	0.527	3	0.526	0.526	0.527

# CHAPTER 5

## COMPARISON OF PROBABILISTIC DAMAGE TOLERANCE ANALYSIS APPROACHES

Several approaches to PDTA (Probabilistic Damage Tolerance Analysis) have been presented in previous chapters:

- PROF
  - Analytical approach using numerical integration and hazard function representation of SFPOF (Single Flight Probability Of Failure)
  - Very short runtime
- Explicit MC (Monte Carlo)
  - Flight-by-flight approach which simulates actual failures
  - Computationally expensive, straightforward approach
- IS (Importance Sampling) MC
  - Similar to the explicit MC approach using IS to set the initial parameters

- Faster convergence than the explicit MC approach, but cannot include scheduled inspections
- HMM (Hidden Markov Model)/SIS (Sequential Importance Sampling)
  - Simulation approach using Bayes' updating of importance weights instead of simulating failures
  - Runtime much shorter than the explicit MC approach, and capable of using observed evidence to update the model

This chapter compares the above approaches through several example problems from the documentation of the PROF software.

SFPOF plots for CP4, CP6, CP7 and CP7ext are shown in Figure 5.1, followed by PCD results in Table 5.2. The SIS routine utilized 5m particles for these runs, calculating SFPOF on a flight-by-flight basis (see Section 4.3.1 for a discussion of SFPOF calculation in the SIS routine). Note that all SFPOF estimates have been given an artificial minimum of  $1 \times 10^{-16}$ .

The MC SFPOF estimates of Figure 5.1 are calculated by pooling failures in 50 flight intervals. In addition to the pooled MC point estimates of SFPOF, 95% confidence bounds are obtained for several selected flights by re-sampling the simulation results (see Section 3.3). These bounds are given in Table 5.1 along with the point estimates of the other approaches.

For all examples the SIS routine yields SFPOF results similar to the MC routine. This demonstrates that the HMM and the SIS approach of updating the importance weights after each flight is equivalent to performing an SFPOF calculation utilizing Equation 3.9. The agreement between the SIS and MC routines after inspections shows that the methodology for modeling inspections (see Section 4.3.4) is capable of accurately representing the situation.

According to the benchmark set by the IS MC routine, PROF underestimates SFPOF for all examples in the early portion of the service life; particularly for CP4. Underestimation at such low SFPOF levels should not result in a serious safety issue. Because the PROF source code is not available it is unknown whether this underestimation of SFPOF can occur at higher risk

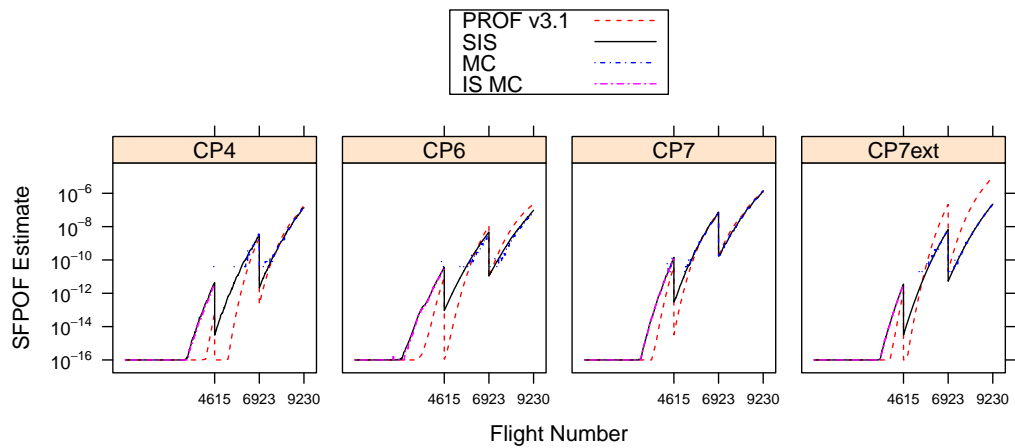


Figure 5.1: Single Flight Probability Of Failure (SFPOF) estimates for Examples CP4, CP6, CP7 and CP7ext using the PRobability Of Fracture (PROF) v3.1 software, Monte Carlo (MC) simulation, and Sequential Importance Sampling (SIS) approaches (with 5m particles for each). The MC estimates provide the benchmark for comparison. Importance sampling is used for the MC estimates prior to the first inspection. The SIS estimates agree very well with the MC estimates. PROF variously underestimates and overestimates SFPOF by up to two orders of magnitude.

Table 5.1: Single Flight Probability Of Failure (SFPOF) estimates at several selected flights (during the first interval and just prior to the three scheduled inspections) for Examples CP4, CP6, CP7 and CP7ext. The benchmark Monte Carlo (MC) results are presented as the upper and lower bounds of a 95% confidence interval characterizing the MC error. The Sequential Importance Sampling (SIS) SFPOF estimates fall within (or very near to) the bounds of the MC routine for all examples. The PProbability Of Fracture (PROF) v3.1 estimates are outside the MC bounds by two orders of magnitude in either direction for several estimates.

(a) Example CP4

Flight	MC lwr	MC upr	SIS	PROF
3846	$1.32 \times 10^{-14}$	$5.01 \times 10^{-14}$	$3.64 \times 10^{-14}$	$1.00 \times 10^{-16}$
4615	$9.59 \times 10^{-13}$	$4.78 \times 10^{-12}$	$4.40 \times 10^{-12}$	$3.24 \times 10^{-14}$
6923	$1.03 \times 10^{-10}$	$1.13 \times 10^{-08}$	$2.87 \times 10^{-09}$	$1.05 \times 10^{-09}$
9230	$1.07 \times 10^{-07}$	$1.72 \times 10^{-07}$	$1.35 \times 10^{-07}$	$1.88 \times 10^{-07}$

(b) Example CP6

Flight	MC lwr	MC upr	SIS	PROF
3846	$2.03 \times 10^{-13}$	$8.56 \times 10^{-13}$	$6.53 \times 10^{-13}$	$8.28 \times 10^{-15}$
4615	$1.12 \times 10^{-11}$	$4.92 \times 10^{-11}$	$3.63 \times 10^{-11}$	$4.70 \times 10^{-12}$
6923	$1.10 \times 10^{-09}$	$1.46 \times 10^{-08}$	$4.76 \times 10^{-09}$	$5.57 \times 10^{-09}$
9230	$4.37 \times 10^{-08}$	$8.80 \times 10^{-08}$	$9.52 \times 10^{-08}$	$2.36 \times 10^{-07}$

(c) Example CP7

Flight	MC lwr	MC upr	SIS	PROF
3846	$5.40 \times 10^{-13}$	$1.20 \times 10^{-12}$	$7.93 \times 10^{-13}$	$1.92 \times 10^{-14}$
4615	$3.26 \times 10^{-11}$	$1.27 \times 10^{-10}$	$1.43 \times 10^{-10}$	$2.09 \times 10^{-11}$
6923	$5.10 \times 10^{-08}$	$8.28 \times 10^{-08}$	$7.49 \times 10^{-08}$	$3.40 \times 10^{-08}$
9230	$1.38 \times 10^{-06}$	$1.53 \times 10^{-06}$	$1.41 \times 10^{-06}$	$1.19 \times 10^{-06}$

(d) Example CP7ext

Flight	MC lwr	MC upr	SIS	PROF
3846	$4.69 \times 10^{-15}$	$1.58 \times 10^{-14}$	$9.22 \times 10^{-15}$	$1.00 \times 10^{-16}$
4615	$1.36 \times 10^{-12}$	$5.04 \times 10^{-12}$	$3.53 \times 10^{-12}$	$6.09 \times 10^{-13}$
6923	$4.05 \times 10^{-09}$	$1.58 \times 10^{-08}$	$6.66 \times 10^{-09}$	$1.07 \times 10^{-07}$
9230	$1.92 \times 10^{-07}$	$2.50 \times 10^{-07}$	$2.21 \times 10^{-07}$	$1.12 \times 10^{-05}$

levels. Near the end of the service life, PROF yields SFPOF estimates within or near the explicit MC results for CP4, CP6, and CP7, but overestimates SFPOF for CP7ext by two orders of magnitude. Recall, CP7ext utilizes DTA data which has been extended (at PROF's suggestion) because the data as originally specified for CP7 are less than ideal.

PCD estimates from the various PDTA approaches are shown in Table 5.2. The SIS routine agrees well with the benchmark MC results. PROF tends to significantly underestimate, particularly for the third inspection.

Table 5.2: Probability of Crack Detected (PCD) estimates for Examples CP4, CP6, CP7 and CP7ext using Monte Carlo (MC) simulation, Sequential Importance Sampling (SIS), and the PRobability Of Fracture (PROF) v3.1 software. Point estimates are shown for PCD of the MC routine because at three decimal places the 95% confidence bounds shown in Table 3.5d are equivalent. The SIS routine yields PCD estimates nearly identical to those of the benchmark MC routine. PROF, on the other hand, tends to significantly underestimate PCD, particularly for the third inspections. Note the results for Examples CP7 and CP7ext are identical.

(a) Example CP4				(b) Example CP6			
Insp	MC	SIS	PROF	Insp	MC	SIS	PROF
1	0.023	0.023	0.021	1	0.033	0.033	0.033
2	0.174	0.174	0.110	2	0.115	0.116	0.109
3	0.592	0.592	0.339	3	0.301	0.302	0.237

(c) Example CP7				(d) Example CP7ext			
Insp	MC	SIS	PROF	Insp	MC	SIS	PROF
1	0.070	0.070	0.068	1	0.070	0.070	0.068
2	0.241	0.241	0.220	2	0.241	0.241	0.220
3	0.526	0.526	0.426	3	0.526	0.526	0.426

# CHAPTER 6

## IMPROVED REPAIR MODELING

The traditional approach to PDTA (Probabilistic Damage Tolerance Analysis) as described in Section 3.1 involves the prediction of future repairs, which results in the resetting of a portion of the crack size distribution to a repair EIFS (Equivalent Initial Flaw Size) distribution. While a different EIFS distribution may be used to represent repairs, after repair the crack growth and  $K/\sigma$  data are unaltered. That is, the repaired cracks are assumed to behave exactly the same as the as-manufactured cracks. This is clearly not true in some cases as the repair may significantly alter the growth rate and stress intensity at the location of interest (be it due to an oversized fastener, installed fitting, or other repair type). The HMM (Hidden Markov Model)/SIS (Sequential Importance Sampling) approach provides a flexible framework which allows for any number of different types of repairs, the behavior of which can be realistically modeled. The modeling approach is given in Section 6.1. This is demonstrated with two altered versions of Example CP7ext, a simple example in Section 6.2 using a repair type that modifies the behavior of cracks, and a more realistic example in Section 6.3 including various repair types and the prediction of repair costs.

## 6.1 Modeling Multiple Repair Types

The HMM/SIS model described in Chapter 4 includes the variables crack length  $a$ , fracture toughness  $K_c$ , and importance weights  $w$ , with each particle defined by these three values. When crack growth occurs or the probability of failure is calculated, the crack growth and  $K/\sigma$  tables are consulted to perform those operations. This assumes all particles will behave in the same manner.

Suppose that a certain repair type will be utilized for a given structure, and as a result the crack growth and normalized stress intensity will be significantly altered due to this repair. In this case a second set of DTA data would be used in the SIS for the repaired particles. In order to differentiate the repaired particles from the as-manufactured particles, an additional classification variable,  $c$ , is added to the SIS model.

This is demonstrated through two examples, each based on Example CP7ext. The *simple* example in Section 6.2 assumes that initially the component is of the as-manufactured type ( $c = 1$ ), and all repairs will be of a certain modified type ( $c = 2$ ). In the *complex* example of Section 6.3 the initial state is again known to be as-manufactured ( $c = 1$ ), and there are two different types of repair ( $c = 2, 3$ ), as well as the possibility of part replacement back to the as-manufactured condition; thus the domain of  $c$  is  $\{1, 2, 3\}$ .

## 6.2 Simple Modified Repair Example

Suppose that for Example CP7ext it is assumed that after repair the structure is weakened; crack growth speed is increased by 60%, and  $K/\sigma$  is increased by 30%. PROF specifies a repair EIFS distribution for its example problems that is more severe than the as-manufactured EIFS distribution, hence the weakening utilized here. In general a strengthening as a result of repair may be appropriate. For this simple repair example the EIFS distribution used for repairs is the same as that used for the initial state, and the inspection times are those indicated in Section 3.2.2 for CP7ext, i.e., inspections after 6,000,

9,000, and 12,000 FH. The as-manufactured data is referred to with classification  $c = 1$ , and the repaired data is referred to as classification  $c = 2$ . The modified DTA data are shown in Figure 6.1.

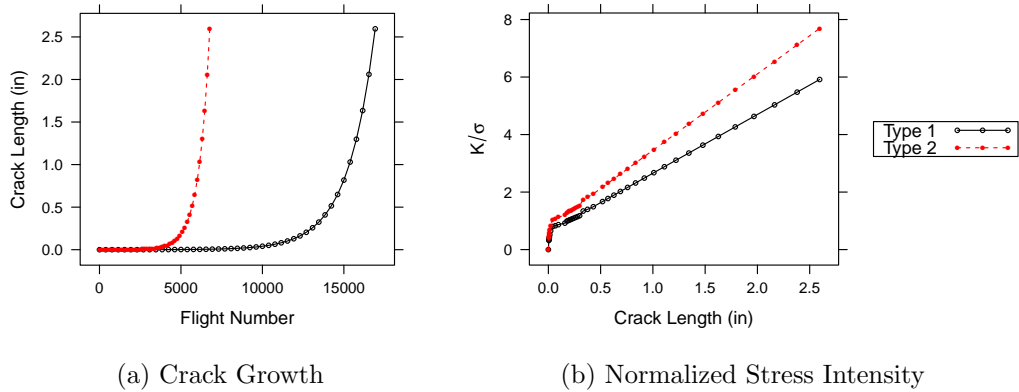


Figure 6.1: Damage Tolerance Analysis (DTA) data for a modified version of Example CP7ext, referred to as the *simple* repair scenario. Type 2 exhibits more severe crack growth and stress intensity. In the Sequential Importance Sampling (SIS) routine, all particles will start as classification  $c = 1$ . Particles will be repaired to classification  $c = 2$  for this simple example. Increased severity is used for this example because the repair Equivalent Initial Flaw Size (EIFS) distribution specified for this problem was more severe than the as-manufactured EIFS distribution, indicating that the repair appropriate for this example yields a component which exhibits increased risk.

This example is also run in the explicit MC routine using 100m trials, the results of which are partitioned into 50 flight intervals to improve the plot (see Section 3.3.2). The SFPOF results are shown in Figure 6.2 along with the SFPOF results of the standard SIS routine for Example CP7ext which does not include multiple types of repairs. The increase in SFPOF estimates of the SIS and MC routines as a result of the possibility of increased crack growth speed and stress intensity for classification  $c = 2$  particles is evident. Note the SIS routine for modeling multiple types of repairs yields SFPOF estimates

equivalent to those of the explicit MC routine.

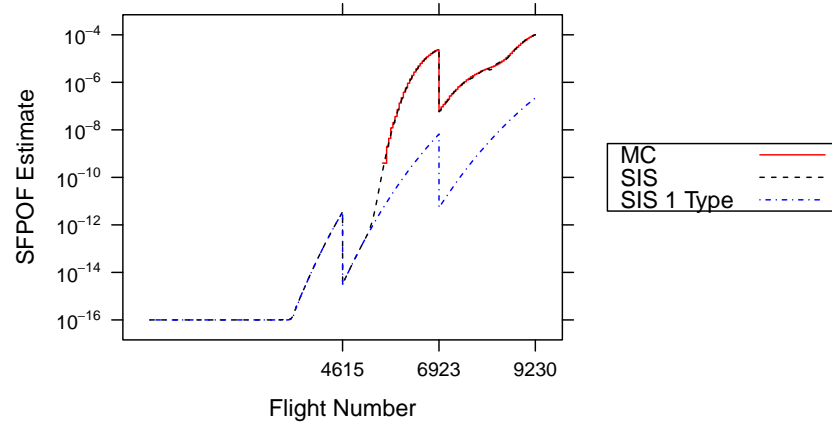


Figure 6.2: Single Flight Probability Of Failure (SFPOF) estimates for modified Example CP7ext; *simple* repair scenario. Estimates are obtained using the explicit MC routine for multiple repair types, the SIS routine for multiple repair types, and the standard SIS routine for the original specification of Example CP7ext (“SIS 1 Type”). The SIS and MC SFPOF estimates are equivalent. When utilizing the more severe reclassification  $c = 2$  repair (in SIS and MC), SFPOF estimates increase dramatically after the first inspection (the first opportunity for repairs to be made).

The PCD (Probability of Crack Detection) results for the *simple* example are shown in Table 6.1. As with SFPOF, PCD estimates from the MC and SIS routines are very similar and are well in excess of the results obtained using the standard SIS routine for Example CP7ext.

### 6.3 Complex Modified Repair Example

Consider a more complex and realistic example which utilizes multiple repair types. The attributes of the three particle types are as follows, including a fourth type which indicates a part replacement to  $c = 1$ . This extends the discussion of Section 4.3.4, in which for the typical PDTA problem there were

Table 6.1: Probability of Crack Detection (PCD) estimates for Example CP7ext; *simple* repair scenario. The increased crack growth speed after repair leads to larger PCD estimates at the second and third inspections.

Insp	MC	SIS	SIS 1 Type
1	0.070	0.070	0.070
2	0.268	0.266	0.241
3	0.634	0.632	0.526

only two possible outcomes for a repair (detection or no detection). Note these numbers are arbitrary and are selected for demonstration purposes.

1. As-manufactured class,  $c = 1$ 
  - Parameters are those of Example CP7ext
2. Oversize fastener,  $c = 2$  ( $a < 0.05''$ )
  - Crack growth rate is increased by 20%
  - $K/\sigma$  and EIFS distribution are identical to Type 1
  - Cost of repair = \$1,000
3. Repair fitting,  $c = 3$  ( $0.05'' \leq a < 0.25''$ )
  - Crack growth rate is decreased by 50%
  - $K/\sigma$  increased by 50%
  - EIFS distribution is more severe: Exponential(rate=138.1559<sup>1</sup>)
  - Cost of repair = \$5,000
4. Part replacement,  $c = 1$  ( $a \geq 0.25''$ )
  - Cost of replacement = \$15,000

Note it is also assumed that any crack smaller than 0.25'' found on an oversize fastener hole ( $c = 2$ ) will be repaired with the fitting, and any crack found on a fitting ( $c = 3$ ) will cause replacement of the part, regardless of the size of the found crack. There is no way to go from a more extensive repair to

<sup>1</sup>This EIFS is the repair EIFS indicated for Example CP7 in the PROF manual, which is equivalent to a Weibull distribution with shape=1 and scale=0.0072382.

a simpler repair (except for part replacement). The various modified data are shown in Figure 6.3.

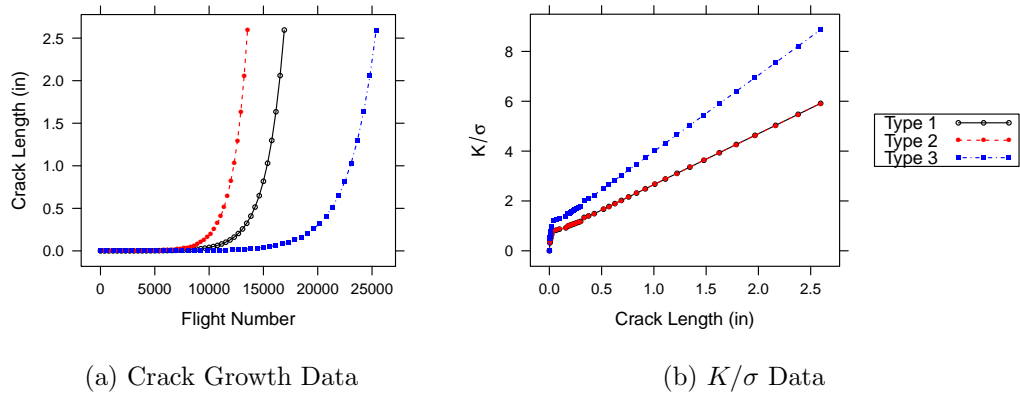


Figure 6.3: Damage Tolerance Analysis (DTA) data for a modified version of Example CP7ext, referred to as the *complex* repair scenario. Classification  $c = 1$  is the as-manufactured component, classification  $c = 2$  is an oversize fastener repair, and classification  $c = 3$  is an installed repair fitting. The behavior of the various repair types is listed in the text. In the Sequential Importance Sampling (SIS) routine, all particles will begin as classification  $c = 1$ . At inspection, the type of repair to be performed for a particle (if a repair occurs) depends on the crack size of that particle at inspection time.

The SFPOF estimates for the complex example using 100k particles are shown in Figure 6.4. The PCD estimates for the complex example are in Table 6.2. Note that the PCD results have been partitioned according to the probability of each type of repair being performed at each scheduled inspection, and the total PCD (probability of any type of repair being performed) is also shown. This is a significant improvement in predictive capability for aircraft fleet managers because this information can be used to both more accurately predict future repair costs and to help make the decision as to whether the engineering work should be done to develop or improve a certain type of repair for this structural component.

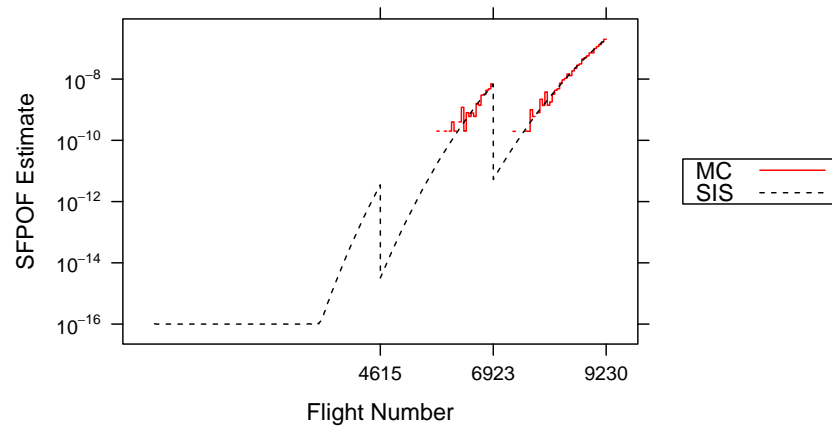


Figure 6.4: Single Flight Probability Of Failure (SFPOF) estimates for Example CP7ext; *complex* repair scenario. The scenario is run using the Sequential Importance Sampling (SIS) routine with 500k particles and the explicit Monte Carlo (MC) routine using 100m trials. SFPOF estimates are very similar later in the service life where MC estimates have converged.

As stated above the PCD results of Table 6.2 can be used to predict the costs due to repairs. The cost of performing each repair type was given in the itemized list earlier in this section. The cost predictions due to repairs at each inspection are calculated by taking the expected value; see Table 6.3.

In the above, PCD estimates are used to find the expected repair costs at the future scheduled inspections. In Chapter 9, costs due to inspections, false calls, and failures are also estimated.

Table 6.2: Probability of Crack Detection (PCD) estimates for Example CP7ext; *complex* repair scenario. The scenario is run using the Sequential Importance Sampling (SIS) routine with 500k particles and the explicit Monte Carlo (MC) routine using 100m trials. The SIS and MC estimates of PCD are nearly identical.

(a) MC

Insp	Oversize	Fitting	Replacement	Total
1	0.062	0.008	0.000	0.070
2	0.154	0.062	0.003	0.218
3	0.274	0.140	0.025	0.439

(b) SIS

Insp	Oversize	Fitting	Replacement	Total
1	0.062	0.008	0.000	0.070
2	0.154	0.062	0.003	0.219
3	0.274	0.140	0.025	0.440

Table 6.3: Cost estimates for Example CP7ext; *complex* repair scenario. The likelihood of occurrence of each repair type, as estimated by the Sequential Importance Sampling (SIS) routine, is used to predict the costs due to each type of repair at each scheduled inspection. This represents a significant improvement in cost prediction capability over the typical industry approach to Probabilistic Damage Tolerance Analysis (PDTA).

Insp	Oversize(\$)	Fitting(\$)	Replacement(\$)	Total(\$)
1	62.47	39.16	0.13	101.76
2	154.14	309.33	40.20	503.67
3	274.30	702.01	379.96	1356.27

# CHAPTER 7

## DIAGNOSTIC MODEL UPDATING

The analysis in previous chapters has been prognostic in nature; i.e., the analysis is performed at time zero and no flights have actually occurred. In reality the model will need to be updated according to what actually occurs when the aircraft is used and inspections or repairs are performed. Such analysis is referred to as diagnostic. The Airframe Digital Twin [18], an on-going multi-million dollar joint research effort of NASA and Air Force Research Laboratories, includes as a goal the use of actual aircraft usage and NDE (Non-Destructive Evaluation) results to update the model throughout the service life to improve safety and reliability. In this chapter these capabilities are demonstrated using the HMM (Hidden Markov Model) / SIS (Sequential Importance Sampling) approach. In Section 7.1, the SIS model is updated to reflect that the actual usage of the aircraft will differ from the usage that was expected to occur. Section 7.2 describes how the model is updated according to what happens at the scheduled inspections once they actually occur.

Note that once the model is updated to the present time, a prognostic analysis is conducted to predict the risks and costs for the remainder of the service life. At this point there is an opportunity to modify the maintenance plan accordingly (using the methods of Chapter 9) and perhaps reduce either

the risk or the maintenance costs for the remainder of the service life.

## 7.1 Aircraft Usage

When the analysis is performed at time zero, an expected fleet usage will be assumed to determine an appropriate maintenance strategy. In the field, each aircraft will experience a different level of usage; either more or less severe. It may also include different configurations of the aircraft, such as carrying heavier payloads or more weapons, which will alter the component-by-component loading across the aircraft.

Once the updated usage information is obtained by fleet managers, the risk analysis for each component on each aircraft will be updated to the present time utilizing that actual, realized usage. In this section a single component is considered and it is assumed that an updated deterministic damage tolerance analysis has been performed (as is generally done in practice) which will provide an updated crack growth analysis and possibly an updated maximum stress per flight distribution. Note the normalized stress intensity table will not be altered since this is a function of crack length; a relationship which has not changed. After the analysis has been diagnostically updated to the present time utilizing the actual loading, a prognostic analysis is then conducted to the end of the service life.

The updating for aircraft usage is rather straightforward. The SIS is simply run up to the present time utilizing the actual DTA data. Then, the data for crack growth and max stress per flight are replaced with the expected data going forward, and the SIS analysis proceeds to the end of the service life. The new run may require alteration of the maintenance strategy (e.g., more or less frequent inspections) based on the SFPOF (Single Flight Probability Of Failure) and PCD (Probability of Crack Detection) results obtained.

### 7.1.1 Aircraft Usage Example

Consider Example CP7ext. Suppose the service life under consideration is 4615 flights (6000 FH) and that the original maintenance plan is to not perform any NDE inspections during the life because the SFPOF remains well below the selected threshold of  $1 \times 10^{-7}$  (see Figure 7.2). After 2308 flights (3000 FH) have been flown, usage data is obtained for a fleet of two identical aircraft. One of these aircraft (aircraft B) experienced usage that is significantly more severe than the other (aircraft A), the usage of which turned out to be as expected. The resulting DTA data for location CP7ext for these aircraft are shown in Figure 7.1 (note these are the same set of DTA data shown in Figure 6.1).

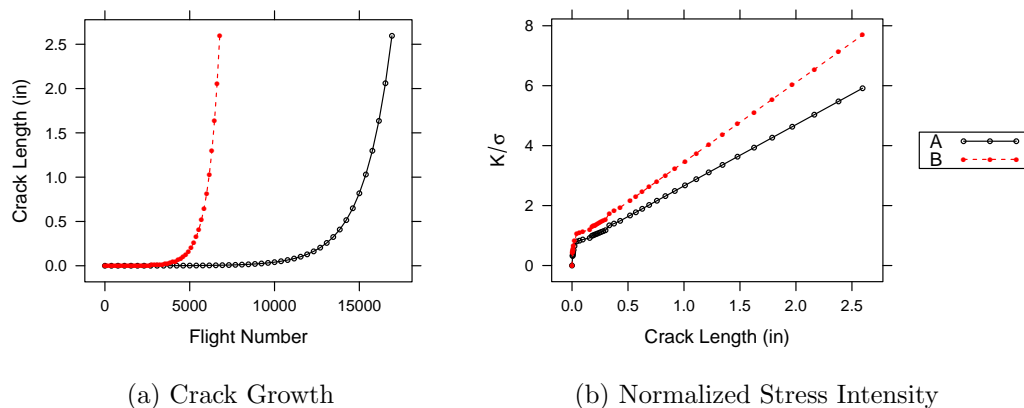


Figure 7.1: Damage Tolerance Analysis (DTA) data for expected-usage aircraft A and severe-usage aircraft B. Note these are the same set of DTA data shown in Figure 6.1.

Assume the usage of aircrafts A and B will revert to the originally expected fleet usage after the present time. In practice, the anticipated future fleet usage would likely be modified to reflect some combination of these usages since overall it appears that the predicted usage is less severe than what may actually be occurring in the field. Also assume that the repair EIFS is the same as the original EIFS for this example. The SFPOF results for aircrafts

A and B are shown in Figure 7.2. For aircraft A, the anticipated usage is low risk and there is no need to perform an inspection at this time. Aircraft B, on the other hand, has experienced significantly increased usage that results in increased SFPOF estimates (even with reversion to the anticipated usage for the remainder of the service life). Note the drop in estimated SFPOF for aircraft B at 2308 flights is a reflection of the reduction in loading that is expected to be seen after this flight. In order for the SFPOF estimates of aircraft B to remain below  $1 \times 10^{-7}$  for the remainder of the service life, an inspection is required at this time.

Because the inspection for aircraft B will occur at the current time, and the results of that inspection will become known, the inspection result could be used to update the SIS model for that aircraft as described in Section 7.2. As time continues to pass and additional actual usage data is obtained, the procedure described here would be performed again. In practice, usage could perhaps be updated on a quarterly basis rather than after 3000 FH (which may represent a decade of flying for a fighter aircraft). The more frequently the model is updated, the better the model will reflect the actual state of the aircraft.

## 7.2 Inspections

Like usage, the inspection results will vary from aircraft to aircraft. These inspection results can be used to inform the model and better predict future failures and repairs. See Cope and Moffett [10] for an example in which inspection results are incorporated in a PDTA analysis using PROF by performing the Bayesian update of the crack size distribution manually outside of the PROF software at each inspection.

The outcomes of the inspections, including part repairs or replacements, should be utilized also. For example, if a part is replaced, the risk analysis for that location should be reset to reflect that a brand new part has been installed. Suppose the first scheduled inspection has been reached. The fol-

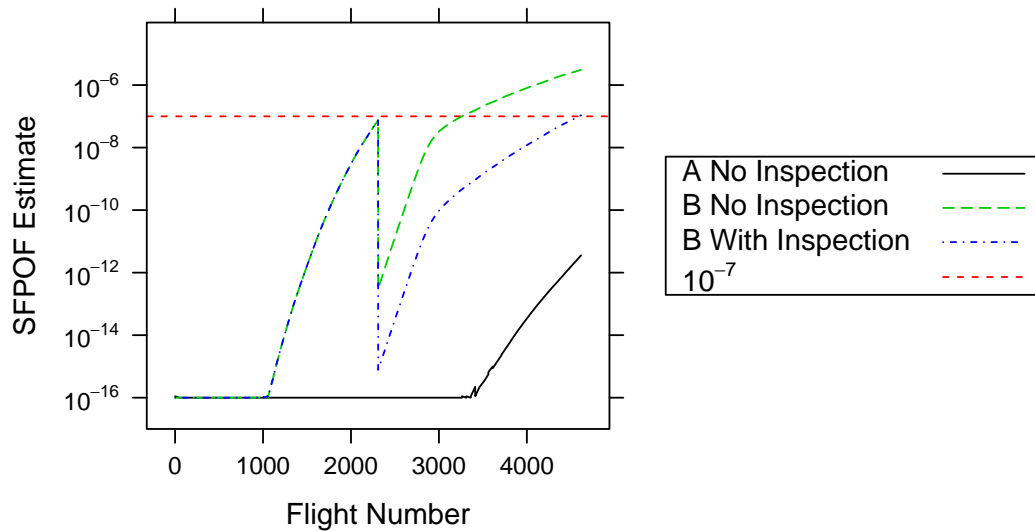


Figure 7.2: Single Flight Probability Of Failure (SFPOF) estimates for expected-usage aircraft A and severe-usage aircraft B, using updated usage. Aircraft A, which experienced the expected fleet usage, has very low risk (identical to the prognostic estimates in this case). Aircraft B, on the other hand, has a significantly increased risk. At 2308 flights, the current time, it has been assumed that the usage going forward will be the expected usage (that of aircraft A). This causes a drop in SFPOF estimates going forward for aircraft B, however, the previous severe usage has likely done some damage. In order to remain below the specified SFPOF threshold of  $1 \times 10^{-7}$  for the next 2308 flights, an inspection is required at this time.

lowing outcomes are possible, each of which implies a different approach to the model update that is required.

1. Uncertain inspection

- It is uncertain whether the scheduled inspection occurred
- Data collection on some aircraft programs is less than perfect, and it may not be known with certainty whether the inspection was in fact performed as intended

2. Uncertain inspection result

- It is known that the inspection was conducted, but whether or not a repair was performed is unknown
- On some programs a small repair may be done in the field and this fact may not be correctly recorded

3. Known repair action

- It is known the inspection occurred, and the result of the inspection was correctly recorded
- This may include a non-finding, a specified type of repair, or a replacement of the part

4. Inspection result obtained

- In this case, the outcome of the inspection is known and the decision as to what repair action to take can be made with the aid of the SIS analysis

Each of the above cases is treated in the following sections.

### **7.2.1 Case 1: Uncertain Inspection**

This case is very similar to the prognostic case and can be solved using traditional PDTA (Probabilistic Damage Tolerance Analysis) software. In the prognostic case, the outcome of the future inspection is not known, so there

is some possibility of a repair and some possibility of no repair, as described by the POD (Probability Of Detection) curve. If an inspection was supposed to have been performed in the past, but it is not certain that it was, the modeling is identical, though the POD curve will include a POI (Probability Of Inspection) parameter. The typical POD curve gives the probability of a crack detection given crack length. If it is uncertain whether the inspection has occurred (or will occur) the curve can be factored down by POI. See the unadjusted and adjusted POD curves in Figure 7.3, where  $POI = 90\%$ .

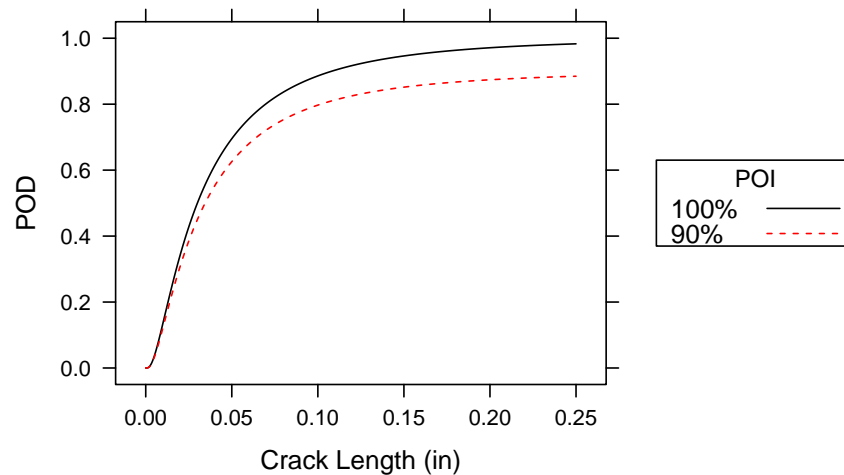


Figure 7.3: Probability Of Detection (POD) curve with and without a Probability of Inspection (POI) parameter. POI causes POD to be factored down uniformly.

### 7.2.2 Case 2: Uncertain Inspection Result

If it is known that the inspection occurred, but whether or not a repair was performed is unknown, then the case is identical to the Uncertain Inspection case with  $POI = 100\%$  (see Figure 7.3). This case can be solved using traditional PDTA software and the SFPOF estimates will behave in a fashion similar to the plots shown previously in this document.

### 7.2.3 Case 3: Known Repair Action

Suppose that it is known that a repair occurred at inspection time. This essentially resets the PDTA analysis for that location since the history prior to that point in time is no longer relevant. The model should be re-initiated using data appropriate to that repair.

If instead it is known that no crack detection occurred, the prognostic approach of the PROF software is lacking. Because an inspection was conducted and no crack was found, this suggests that the larger crack sizes in the support of that distribution are less likely to reflect the actual state of the model. To utilize the PROF-approach to repairs by removing some amount of weight from the crack size distribution and placing that weight onto an EIFS distribution would be incorrect since it is known that no repair occurred.

The correct approach is to perform a Bayesian update of the model given that no crack was found. The HMM/SIS approach can be used to perform such an update. Suppose  $Y$  is an observable variable representing crack detection. Bayes' rule is utilized to update the particle weights and obtain the posterior distribution of the model state (see Equation 4.3).

The situation is shown in Figure 7.4 (units in inches). The crack size distribution  $f(a)$  prior to inspection is Weibull( $k = 1.5, \lambda = 0.03$ ). The POD curve is the CDF of a log-normal distribution with median 0.03 and slope 1. The probability of detection at this inspection is  $PCD = \int_0^\infty \text{POD}(a)f(a)da = 39.77\%$ . The portion of  $f(a)$  missed at inspection is shown in the figure, as well as its normalized counterpart. This normalized  $f(a)$  is the appropriate distribution of crack length to utilize given that no crack was detected at the inspection.

In the SIS routine, the evidence that detection  $Y = \text{FALSE}$  is used to update the model; the likelihood for each particle is  $f(Y = \text{FALSE}|X) = 1 - \text{POD}(a)$ . Each particle's weight is reduced by the probability that a crack of that size would have been missed. This is followed by a normalization of the weights, and the update is complete.

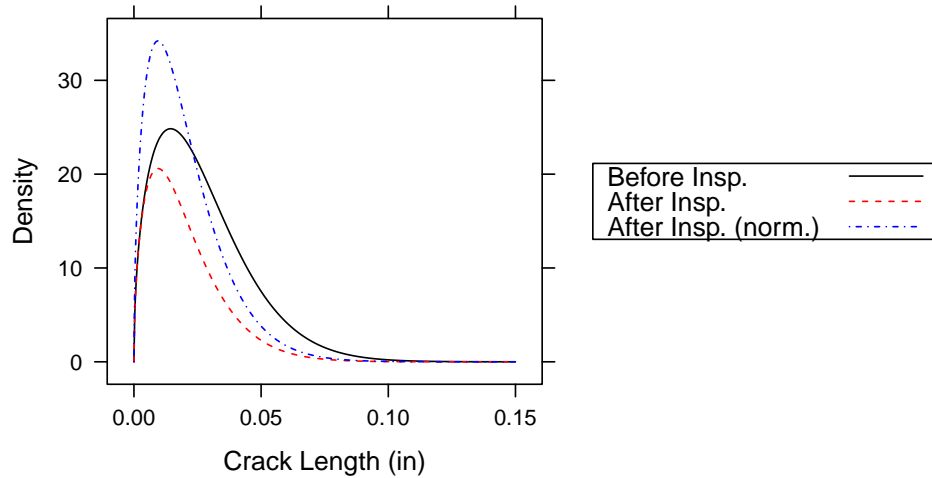


Figure 7.4: Crack size distribution before and after inspection given that there was no detection. This is obtained via an application of Bayes' rule using the Probability Of Detection (POD) curve to obtain the likelihood of a non-detection given crack length, followed by normalization of the distribution.

#### 7.2.4 Case 4: Inspection Result Obtained

The final case to consider demonstrates that it may be very useful to utilize the SIS model to inform fleet maintainers as to what action should be taken, if any, given an inspection result. There are two types of NDE data which can be obtained, as described in the Department of Defense handbook 1823A [38], hit/miss data and  $a$  vs.  $\hat{a}$  data. With hit/miss data, a crack is either found, or it is not. With  $a$  vs.  $\hat{a}$  data, the crack indication  $\hat{a}$  will be correlated with the length of the crack; a larger value of  $\hat{a}$  indicates that it is more likely that a crack is present. Note that false calls are possible with both NDE data types. Regardless of the data type, the approach involves performing a Bayesian update given the indication received from the NDE system.

For hit/miss data, the response is binary and the POD curve can be utilized to perform the Bayesian update since this reflects the probability of a hit or miss given crack length:  $f(Y = y|X = a)$ ,  $Y \in \{\text{hit}, \text{miss}\}$ . That is, for

a binary response the POD curve is itself a representation of the likelihood distribution, which is Bernoulli distributed given crack length. For  $a$  vs.  $\hat{a}$  data,  $\hat{a}$  is a continuous response and the statistical model used to obtain the POD curve provides the likelihood distribution  $f(Y = \hat{a}|X = a)$ . In this section Example 1 from 1823A is described, and the obtained POD curve is utilized along with the Bayesian updating approach to demonstrate how an SIS model can be updated using realized inspection results.

The data set for Example 1 consists of specimens of known crack lengths  $a$  and a corresponding  $\hat{a}$  value from the NDE system for each specimen. Each data point is the result of an inspection performed as part of a physical experiment. In Figure 7.5, the data are plotted with the  $x$ -axis (log-scale) representing the actual crack length  $a$  and the  $y$ -axis representing the dimensionless response  $\hat{a}$  from the NDE system. It is also necessary to characterize the distribution of  $\hat{a}$  which results from inspecting undamaged parts; this is referred to as the noise distribution. The noise is important because it provides the false call rate associated with the POD curve. For Example 1, independent noise data from the testing of pristine structure is not available, thus as is described in 1823A the noise is characterized by assuming that the data points below a specified value of  $a$  (0.0085" in this example) are equivalent to noise. In this case the eight data points below 0.0085" appear to be approximately normally distributed (see 1823A for details). In Figure 7.5, the density of the Gaussian noise distribution is shown in the lower-left corner. The POD curve, shown in the sub-window above the data, is obtained by calculating the probability that a given crack length  $a$  will yield an indication  $\hat{a}$  above a selected *decision threshold*. The decision threshold for this curve (238.108) was selected as that which yields a false call rate of 1% (by finding the 99<sup>th</sup> quantile from the Gaussian noise distribution). Note the detection capability can be increased if the threshold is reduced. This will, however, result in an increase in the false call rate. A regression analysis is performed and the resulting regression line is shown. The standard error from the regression is used to determine the variance of  $\hat{a}$  given  $a$ . At three selected crack sizes, the distribution of  $\hat{a}$

given  $a$  is shown (Gaussian) and the area under each curve *above* the decision threshold is the POD for that value of  $a$  (indicated in the inlaid POD curve plot with a “+”).

The likelihood distribution of  $\hat{a}$  given  $a$  is required for the SIS routine to perform a Bayes’ update of the crack size distribution given an indication  $\hat{a}$  from the NDE system. The regression coefficients obtained using the 1823A software are  $\hat{\beta}_0 = 2757.8$  and  $\hat{\beta}_1 = 540.41$ . The standard error of the residuals is  $\hat{\tau} = 154.24$ . Note that it has been assumed that for a crack length  $a$  below 0.0085”, the noise distribution is appropriate. Thus the likelihood distribution is as follows.

$$f(\hat{a}|a) = \begin{cases} N(\mu = 157.5, \sigma = 34.65), & \text{if } a < 0.0085'' \\ N(\mu = 2757.8 + 540.41 \times \ln(a), \sigma = 154.24), & \text{if } a \geq 0.0085'' \end{cases}$$

The POD curve obtained is a Log-Normal CDF with median 0.009443 and slope 0.28542; this is the POD curve depicted in the sub-window of Figure 7.5.

Consider Example CP7ext (see Section 3.2.2 for details). First, this example is run in the SIS routine to an SFPOF level of  $1 \times 10^{-7}$ , at which time a future inspection is performed using the POD curve obtained above, and the SIS is subsequently run until the SFPOF level again reaches  $1 \times 10^{-7}$ . This procedure will yield the maximum inspection intervals that can be utilized when maintaining SFPOF below  $1 \times 10^{-7}$  as a requirement. Note that other inspection schedules may be superior regarding cost estimates (see Chapter 9). The SFPOF estimates resulting from this prognostic run are shown in Figure 7.7 (along with the diagnostic results described below), utilizing 100k particles and inspections after 6,700 and 10,500 flights, respectively.

Suppose the usage at a particular failure location turns out to be as expected for two aircraft (C and D) – i.e., no update for usage is required – and 6,700 flights have occurred, followed by the first scheduled inspection for that location. The inspection results for aircrafts C and D are  $\hat{a}_C = 400$  and  $\hat{a}_D = 1500$ , respectively. The  $\hat{a}$  value for aircraft C is much lower than that

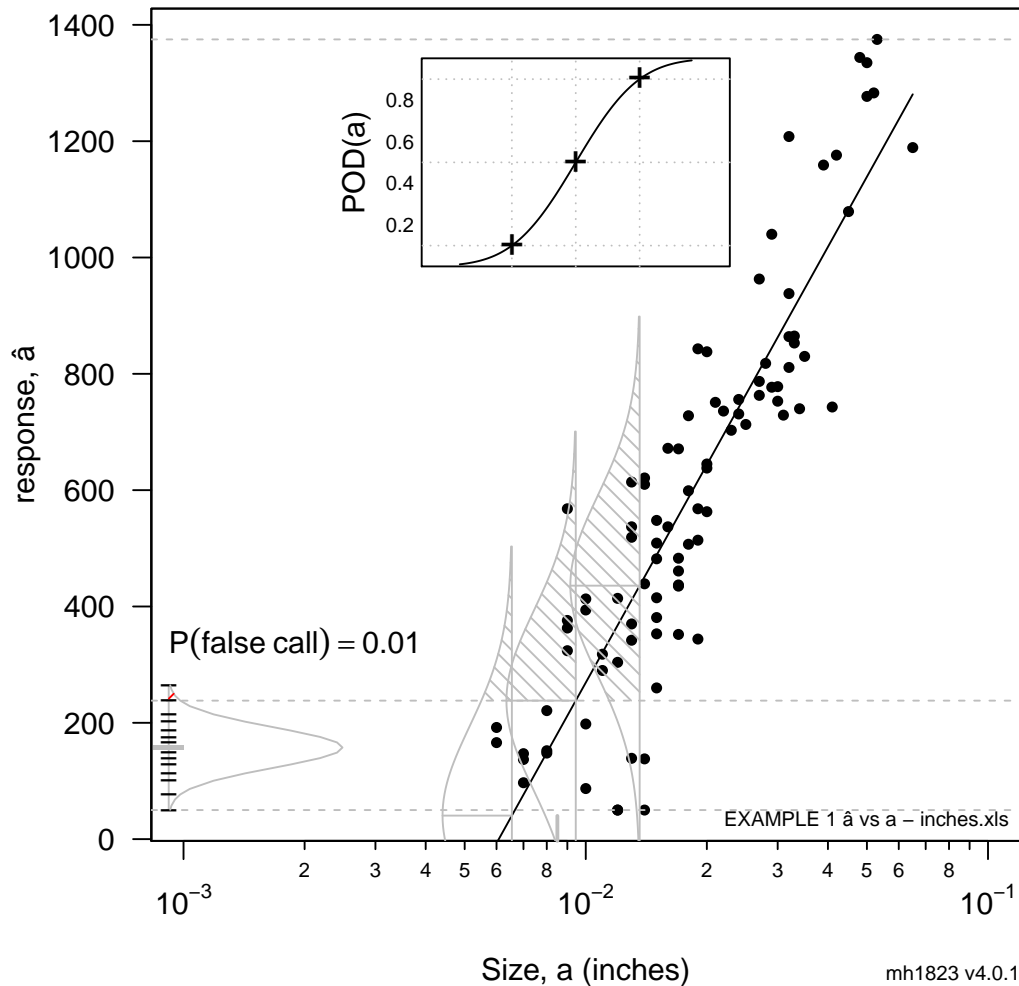


Figure 7.5: 1823A Example 1. The data points represent the  $a$  vs.  $\hat{a}$  data. A regression analysis is conducted to model the relationship between  $a$  and  $\hat{a}$ . The detection threshold at  $\hat{a} = 238$ , along with the regression model, yields the Probability Of Detection (POD) curve, inlaid at the top of the figure. The POD curve is the probability that, according to the model, a crack of a given length will yield an  $\hat{a}$  value above the detection threshold. The probability of a false call (an erroneous detection) is 1%; note the noise density at the bottom left.

of aircraft D, however, given that the decision threshold for this POD curve is 238.108, the traditional approach would suggest that an immediate repair be performed for both aircraft. Instead of utilizing the pre-defined POD curve, the  $\hat{a}$  values will each be used to update the SIS model. In Figure 7.6, the crack size distribution at the first inspection is shown; this was obtained in R using kernel density estimation [56]. Also shown are the updated distributions given the  $\hat{a}$  values. These updated distributions are obtained for each case by multiplying the particle weights prior to inspection by the likelihood of the evidence for each particle, normalizing the weights, and performing a kernel density estimate of the weighted particles.

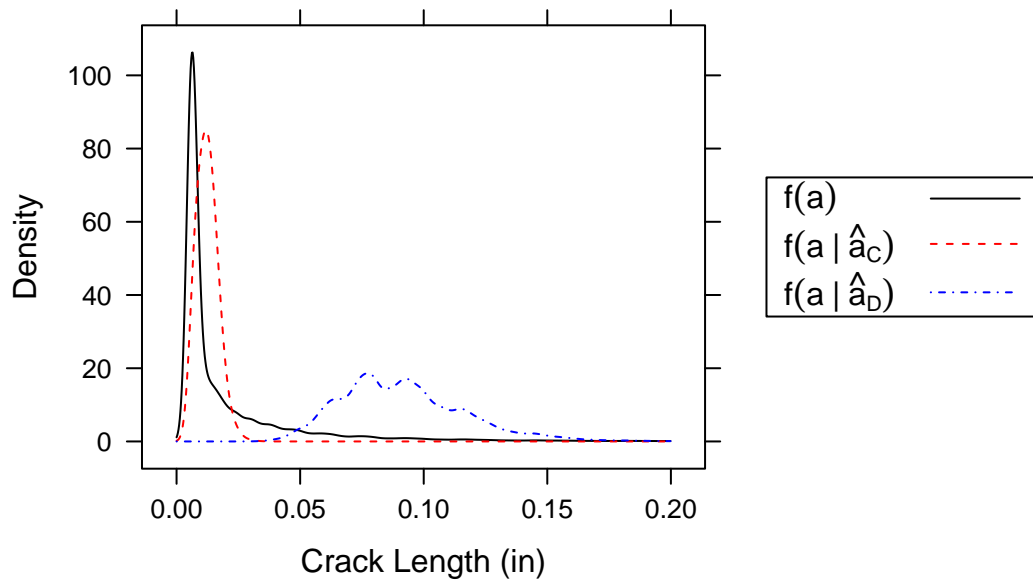


Figure 7.6: 1823A Example 1; crack length distributions at inspection in the Sequential Importance Sampling (SIS) routine.  $f(a)$  is the density prior to obtaining an inspection result. Inspection result C (and subsequent Bayes' updating of the density) yields  $f(a|\hat{a}_C)$ ; likewise for inspection result D. Result D, being a much larger value of  $\hat{a}$ , yields an updated crack length distribution which is far more severe than that of result C.

To determine what maintenance action to take, the SIS routine is run for the second inspection interval for each case. In Figure 7.7, SFPOF estimates are shown for the following cases:

- Prognostic
  - POD curve is used at the first inspection and may or may not result in a repair
- Result C – No Repair
  - Bayes' update at inspection 1 using  $\hat{a}_C$ , with no repair after inspection
  - SFPOF estimates remain below  $1 \times 10^{-7}$ , so no repair is required
- Result D – No Repair
  - Bayes' update at inspection 1 using  $\hat{a}_D$ , with no repair after inspection
  - SFPOF estimates quickly exceed  $1 \times 10^{-7}$ , so a repair is required or the next inspection must be performed sooner than expected
- Result D – Repair
  - Bayes' update at inspection 1 using  $\hat{a}_C$ , with repair immediately after inspection
  - The repair resets the SIS routine using the Repair EIFS distribution (Case 3)
  - Note, the resulting SFPOF estimates are incidentally similar to prognostic case; this is largely due to the fact that the Repair EIFS distribution for CP7ext is relatively severe

This example has shown that unnecessary repairs can potentially be avoided by utilizing the inspection results to update the SIS model, and that in general the SIS routine is capable of efficiently updating the PDTA model given observed evidence. In practice, the model should be updated frequently throughout the service life according to the realized usage of the aircraft and the

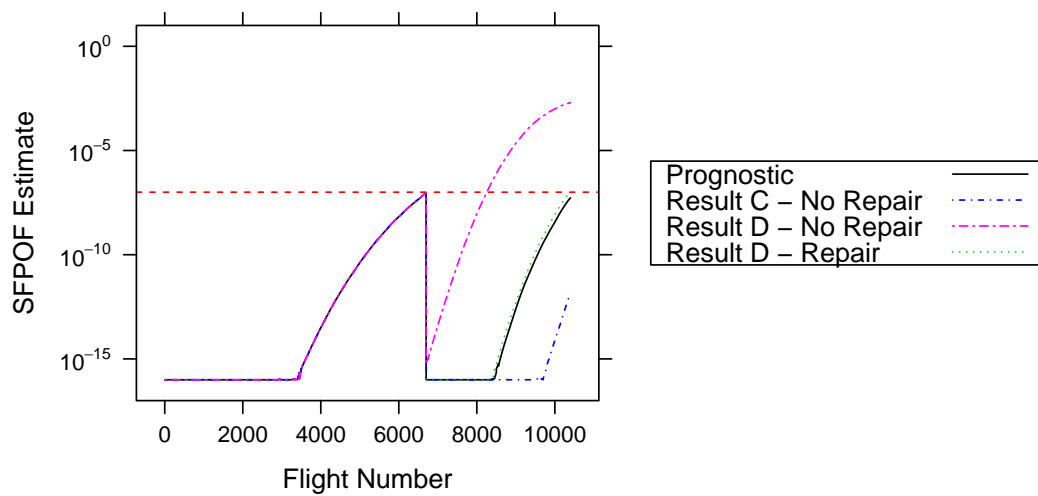


Figure 7.7: 1823A Example 1; diagnostic Single Flight Probability Of Failure (SFPOF) estimates from the Sequential Importance Sampling SIS routine. The Prognostic result uses the traditional approach to modeling a future scheduled inspection. Result C, being a relatively low value of  $\hat{a}$ , suggests that the crack length is likely small and the SFPOF estimates remain low without the need for conducting a repair. Result D, on the other hand, suggests that a relatively large crack exists, therefore a repair is required in order to maintain SFPOF to acceptable levels.

obtained inspection results, followed by a re-assessment of the maintenance strategy for each aircraft.

In this section, the decision as to what repair action to take has been made solely according to an SFPOF requirement. From a maintenance cost perspective, the methods of Chapter 9 should be used after updating the model to obtain a maintenance strategy that also minimizes unnecessary costs.

## CHAPTER 8

# CONTINUING DAMAGE

Typically, for damage-tolerant aerospace structures which are susceptible to fatigue cracking, analysis must show that the crack will grow slowly enough that it will not grow to critical size before a scheduled inspection occurs. Some damage-tolerant structures will not fail when a single crack grows to critical size, but rather will fail only when a second crack forms nearby and grows to critical size. This situation is referred to as continuing damage. The United States Air Force damage tolerance design guidelines provided in the Joint Service Specification Guide JSSG-2006 [28] defines the continuing damage problem and provides requirements for performing a traditional DTA (Damage Tolerance Analysis) for such structures. The majority of continuing damage locations involve a single fastener hole in which cracks may form on either side of the hole. This is the typical situation, though it is possible that two fastener holes in close proximity could be similarly analyzed with a continuing damage approach. Also note that in extreme cases three, four or more cracks could be considered. The focus in this chapter is on the typical continuing damage problem with two cracks growing from either side of a fastener hole.

The more severely loaded location, where cracking is more likely to occur, is referred to as the *primary* location, and the less severe is the *secondary* location. The deterministic method prescribed in JSSG-2006 for this situation

is described at a high level below:

- Assume an initial crack length of 0.050" at the primary location
- Assume an initial crack length of 0.005" at the secondary location
- Analytically grow the primary crack until it reaches critical length at time  $t_{\text{primary}}$  assuming no crack is present at the secondary location
- Grow the secondary crack for time  $t_{\text{primary}}$  assuming no crack is present at the primary location
- Continue growing the secondary crack from time  $t_{\text{primary}}$  to failure at time  $t_{\text{total}}$ , assuming the primary location has failed
- The total time to failure  $t_{\text{total}}$  is the fatigue life used to schedule structural inspections

The secondary crack is analytically grown under two different conditions: primary location intact, and primary location critical. If the primary has gone critical, the secondary will be more heavily loaded since the primary location no longer provides stiffness to the part; this is referred to as the **hot** state for the secondary crack. When the primary is intact, the secondary is **cold**. Such traditional analysis therefore requires three deterministic damage tolerance analyses: **primary**, **secondary cold**, and **secondary hot**. The continuing damage problem is depicted graphically in Figure 8.1 below.

In PDTA (Probabilistic Damage Tolerance Analysis), the initial crack length is not an assumed constant, but rather is described by an EIFS (Equivalent Initial Flaw Size) distribution. If the initial crack at the secondary location is unusually large, the secondary location can fail prior to the primary location. Hence a fourth deterministic damage tolerance analysis is required for PDTA: **primary hot**. Continuing damage in PDTA is an open problem. The approaches to continuing damage using MC (Monte Carlo) and HMM (Hidden Markov Model) / SIS (Sequential Importance Sampling) described in this chapter are original contributions of this work. The MC routine is discussed in Section 8.1, and the HMM/SIS routine is presented in Section 8.2. An example problem is presented in Section 8.3.

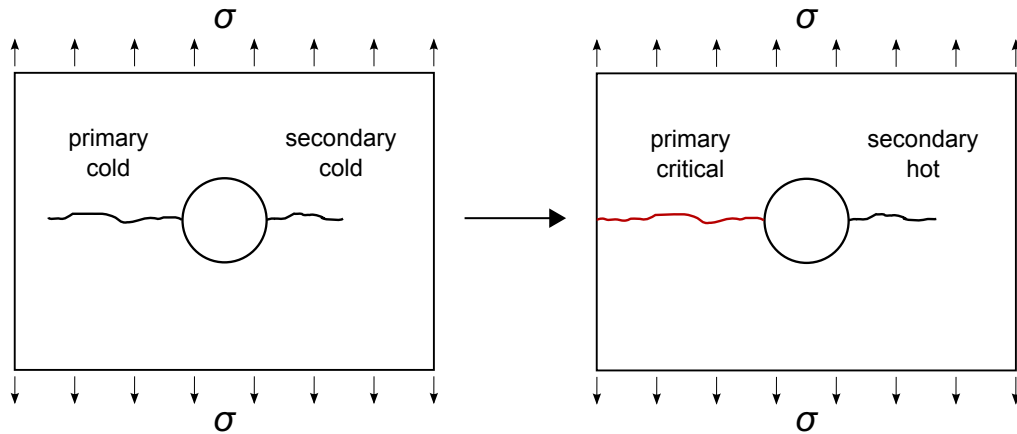


Figure 8.1: Diagram of the typical continuing damage case where two cracks emanate from a single fastener hole.

## 8.1 Continuing Damage Using Explicit MC

An explicit MC approach to solving the single-crack PDTA problem was described in Chapter 3. A flow chart for that routine is shown in Figure 3.8. That routine was used to benchmark the SFPOF (Single Flight Probability Of Failure) and PCD (Probability of Crack Detection) results against which to compare the results of the SIS routine. A similar routine is described in this section for solving the typical continuing damage PDTA problem.

Some notable details regarding the continuing damage MC routine are as follows:

- the length and growth of two cracks must be modeled,
- because the two cracks are located at the same fastener hole, the fracture toughness is assumed to be the same for both cracks,
- again due to co-location, the maximum applied stress per flight is identical for both cracks,
- each crack is in the cold state until the other crack reaches a specified length, at which time it becomes hot,
- detection of either crack at inspection is assumed to be independent,

- if either crack is found, *both* cracks are repaired.

In the example in Section 8.3 the transition from **cold-to-hot** occurs at the critical crack length. Thus a the second crack does not become **hot** until the first crack reaches what would be a failure condition in a single-crack model. Note this stepwise increase in severity is a simplification. In reality, there will be a smooth transition between the **cold** and **hot** states. This is discussed further in Section 8.2.2.

Note the MC routine as written includes only one *type* (in the context of the improved repair modeling of Chapter 6). It could be expanded to utilize multiple repair types. The example later in this chapter utilizes repair back to the as-manufactured condition.

### 8.1.1 Inspection Modeling in Continuing Damage MC

The POD (Probability Of Detection) curve provides the probability that a single crack will be found given its length. In continuing damage there are two cracks at locations which are each inspected. As stated above, if either crack is found a repair will be performed on *both* cracks; thus the probability of finding either crack determines whether a repair is performed. Assuming the inspections for the two cracks are independent, the probability of finding either crack is as follows.

$$\text{POD}(a_p \cup a_s) = \text{POD}(a_p) + \text{POD}(a_s) - \text{POD}(a_p) \times \text{POD}(a_s) \quad (8.1)$$

The methodology for determining if a repair occurs in the continuing damage MC routine is identical to that of the single-crack MC routine, utilizing  $\text{POD}(a_p \cup a_s)$  instead of  $\text{POD}(a)$ .

For the less typical case where the primary and secondary cracks are at separate fastener holes, the type of repair may determine whether one or both cracks may be repaired. For example, use of an oversize fastener would treat a single hole, but the attachment of a repair fitting may involve the entire nearby area. This more complex case is not considered in this work.

### 8.1.2 Importance Sampling in Continuing Damage MC

As in the explicit MC approach for a single crack, importance sampling may be used to initialize a trial. This leads to vastly improved convergence, but as a consequence scheduled inspections cannot be modeled. Results for the example problem in Section 8.3 utilize this importance sampling modification prior to the first inspection. Details regarding how the initial importance weights are determined in the two-crack model are given in Section 8.2.1.

## 8.2 Continuing Damage Using HMM/SIS

The HMM description of the continuing damage problem is identical to that of the typical PDTA analysis, where the hidden state includes two cracks rather than a single crack. Recall, in the prognostic SIS routine, the approach involves generating the initial state, growing the cracks over time while updating the importance weights (either at each flight or in intervals of flights), and performing structural inspections at the scheduled times. Each of these components of the SIS model is discussed in this section.

### 8.2.1 Generating the Initial State in Continuing Damage SIS

The quantities of interest are the initial crack size for the primary and secondary locations, fracture toughness, importance weights, and possibly repair type (if more than one type of repair is possible, as in Chapter 6). As in the standard SIS routine, the type at time zero is *as-manufactured* for every particle, thus the type is not a consideration when setting the initial state.

The initial crack sizes  $a_{p,0}$  and  $a_{s,0}$  at the primary and secondary locations may or may not be correlated. Regarding the modeling the distinction is not important since all that is required is the joint distribution of the initial crack sizes,  $f_{A_{p,0},A_{s,0}}(a_{p,0}, a_{s,0})$ . In the example problem of Section 8.3, they

are assumed to be independent.

Fracture toughness is assumed to be common to the primary and secondary locations because they are co-located on the same component. In addition, as in the standard SIS approach, fracture toughness is assumed to be independent of the initial crack length. The pdf of fracture toughness is  $f_{K_c}(k_c)$ .

The initial importance weights are set in a fashion similar to the standard SIS routine. Because importance sampling is used to set the initial state, the joint sampling distribution for  $a_p$ ,  $a_s$ , and  $K_c$  –  $g_{A_{p,0},A_{s,0},K_c}(a_{p,0}, a_{s,0}, k_c)$  – is required, along with the actual joint distribution  $f_{A_{p,0},A_{s,0},K_c}(a_{p,0}, a_{s,0}, k_c)$ . With  $a_p$ ,  $a_s$ , and  $K_c$  independent, and with direct sampling used to generate  $K_c$ , the sampling distribution is  $g_{A_{p,0}}(a_{p,0}) \times g_{A_{s,0}}(a_{s,0}) \times f_{K_c}(k_c)$  and the actual distribution is  $f_{A_{p,0}}(a_{p,0}) \times f_{A_{s,0}}(a_{s,0}) \times f_{K_c}(k_c)$ .

## 8.2.2 Flight-by-Flight Updating in Continuing Damage SIS

At any time the primary location is either *hot* or *cold*, depending on whether the secondary location is or is not critical; and vice versa. Failure occurs only when *both* cracks fail. Recall, the definition of SFPOF requires that a failure has not occurred in a previous flight.

A mechanism for determining when a crack is critical is required so that the correct failure calculation is used. A simple approach involves considering a crack to have gone critical when it has grown to a specified size, at which time the focus shifts to the other, now *hot* crack. This is a simplification. In reality, as one crack lengthens the stiffness on that side of the hole is decreased and the other side will experience increased loading. It is more realistic to model the stress intensities of each crack as a function of the length of both cracks, though such an approach is not trivial. For an example of a deterministic approach to continuing damage that accounts for interactions between the two crack lengths, see Bombardier, Liao, and Renaud [7].

Recall, in the single-crack MC and SIS models, the critical crack length  $a_c$  is

a crack length at which failure is assumed to occur with certainty. Suppose in the continuing damage context there are four critical crack lengths of interest.

- $a_{c,pc}$ 
  - length at which a **primary cold** crack goes critical, causing the secondary crack to become hot
- $a_{c,sc}$ 
  - length at which a **secondary cold** crack goes critical, causing the primary crack to become hot
- $a_{c,ph}$ 
  - length at which a **primary hot** crack will cause part failure (secondary crack has already gone critical)
- $a_{c,sh}$ 
  - length at which a **secondary hot** crack will cause part failure (primary crack has already gone critical)

For any given flight, the component will fail if one of the following occurs.

- the applied stress  $\sigma_{\max}$  is large enough to cause failure of the less severe crack
  - that is, failure occurs if  $\min(K_{\max,p}, K_{\max,s}) > K_c$ , where  $K_{\max,p}$  and  $K_{\max,s}$  are the maximum stress intensities of the primary and secondary cracks, respectively, utilizing the correct set of DTA data given the hot/cold status
- a **primary hot** crack reaches length  $a_{c,ph}$
- a **secondary hot** crack reaches length  $a_{c,sh}$

Note that if both  $a_p$  and  $a_s$  have reached critical length in a previous flight, the particle has zero weight (since it cannot have survived to the current time) and cannot affect SFPOF or PCD estimates.

Given the above failure conditions, the probability of failure for each particle is calculated as in the single-crack SIS model. Subsequently SFPOF is estimated and importance weights are updated in a manner identical to that of the standard SIS routine.

### 8.2.3 Interval Weight Updating in Continuing Damage SIS

Like the standard SIS routine, the continuing damage routine can utilize a flight-by-flight approach or an approximate interval approach which proceeds a number of flights at-a-time. Note the interval approach for a continuing damage run involves an additional simplification that the hot or cold status of a crack is set before the interval occurs, otherwise the approach is identical to that of the standard SIS interval routine. By advancing a number of flights at a time, the runtime can be drastically reduced. Also, the convergence speed of the single-crack SIS interval routine has been shown to be faster for problems in which the critical crack failure mode has a strong influence. These characteristics hold when the interval approach is used to model the simultaneous growth of two cracks. Results utilizing both the flight-by-flight and interval routines are given in Section 8.3.

### 8.2.4 Inspection Modeling in Continuing Damage SIS

As in the explicit MC routine for continuing damage at a single hole, both cracks are repaired if either crack is found. Thus the relevant probability of detection for a particle is  $\text{POD}(a_p \cup a_s)$  (see Section 8.1.1). Otherwise, the SIS model regarding inspections is unchanged.

### 8.3 Continuing Damage Example Problem

The previously shown example problems are not of the continuing damage variety. The general approach to continuing damage addressed in this chapter can, however, be demonstrated by modifying a standard example. Consider Example CP7 from the PROF manual. Suppose this example involves a second crack at the same location. This second crack has the same characteristics regarding fracture toughness, probability of detection, and initial flaw size.

The crack growth and  $K/\sigma$  data from Example CP7 have been factored to varying degrees of severity as shown in Figure 8.2. Specifically, the flights of the **primary hot** case are reduced by 20% to increase crack growth speed, and the corresponding  $K/\sigma$  values are increased by 20%. Similarly, **secondary cold** is 5% less severe than **primary cold**, and **secondary hot** is 15% more severe than **secondary cold**. Recall, the transition from cold-to-hot occurs for the secondary crack if the primary crack reaches a critical length (or vice versa). For this example the critical crack length for CP7 is used for transition from cold-to-hot as well as for failure of both cracks. That is,  $a_{c,pc} = a_{c,sc} = a_{c,ph} = a_{c,sh} = 0.518''$ .

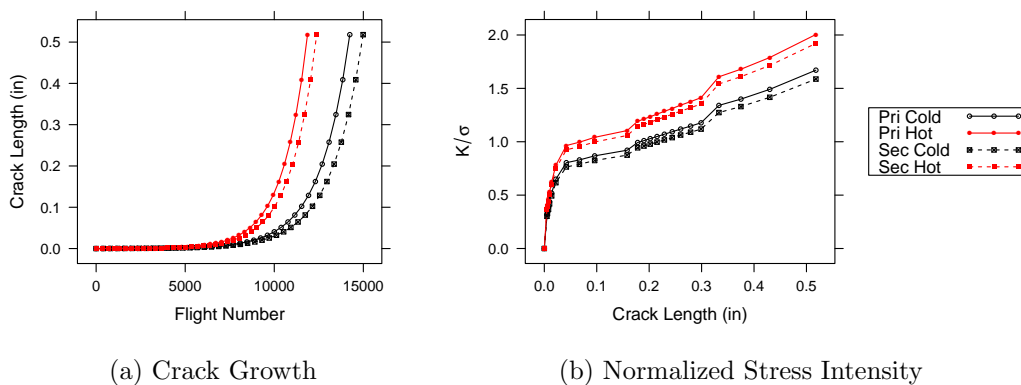


Figure 8.2: Continuing Damage; modified Example CP7 Damage Tolerance Analysis (DTA) data. The hot data are more severe than the cold data.

The inspection times for the single-crack version of Example CP7 lead to

very low SFPOF estimates when considering a second crack. The inspections are rescheduled for this example so that agreement between the MC and SIS approaches can be demonstrated. The inspection times for this example are at 8,000 and 11,000 flights, respectively. Figure 8.3 shows the results when running the flight-by-flight and interval routines in five independent sequences using 200k particles in each sequence. The mean lines are depicted as well.

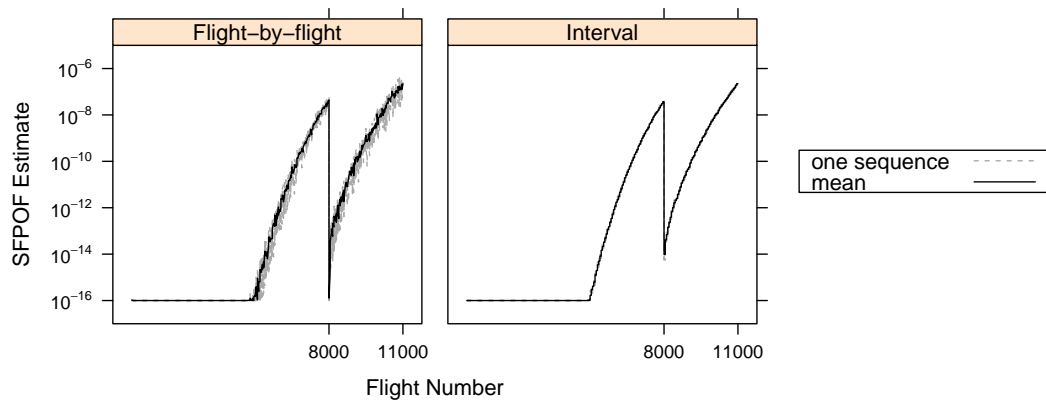


Figure 8.3: Continuing Damage Example CP7 results using the flight-by-flight and interval SIS routines. The estimates of five independent sequences of 200k particles are shown along with the mean estimates. Convergence of the interval routine is excellent.

Figure 8.4 compares the SFPOF estimates from the interval SIS routine to those of the MC routine (using importance sampling prior to the first inspection). Agreement between the SIS routine and the MC is excellent. Also depicted are the SFPOF estimates obtained from running the single crack model on Example CP7 with these inspection times. Note that the single-crack model exhibits much higher SFPOF estimates due to the fact that there is no second crack providing additional life.

PCD estimates from each sequence of the flight-by-flight SIS, interval SIS, and MC routines are shown in Table 8.1. The SIS routines were each run with 5 parallel sequences of 200k particles. The MC analysis was run in five

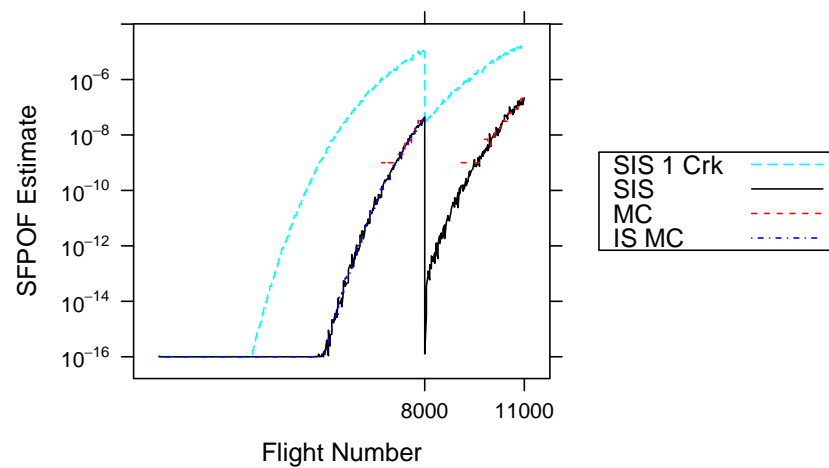


Figure 8.4: Continuing Damage Example CP7 Single Flight Probability of Failure (SFPOF) estimates using the interval Sequential Importance Sampling (SIS) routine and the explicit Monte Carlo (MC) routine. The SIS routine used 1m particles. The MC routine used 10m trials. The “IS MC” results are those of the importance sampling routine run up to the first inspection (using 100k trials). Also depicted are the SIS results for the single-crack version of CP7 using 100k particles. Agreement between the SIS routine and the MC is excellent. Note that the single-crack model exhibits much higher SFPOF estimates due to the fact that there is no second crack providing additional life.

batches with 2m trials in each run. Variability between sequences is low thus convergence is judged to be acceptable. The SIS routines yield PCD estimates similar to those of the MC routine, though the interval routine yields a slight underestimate for the second inspection.

Table 8.1: Continuing Damage Example CP7 PCD estimates from five sequences using flight-by-flight Sequential Importance Sampling (SIS), interval SIS, and explicit Monte Carlo (MC) routines. Each sequence of the SIS routine used 200k particles. Each run of the MC routine used 2m particles. Variability between sequences is low thus convergence is judged to be acceptable. The SIS routines yield PCD estimates similar to those of the MC routine, though the interval routine yields a slight underestimate for the second inspection.

(a) First Inspection				(b) Second Inspection			
Seq	Int SIS	FBF SIS	MC	Seq	Int SIS	FBF SIS	MC
1	0.6404	0.6417	0.6415	1	0.8121	0.8176	0.8102
2	0.6413	0.6413	0.6412	2	0.8029	0.8046	0.8101
3	0.6405	0.6431	0.6409	3	0.8005	0.8060	0.8103
4	0.6433	0.6408	0.6412	4	0.8082	0.8102	0.8101
5	0.6418	0.6413	0.6408	5	0.8077	0.8060	0.8099
Mean	0.6415	0.6416	0.6411	Mean	0.8063	0.8089	0.8101

# CHAPTER 9

## MAINTENANCE COST MODELING

As previously shown SFPOF (Single Flight Probability Of Failure) estimates tend to increase from flight-to-flight until a scheduled inspection is reached. When the maintainers of an aircraft fleet are determining the inspection schedule to use for a structural location they should consider both the SFPOF estimates resulting from that schedule and the cost of implementing that maintenance strategy. The safest strategy would be to perform a thorough inspection after every flight, though this is clearly not possible. It is generally the case with structures that there is a trade-off between failure probability and economics. The goal is often to maintain SFPOF below some specified threshold and minimize unnecessary maintenance costs. Maintenance costs can be attributed to the following four sources [24]: inspections, repairs, false calls, and failures. Each of these cost sources is discussed in Section 9.1. The complex repair example from Chapter 6 is continued in Section 9.2 to demonstrate the approach. Finally, some extensions to the problem as defined in this chapter are given in Section 9.3

## 9.1 Cost Modeling

The PDTA (Probabilistic Damage Tolerance Analysis) problem is primarily concerned with the estimation of SFPOF for the future flights in the service life, and PCD (Probability of Crack Detection) for the future scheduled inspections. Inspecting more often, or utilizing a different inspection sensitivity, will have a significant impact on SFPOF and PCD estimates; see Section 7.2 for details regarding the detection capability of an NDE system. For a given structural feature there are many maintenance strategies which are capable of maintaining SFPOF below the specified threshold, thus some other measure should be identified by which to compare various acceptable strategies. Typically this criterion will be either maintenance costs, labor hours, or aircraft downtime, each of which should be minimized. These criteria are closely related and for some cases the selection may not alter the recommended strategy. In this chapter we consider maintenance costs as the sole criteria. In some special cases it may be beneficial to consider multiple criteria, though that is not considered here.

There may some restriction on when NDE inspections can be performed; the location of interest may be impossible to access in the field and thus can only be inspected at infrequent intervals when the aircraft is at the maintenance depot (perhaps once every several years). It may also be the case that the fleet owners have decreed (possibly for reasons of available labor or to minimize downtime) that some minimum number of flights must occur between structural inspections for each aircraft.

The maintenance costs problem considered in this work is described in the following. Note these guidelines are discussed further in Section 9.3 where possible extensions and generalizations are described.

- One structural location is considered (e.g., a single fastener hole)
- SFPOF estimates for this location must remain below a specified threshold throughout the service life

- Maintenance costs are to be minimized; for simplicity this is done without discounting to today dollars
- Sources of costs are inspections, repairs, false calls, and failures
- The costs of each type of maintenance event are assumed constant
- The maintenance strategy is assumed to remain fixed for the remainder of the service life; i.e., the strategy won't be modified during the service life because of altered usage or inspection results (see Chapter 7)

In this chapter individual costs (dollars) are represented by  $c$ , and the probability of occurrence of those costs by  $p$ . Total costs will use upper case  $C$ . The expected costs due to the events: inspections ( $I$ ), repairs ( $R$ ), false calls ( $L$ ), and failures ( $F$ ), are independently estimated and summed. Thus the total maintenance cost estimate is

$$\mathbb{E}(C) = \mathbb{E}(C_I) + \mathbb{E}(C_R) + \mathbb{E}(C_L) + \mathbb{E}(C_F).$$

The calculation of expected costs for each type of maintenance event is detailed in the following sections.

### 9.1.1 Inspection Costs

The cost for a single inspection is relatively simple to quantify. The typical fleet maintenance guide for a particular aircraft will indicate the labor hours required to perform the inspection. Thus the cost of an individual inspection is the labor hours multiplied by the labor rate (ignoring incidental costs such as expended materials, which could also be included). For inspection number  $j$ , the cost is  $c_I^{(j)}$ , which is assumed to be constant. As is discussed in Section 7.2, the probability of a scheduled inspection actually occurring may be less than 1; referred to in that section as POI (Probability Of Inspection). Here, the probability of an inspection  $j$  occurring is represented by  $p_I^{(j)}$ . If for a given maintenance strategy  $m$  inspections are scheduled in the service life, then the expected total inspection cost is

$$\mathbb{E}(C_I) = \sum_{j=1}^m c_I^{(j)} p_I^{(j)}.$$

In the specification of the maintenance cost problem given in this section,  $p_I$  and  $c_I$  are assumed to be the same for each inspection in the service life; in that case  $\mathbb{E}(C_I) = m \times c_I \times p_I$ .

### 9.1.2 Repair Costs

An example of the estimation of repair costs resulting from future scheduled inspections was given in Section 6.3. In that example, multiple types of repairs were possible (including part replacement for extensive damage). The cost of performing each possible type of repair must be determined, generally including material and labor costs. The probability of occurrence of each repair cost is given by the appropriate estimate of PCD from the PDTA analysis. In Section 9.3, additional possible cost sources are discussed, such as transporting the aircraft to a maintenance depot.

For the sake of generality, the cost of performing the various repairs may vary between scheduled inspections (which may be true if, for example, an inspection will occur in the field as opposed to the maintenance depot). The cost of performing repair type  $k$  at inspection  $j$  is  $c_{R,k}^{(j)}$ , and the corresponding PCD estimate is  $p_{R,k}^{(j)}$ ; thus the expected type  $k$  repair cost at inspection  $j$  is  $c_{R,k}^{(j)} \times p_{R,k}^{(j)}$ . If for a given maintenance strategy there are  $m$  inspections and  $q$  repair types, the expected total cost due to repairs is

$$\mathbb{E}(C_R) = \sum_{j=1}^m \sum_{k=1}^q c_{R,k}^{(j)} \times p_{R,k}^{(j)}.$$

In the example problem given in Section 9.2, the cost of each type of repair is assumed constant.

### 9.1.3 False Call Costs

If a POD (Probability Of Detection) curve is developed according to the Department of Defense handbook 1823A, there will be a false call rate associated with each inspection. A false call is defined as an indication from inspection that a crack is present, when in fact there is no crack. In practice the false call rate is often assumed to be zero, which is not overly relevant from a safety perspective. However, from a maintenance perspective, the false call rate can impact the overall maintenance costs or labor hours for a fleet of aircraft as each false call will involve several hours or more of unnecessary investigation or repair. Under the guidelines given earlier in this section, the maintenance strategy is assumed to be fixed. A POD curve is specified for each future scheduled inspection and the false call rate is a characteristic of that POD curve.

The cost of the occurrence of a false call is not obvious. A legitimate crack finding may involve a crack that is 0.003" in length; a size that is not visible by the human eye. If a false call is indicated by the NDE system, the maintainers will be unaware that there is no crack present. In this case, the most likely outcome is that a minor repair is performed, such as a spot weld or the installation of an oversize fastener. This suggests that the cost of a false call can be reasonably modeled as cost of performing a minor repair. Note that when a minor repair is performed on an undamaged part, the state of that part has been altered. If it is believed that false calls are possible for an inspection approach (which is almost certainly the case in general), and the POD curve being utilized intersects the origin (as specified by 1823A), there is a disconnect between the PDTA model and the cost model. If false calls are possible, there should be some probability that at any scheduled inspection a minor repair is performed which alters the model state accordingly. This can be accomplished by utilizing a POD curve which does not intersect the origin, but rather has a minimum value at the false call probability, as suggested by Straub [53]. 1823A states that such POD curves are not compatible with the

provided software for developing POD curves.

For inspection number  $j$ , the cost of a false call is  $c_L^{(j)}$ . The false call rate for inspection  $j$  (a characteristic of the POD curve) is  $p_L^{(j)}$ . If there are  $m$  scheduled inspections the expected total false call cost is

$$\mathbb{E}(C_L) = \sum_{j=1}^m c_L^{(j)} p_L^{(j)}.$$

#### 9.1.4 Failure Costs

Failures may occur at a structural location during any flight in the service life. The cost of failure for an individual part will largely depend on whether that part is designated as “safety-of-flight”, i.e., if loss of that part will lead to loss of the aircraft either through catastrophic failure or retirement due to excessive damage. If so, the failure cost should be either the purchase or replacement cost of that aircraft. If the part is not “safety-of-flight”, the failure will lead to replacement of the part, similar to a repair cost. It is assumed that the cost of a failure is constant<sup>1</sup>. Failure cost is given by  $c_F$ .

The probability of failure for flight  $i$  is  $p_F^{(i)}$ , given by the SFPOF estimate for flight  $i$ . If a service life consists of  $n$  flights, the expected total failure cost is

$$\mathbb{E}(C_F) = \sum_{i=1}^n c_F \times p_F^{(i)} = c_F \sum_{i=1}^n p_F^{(i)}.$$

Note the above equation assumes that an SFPOF estimate is available for every flight. In many cases a PDTA software package will provide SFPOF estimates at selected flights, rather than at every flight. This is done either to reduce the size of the output (as is done in the flight-by-flight SIS (Sequential Importance Sampling) routine described in this work) or because the analysis methodology involves advancing through the service life in flight intervals

---

<sup>1</sup>It may be possible for failure costs to depend on the flight number if, for example, it is known that the aircraft will be temporarily located and flown at a training base which is also the location of a maintenance depot for that aircraft. This possibility is omitted.

rather than flight-by-flight (as is done in PROF and the fast/interval version of the SIS routine). In this case interpolation is required to obtain SFPOF estimates at each flight.

## 9.2 NDE Cost Minimization Example

In this section the cost modeling for PDTA is demonstrated for CP7ext where the POD curve is fixed and the inspection times are variable. The complex repair example of Chapter 6 is used, which allows for various types of repairs to occur. The goal is to set the inspection times such that SFPOF is held below  $1 \times 10^{-7}$  and total maintenance costs are minimized. This is done assuming a reasonable false call rate of 1%.

The PROF manual does not provide cost parameters. The various maintenance costs for CP7ext were arbitrarily specified in Section 6.3. The NDE inspection cost is \$500, the false call cost is \$1000, and the failure cost is \$1m. The repair types and associated costs are repeated below for convenience.

1. As-manufactured class,  $c = 1$ 
  - Parameters are those of Example CP7ext
2. Oversize fastener,  $c = 2$  ( $a < 0.05$ " )
  - Crack growth rate is increased by 20%
  - $K/\sigma$  and EIFS distribution are identical to Type 1
  - Cost of repair = \$1,000
3. Repair fitting,  $c = 3$  ( $0.05$ "  $\leq a < 0.25$ " )
  - Crack growth rate is decreased by 50%
  - $K/\sigma$  increased by 50%
  - EIFS distribution is more severe: Exponential(rate=138.1559<sup>2</sup>)
  - Cost of repair = \$5,000

---

<sup>2</sup>This EIFS is the repair EIFS indicated for Example CP7 in the PROF manual, which is equivalent to a Weibull distribution with shape=1 and scale=0.0072382.

4. Part replacement,  $c = 1$  ( $a \geq 0.25$ )

- Identical to Type 1
- Cost of replacement = \$15,000

Typically NDE inspections are scheduled with a first inspection interval and a subsequent interval (possibly different from the first) that is repeated; these intervals are referred to as DI and  $\Delta$ DI, respectively. Often these are given in flight hours, but due to the flight-by-flight nature of the SIS routine, DI and  $\Delta$ DI are in units of number of flights in this section. For example, the problems from the PROF manual have inspections scheduled at 6000, 9000, and 12000 flight hours, corresponding to DI = 6000 hours and  $\Delta$ DI = 3000 hours. The typical flight for these is 1.3 hours, thus the examples shown in earlier chapters have DI = 4615 flights and  $\Delta$ DI = 2308 flights.

To begin the analysis, the flight-by-flight SIS routine is run using 100k particles through the complete service life without inspections to determine when the first inspection needs to occur. The resulting SFPOF estimates are shown in Figure 9.1.

The SFPOF threshold of  $1 \times 10^{-7}$  is breached near flight 6500, thus the first inspection needs to occur before this number of flights have occurred. To assess what DI and  $\Delta$ DI values will be competitive from a cost perspective, DI values of 2000, 4000, and 6000 flights are arbitrarily considered, along with  $\Delta$ DI values of 1000, 2000, and 3000 flights. There are nine permutations of DI and  $\Delta$ DI in this case. See Table 9.1 for the results of runs of the interval SIS routine using 500k particles and 50 flight intervals. Costs in the table are calculated using the methods described earlier in this chapter.

The run which minimizes costs while maintaining SFPOF below  $1 \times 10^{-7}$  uses DI = 6000 and  $\Delta$ DI = 2000. A second permutation is run around these values with DIs of 5500, 6000, and 6500, and  $\Delta$ DIs of 1500, 2000, and 2500. The best strategy from this run has DI = 5500 and  $\Delta$ DI = 2000. Finally, a third permutation is run with DI values of 5250, 5500, and 5750, and with  $\Delta$ DI values of 1750, 2000, and 2250. The total costs and peak SFPOF values

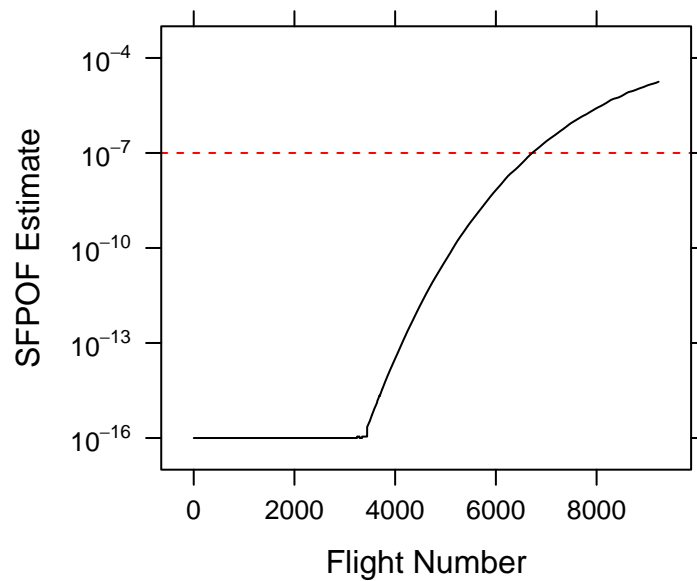


Figure 9.1: Single Flight Probability Of Failure (SFPOF) estimates for CP7ext with no inspections in the service life. The Sequential Importance Sampling (SIS) routine used 100k particles for this run. This result is used to determine the latest time at which an inspection can occur according to the specified SFPOF threshold of  $1 \times 10^{-7}$ , which is breached near flight 6500.

Table 9.1: Cost Estimates for a modified Example CP7ext Through Several Permutations of DI and  $\Delta$ DI Non-Destructive Inspection Intervals. Each run used 500k particles in the interval version (50 flight intervals) of the Sequential Importance Sampling (SIS) routine. Costs are calculated for inspections (Insp), repairs (Rep), false calls (FC), and failures (Fail). Using a Single Flight Probability of Failure (SFPOF) threshold of  $1 \times 10^{-7}$ , the optimal inspection schedule shown here uses DI = 6000 and  $\Delta$ DI = 2000 (marked with an asterisk).

Run	DI	$\Delta$ DI	Insp(\$)	Rep(\$)	FC(\$)	Fail(\$)	Total(\$)	Max SFPOF
1	2000	1000	4500	5934	90	0	10524	8.33E-10
2	2000	2000	2500	5776	50	3	8329	7.03E-09
3	2000	3000	2000	6059	40	41	8140	1.19E-07
4	4000	1000	3500	5861	70	0	9431	9.48E-12
5	4000	2000	2000	5742	40	4	7786	1.05E-08
6	4000	3000	1500	5745	30	77	7352	2.25E-07
7	6000	1000	2500	6084	50	2	8635	5.37E-09
*8	6000	2000	1500	5866	30	19	7416	5.05E-08
9	6000	3000	1500	6644	30	368	8542	9.48E-07

resulting from the 27 runs are given in Table 9.2. The optimal run from each of the three iterations is marked in the table with an asterisk. Note that each run of the routine uses three parallel sequences so the convergence of the cost estimates can be qualitatively assessed. Also note that the interval SIS routine is used for these runs to decrease the runtime.

The permutation exercise summarized in Table 9.2 identifies that  $DI = 5250$  and  $\Delta DI = 2000$  yields minimal costs and maintains SFPOF below the specified  $1 \times 10^{-7}$  threshold. Note that according to these results many similar strategies yield essentially equivalent cost estimates, thus for this example there is no need to further refine the strategies. Due to the number of cases that needed to be run, the interval SIS routine was used to generate Table 9.2. To complete this exercise the optimal strategy is run in the flight-by-flight routine until convergence of cost and peak SFPOF estimates is achieved. The SFPOF estimates of the winning strategy are shown in Figure 9.2. Corresponding PCD estimates are shown in Table 9.3. Finally, the cost estimates of the optimal strategy are given in Table 9.4.

Note that for this example, the false call rate of 1% is clearly not a strong factor in determining the ideal strategy because false calls account for less than 1% of total costs. The inspection and repair costs are responsible for the majority of total costs.

### 9.3 Extensions to the Maintenance Cost Minimization Problem

In the previous section a simple example was given to give a general idea of how the selection of a maintenance strategy may proceed. For that problem, it was sufficient to permute combinations of  $DI$  and  $\Delta DI$  to find the optimal strategy. There are many ways in which the problem can become more complex, which would require more sophisticated approaches. In this section, some potential complications are presented.

Table 9.2: Cost estimates (sum of costs from inspections, repairs, false calls, and failures) and risk estimates (peak values of Single Flight Probability of Failure) for modified Example CP7ext through several permutations of DI and  $\Delta$ DI inspection intervals. Each DI/ $\Delta$ DI pair is run in the interval Sequential Importance Sampling (SIS) routine using 500k particles with 50 flight intervals. Three independent sequences are run for each so that convergence of cost and risk estimates can be examined. The strategy which minimizes costs while maintaining SFPOF below  $1 \times 10^{-7}$  is identified with an asterisk in each batch of 9 runs. Cost estimates for competing strategies are similar in the last batch. If more refinement is desired, this procedure can be continued.

Run	DI	$\Delta$ DI	Cost1(\$)	Cost2(\$)	Cost3(\$)	Risk1	Risk2	Risk3
1	2000	1000	10524	10557	10540	8.3E-10	1.2E-08	6.6E-12
2	2000	2000	8329	8326	8327	7.0E-09	7.0E-09	7.1E-09
3	2000	3000	8140	8146	8548	1.2E-07	1.2E-07	8.3E-06
4	4000	1000	9431	9426	9418	9.5E-12	9.4E-12	9.6E-12
5	4000	2000	7786	7794	7785	1.1E-08	1.1E-08	1.1E-08
6	4000	3000	7352	7348	7353	2.3E-07	2.2E-07	2.2E-07
7	6000	1000	8635	8624	8625	5.4E-09	5.4E-09	5.4E-09
*8	6000	2000	7416	7417	7419	5.1E-08	5.0E-08	5.0E-08
9	6000	3000	8542	8548	8542	9.5E-07	9.5E-07	9.5E-07
10	5500	1500	7892	7888	7895	4.7E-09	4.7E-09	4.7E-09
*11	5500	2000	7199	7198	7202	3.9E-08	3.9E-08	3.8E-08
12	5500	2500	7493	7494	7489	9.9E-08	1.0E-07	9.9E-08
13	6000	1500	8358	8356	8346	9.7E-09	9.8E-09	9.7E-09
14	6000	2000	7410	7417	7418	5.0E-08	5.0E-08	5.0E-08
15	6000	2500	7832	7827	7826	2.5E-07	2.5E-07	2.5E-07
16	6500	1500	7421	7420	7414	3.8E-08	3.8E-08	3.8E-08
17	6500	2000	7782	7782	7781	1.3E-07	1.3E-07	1.3E-07
18	6500	2500	8366	8365	8366	5.2E-07	5.2E-07	5.2E-07
19	5250	1750	8150	8144	8148	1.7E-08	1.7E-08	1.7E-08
*20	5250	2000	7152	7157	7151	6.9E-08	6.9E-08	6.9E-08
21	5250	2250	7250	7253	7251	4.8E-08	4.8E-08	4.8E-08
22	5500	1750	8375	8372	8378	2.4E-08	2.4E-08	2.4E-08
23	5500	2000	7205	7198	7205	3.8E-08	3.8E-08	3.9E-08
24	5500	2250	7327	7325	7334	4.3E-08	4.3E-08	4.3E-08
25	5750	1750	7179	7173	7177	3.1E-08	3.1E-08	3.1E-08
26	5750	2000	7287	7295	7295	3.0E-08	3.0E-08	3.0E-08
27	5750	2250	7447	7450	7446	7.2E-08	7.2E-08	7.2E-08

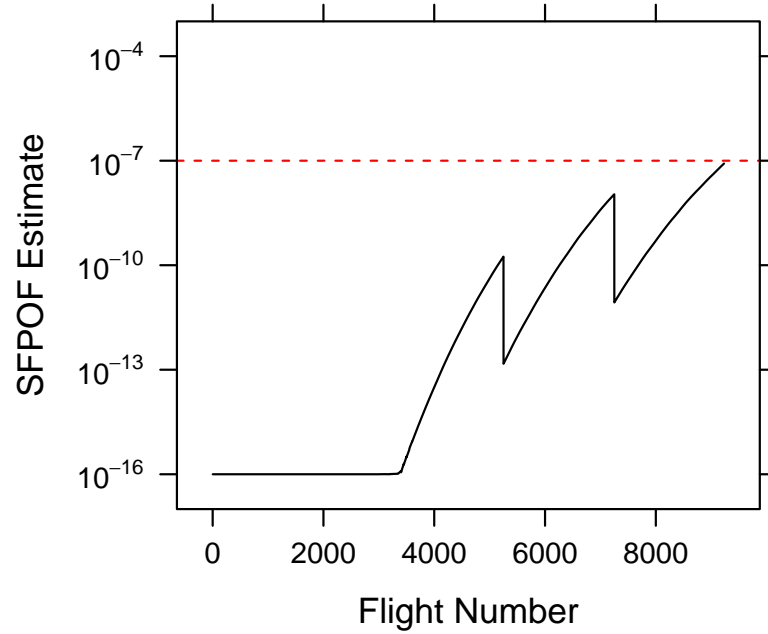


Figure 9.2: Single Flight Probability Of Failure (SFPOF) estimates for the optimal strategy of modified CP7ext. Results shown utilized the flight-by-flight sequential importance sampling routine using 1m particles. With inspections after 5250 flights and 7250 flights, Single Flight Probability of Failure (SFPOF) is kept below the  $1 \times 10^{-7}$  threshold (reaching a peak value of  $8.3 \times 10^{-8}$ ).

Table 9.3: Probability of Crack Detection (PCD) estimates for the optimal strategy of modified Example CP7ext. The PCD estimates are used to predict the future repair costs.

Insp	Oversize	Fitting	Replacement	Total
1	0.087	0.019	0.000	0.107
2	0.165	0.067	0.006	0.238
3	0.263	0.114	0.024	0.401

Table 9.4: Cost estimates for the optimal strategy of modified Example CP7ext. Costs are calculated for inspections (Insp), repairs (Rep), false calls (FC), and failures (Fail). Note that the total cost predicted using the flight-by-flight routine is \$7130, where the interval routine estimate (using fewer particles) is 7153. The peak SFPOF estimate of the flight-by-flight routine is slightly higher than that of the interval routine, though still below the specified SFPOF threshold of  $1 \times 10^{-7}$ .

Insp(\$)	Rep(\$)	FC(\$)	Fail(\$)	Total(\$)	Max SFPOF
1500.00	5575.36	30.00	24.98	7130.34	8.31E-08

### 9.3.1 Variable POD Curve Detection Capability

Following 1823A, any number of POD curves can be generated for a crack detection system by altering the detection threshold (see Section 7.2.4). This detection capability may be a variable which can be altered by the maintainers of a fleet to optimize a maintenance strategy. Increasing the detection threshold will lead to fewer false calls and reduced detection capability. This feature may be particularly useful when utilizing automated inspection technology, as is described in the next section.

### 9.3.2 Automated Inspections of Inaccessible Locations

Automatic inspection technologies, often referred to as Structural Health Monitoring, are the subject of active research in the aerospace industry. In this, embedded or in-situ sensors are employed to conduct structural inspections without requiring access to the location. With such technology it is possible to perform inspections very frequently; for example, after every flight. The ability to perform frequent inspections on difficult-to-access structure has the potential to increase safety and reduce maintenance costs. Such sensors are not immune to the possibility of false calls, however, and the occurrence of a false call can be costly since the location is not easily accessed and may require grounding of the aircraft to verify the inspection results and perform

any necessary repairs.

In addition, the traditional POD curve is developed assuming that inspections are independent. For infrequent NDE inspections, which may be conducted with various equipment and operators, the independence assumption may be reasonable. However, with embedded sensors and frequent inspections, the assumption of independence from inspection-to-inspection is clearly incorrect. The correlation between subsequent inspections in an embedded sensor system is an open question.

Setting aside the issue of correlation between subsequent inspections, there is an advantage to be had in using a POD curve with a low false call rate when conducting automated inspections in the field. This will lead to fewer false calls and associated costs. When the aircraft is in the maintenance depot, where the findings of the inspection system can be verified at lower cost, it may be advantageous to use a POD curve with a higher detection capability and higher false call rate. In the search for an optimal maintenance strategy, the POD curve to utilize in the field and in the maintenance depot are thus separate variables.

Note that if  $DI$ ,  $\Delta DI$ ,  $POD_{\text{field}}$ , and  $POD_{\text{depot}}$  are each alterable maintenance parameters, the simple approach to optimization demonstrated by example in the previous section is more time-consuming due to the number of runs that would be required. In that case, more sophisticated approaches to seeking out an optimal maintenance strategy may be beneficial.

### 9.3.3 Non-Typical Usage or Incorporation of Inspection Results

The cost predictions of this chapter are based on predicted usage, where each aircraft is assumed to be flown according to the design usage. As described in Chapter 7, the severity of usage among aircraft can differ, leading to changes in the failure probability and repair probability for that aircraft. Also, the PCD estimates are obtained assuming the detection threshold-based

approach will be used to determine if a crack is found. Chapter 7 also presents methods in which inspection results can be utilized to update the model and better determine whether a repair must be performed or can be delayed. These possible alterations to the maintenance strategy are not part of the cost modeling presented above. In practice, the prediction of maintenance costs should be re-visited when the SIS model is updated.

# CHAPTER 10

## CONCLUSION

Section 10.1 lists the original contributions of this work. A free, publicly licensed software package capable of performing the analyses of this work is described in Section 10.2. Finally, this work concludes with a discussion of future research opportunities involving the HMM (Hidden Markov Model) / SIS (Sequential Importance Sampling) approach to PDTA (Probabilistic Damage Tolerance Analysis) in Section 10.3.

### 10.1 Original Contributions

The original contributions of this work can be summarized as follows:

- an explicit MC (Monte Carlo) approach to PDTA was developed which can be used to validate other PDTA approaches,
- an HMM representation of PDTA solved using SIS was developed; the results of which were shown to agree with those of the MC routine and to outperform a popular industry PDTA tool,
- an improvement to the modeling of the physics regarding potential future repairs was demonstrated using the SIS routine,
- Bayesian updating of model parameters was shown to be efficiently performed in the SIS routine, providing a modeling tool which can evolve over time as evidence regarding the health of the structure is observed,

- the previously unsolved PDTA problem of continuing damage was successfully solved using SIS,
- a method for estimating the costs of a maintenance plan while maintaining a specified level of safety was described,
- a free, publicly licensed and open source PDTA software package was produced.

## 10.2 crackR Software

The MC and SIS analyses of this work utilized an original R package called `crackR`. Any PDTA problem of similar scope to the examples of this work can be analyzed using the `crackR` package. The software is free, publicly licensed, and open source, and can be obtained from the Comprehensive R Archive Network<sup>1</sup> (CRAN). The documentation provided with the package includes detailed descriptions of the package organization as well as instructions on how to use it. Working examples are provided.

PDTA practitioners are encouraged to extend the software and contact the author to suggest changes or improvements. A future possible improvement may include parallelization of the routine for increased computational speed. Also, the capabilities discussed in the next section may be incorporated and the software refined to better suit such analyses.

## 10.3 Future Work

A number of possible avenues for future research involving the SIS approach to PDTA are discussed in this section.

---

<sup>1</sup><http://cran.us.r-project.org/>

### 10.3.1 Other Types of Structural Deterioration

The focus of this work is on fatigue cracking of metallic structures. PDTA analysis involving other types of deterioration in metals, such as corrosion, could be considered. The flexibility of the SIS approach makes such an application possible. In addition to metals, composite materials represent a significant portion of aircraft structures. The damage mechanisms of composites, such as delamination, are fundamentally different from fatigue cracking in metals. These types of damage can involve many random variables. Sequential MC methods in general function well in high dimensions, and an SIS approach to composite failure prediction may be very useful.

Further research into more complex continuing damage scenarios is warranted. Continuing damage could involve three, four, or more cracks. Including additional cracks can be accomplished with the SIS routine developed in this work, though the computation time may become rather long. Also, the continuing damage model in this work involved a discontinuous switch between cold and hot states (see Chapter 8). In reality the crack growth rates and stress intensities for the cracks will be a function of the lengths (and possibly orientations) of both cracks; significantly increasing the model complexity. Again, the flexibility of the SIS approach can accommodate such considerations.

### 10.3.2 Stochastic Crack Growth

As was discussed in Chapter 4, SIS is well equipped to model a stochastic transition from state-to-state. With a stochastic crack growth model, the runtime for the SIS routine would not be dramatically increased since it would simply involve calling a function which includes a random component instead of a table lookup function. While a stochastic crack growth model is more realistic, experts in stochastic crack growth are far more difficult to come by in the aerospace industry than are traditional practitioners. It may nevertheless be the case that a stochastic model will better predict failures and repairs. For a discussion of stochastic crack growth, see Yang, Hsi and Manning [59]

or Yang and Manning [60].

### 10.3.3 Crack Initiation

Opinions vary in aerospace academia and research whether crack initiation needs to be explicitly modeled in PDTA. Much research has been conducted in developing quality EIFS (Equivalent Initial Flaw Size) distributions[15][48][42]. Also, when utilizing deterministic crack growth, the TTCI (Time To Crack Initiation) and EIFS approaches to PDTA may yield equivalent results because of the one-to-one relationship between them as shown in Figure 3.2. Consideration of the PDTA problem suggests that the most realistic approach would involve a stochastic crack initiation period, including the potential for accidental and spontaneous initiation, followed by stochastic crack growth. In addition, this would allow for the model to assess the likelihood that a crack has initiated. When utilizing the PDTA approach presented throughout this document, a crack has been assumed to have already initiated.

If data can be obtained which can well characterize crack initiation with a TTCI distribution, the SIS approach can easily accommodate a crack initiation period. One could add a variable called  $t_0$  to the state, which indicates the flight number (or flight hour) where the crack will initiate. As the model proceeds, any particle which has yet to initiate simply does not grow, has zero probability of failure, and cannot be detected by NDE (false calls disregarded). The initial crack size  $a_0$  would either be generated from a distribution of crack length at initiation (which may be correlated with  $t_0$ ), or could be of fixed length. No other modifications would be required and the crack initiation phase could be included with minimal computational cost.

Crack initiation will eventually occur when cyclic loading is applied to a structure. There are other ways cracks can initiate; for example, a tool can be dropped onto the structural surface during routine maintenance, or a fastener hole can be scratched when a rivet is removed to perform a structural inspection. It may be possible to incorporate such initiations in the determination of

the EIFS or TTCI distribution, though this would not capture the possibility that scheduled maintenance can *cause* a crack to initiate. In the SIS approach to PDTA a model parameter could be specified which yields the probability of crack initiation at an inspection – or at any specified time – allowing for explicit modeling of such event-driven crack initiations.

### 10.3.4 Correlated Inspections

The focus of this work has been on infrequent NDE inspections. In this case, the maintenance technician and NDE hardware will likely differ from inspection to inspection, and subsequent inspections will generally be separated by months or years. As such it is reasonable to assume that subsequent inspections are indeed independent, as has been assumed in this work. That assumption is not necessary, however, and it is possible to relax it<sup>2</sup>.

In addition, there is a growing field of research involving automated inspection techniques, also known as in-situ sensors (see the international journal *Structural Health Monitoring*). Such sensors are embedded in the structure and use techniques similar to those of NDE (e.g., many such sensors are ultrasonic, a common NDE approach). With in-situ sensors an inspection could theoretically be conducted as often as one likes, flight-by-flight or moment-to-moment, and subsequent inspections are certainly correlated in this case. See Shook et al [49] for a discussion of the impact of assuming various levels of correlation.

Recall, the SIS approach requires that observations depend only on the current state, i.e. the likelihood distribution is  $f(\mathbf{y}_t|\mathbf{x}_t)$ . The previous inspection results are not explicitly part of the current state, so as is the model cannot utilize correlated inspections. If the correlated POD model can be developed such that it is limited to require only several previous inspection results, the model can be altered such that a number of variables are added to the state,

---

<sup>2</sup>It may also be appropriate to expand the POD model to include other variables such as orientation, maintainer skill, etc., as is suggested by Coppe et al. [11], though this is outside the scope of this work

one for each previous inspection. (If tens or hundreds of previous results are needed, the high-dimensionality will slow the model considerably.) For example, if the selected correlation model utilizes a correlation function using the previous three inspection results, the variables  $y_{-3}$ ,  $y_{-2}$ , and  $y_{-1}$  could be included as state variables, and a corresponding  $\text{POD}(a, y_{-3}, y_{-2}, y_{-1})$  model would need to be developed.

## REFERENCES

- [1] 787 fact sheet, The Boeing Company. <http://www.boeing.com/commercial/787family/programfacts.html>, retrieved March 2014.
- [2] Aircraft structural integrity program (ASIP). Technical Report MIL-STD-1530C, Department of Defense, 2005.
- [3] C. Annis. *Statistical best-practices for building Probability of Detection (POD) models*, 2012. R package mh1823, version 3.1.2.
- [4] M.S. Arulampalam, S. Maskell, N. Gordon, and T. Clapp. A tutorial on particle filters for online nonlinear/non-gaussian bayesian tracking. *Signal Processing, IEEE Transactions on*, 50(2):174–188, February 2002.
- [5] L.E. Baum and T. Petrie. Statistical inference for probabilistic functions of finite state markov chains. *The Annals of Mathematical Statistics*, 37:1554–1563, 1966.
- [6] A. P. Berens, P. W. Hovey, and D. A. Skinn. Risk analysis for aging aircraft fleets volume 1 - analysis. Technical report, University of Dayton, Oct 1991.
- [7] Y. Bombardier, M. Liao, and G. Renaud. Modelling of continuing damage for damage tolerance analysis. In *ICAF Symposium*, June 2011.

- [8] S.P. Brooks and A. Gelman. General methods for monitoring convergence of iterative simulations. *Journal of Computational and Graphical Statistics*, 7(4):434–455, 1998.
- [9] T.R. Brussat. Recommended methodology updates to improve single flight probability of failure estimation. In *Aircraft Structural Integrity Program*, November 2012.
- [10] D.A. Cope and J.D. Moffett. Bayesian updating of structural health and integrity assessments using real-time inspection results. In *American Institute of Aeronautics and Astronautics Structures, Structural Dynamics, and Materials Conference*, April 2012.
- [11] A. Coppe, R.T. Haftka, N.H. Kim, and C. Bes. A statistical model for estimating probability of crack detection. In *International Conference on Prognostics and Health Management*, October 2008.
- [12] A. Doucet, N. de Freitas, and N. Gordon. *Sequential Monte Carlo Methods in Practice*. Springer, 2 edition, 2010.
- [13] A. Doucet, S. Godsill, and C. Andrieu. On sequential monte carlo sampling methods for bayesian filtering. *Statistics and Computing*, 10:197–208, July 2000.
- [14] T. Drozda, C. Wick, R.F. Veilleux, and R. Bakerjian. *Tool and Manufacturing Engineers Handbook*. Society of Manufacturing Engineers, 1985.
- [15] Fastener hole quality. Technical Report AFFDL-TR-78-206, United States Air Force, 1978.
- [16] A.M. Freudenthal, J.M. Garrelts, and M. Shinozuka. The analysis of structural safety. Technical report, American Society of Civil Engineers, 1966.
- [17] A. Gelman, J.B. Carlin, H.S. Stern, and D.B. Rubin. *Bayesian Data Analysis*. Chapman and Hall/CRC, 2003.

- [18] E.H. Glaessgen and D.S. Stargel. The digital twin paradigm for future NASA and U.S. Air Force vehicles. In *American Institute of Aeronautics and Astronautics Structures, Structural Dynamics, and Materials Conference*, April 2012.
- [19] U.G. Goranson. Damage tolerance facts and fiction. In *International Conference on Damage Tolerance of Aircraft Structures*, September 2007.
- [20] E.J. Gumbel. *Statistical theory of extreme values and some practical applications: a series of lectures*. Applied Mathematics Series. United States Government Printing Office, 1954.
- [21] K. Halbert. crackR: Probabilistic prediction of airframe fatigue damage. In *UseR! Conference*, 2012.
- [22] K. Halbert. *Probabilistic damage tolerance analysis for fatigue cracking of metallic aerospace structures*, 2014. R package crackR, version 0.3-07.
- [23] K. Halbert and L.M. Fitzwater. Sequential importance sampling approach to probabilistic damage tolerance analysis. In *American Institute of Aeronautics and Astronautics SciTech Conference*, January 2014.
- [24] K. Halbert, L.M. Fitzwater, C.L. Davis, J.-B. Ihn, D.S. Jones, J.L. McFarland, T.Y. Torng, and D.A. Wiegand. Cost/benefit analysis for system-level integration of non-deterministic analysis and maintenance technology. In *American Institute of Aeronautics and Astronautics Non-Deterministic Approaches Conference*, 2012.
- [25] K. Halbert, L.M. Fitzwater, H. Smith Jr., and T.Y. Torng. Single flight probability of failure in probabilistic damage tolerance analysis. In *American Institute of Aeronautics and Astronautics Non-Deterministic Approaches Conference*, 2013.
- [26] M.S. Hamada, A.G. Wilson, C.S. Reese, and H.F. Martz. *Bayesian Reliability*. Springer, 2008.

- [27] C. Hellier. *Handbook of Nondestructive Evaluation*. McGraw-Hill, 2001.
- [28] Joint service specification guide aircraft structures. Technical Report JSSG-2006, Department of Defense, 1998.
- [29] M. Liao. Comparison of different single flight (hour) probability of failure (SFPOF) calculations for aircraft structural risk analysis. In *Aircraft Airworthiness and Sustainment*, April 2012.
- [30] M. Liao, Y. Bombardier, and G. Renaud. Probabilistic risk analysis for aircraft structures with limited in-service damages. In *International Congress of the Aeronautical Sciences*, September 2012.
- [31] M. Liao, Y. Bombardier, G. Renaud, N. Bellinger, and T. Cheung. Development of advanced risk assessment methodologies for aircraft structures containing MSD/MED. In *ICAF 2009, Bridging the Gap between Theory and Operational Practice*, May 2009.
- [32] J. W. Lincoln. Method for computation of structural failure probability for an aircraft. Technical report, Aeronautical Systems Division, Wright-Patterson Air Force Base, Jul 1980.
- [33] R.E. Little and E.H. Jebe. *Statistical design of fatigue experiments*. Wiley, 1975.
- [34] J.S. Liu. *Monte Carlo Strategies in Scientific Computing*. Springer Verlag, New York, Berlin, Heidelberg, 2008.
- [35] Y. Liu and S. Mahadevan. Probabilistic fatigue life prediction using an equivalent initial flaw size distribution. *International Journal of Fatigue*, 31(3):476–487, Mar 2009.
- [36] H.O. Madsen, R.K. Skjong, A.G. Tallin, and F. Kirkemo. Probabilistic fatigue crack growth analysis of offshore structures, with reliability updating through inspection. In *Marine Structural Reliability Symposium*, Oct 1987.

- [37] P.C. Miedlar, A.P. Berens, P.W. Hovey, T.R. Boehnlein, and J.S. Loomis. Prof v3 probability of fracture aging aircraft risk analysis update. Technical report, University of Dayton Research Institute, Dayton, OH, 2005.
- [38] Nondestructive evaluation system reliability assessment. Technical Report MIL-HDBK-1823A, Department of Defense, The United States of America, 2009.
- [39] P.C. Paris, M.P. Gomez, and W.E. Anderson. A rational analytic theory of fatigue. *Trend Engineering*, 13(1), 1961.
- [40] R Core Team. *R: A Language and Environment for Statistical Computing*. R Foundation for Statistical Computing, Vienna, Austria, 2012. ISBN 3-900051-07-0.
- [41] R.P. Reed. *The Economic Effects of Fracture in the United States*. National Bureau of Standards, Washington, D.C., 1983.
- [42] G. Renaud, M. Liao, and Y. Bombardier. Calculation of equivalent initial flaw size distributions for multiple site damage. In *American Institute of Aeronautics and Astronautics SciTech Conference*, January 2014.
- [43] B. Ristic. *Particle Filters for Random Set Models*. Springer, 20013.
- [44] C. Robert and G. Casella. *Monte Carlo Statistical Methods*. Springer, 2 edition, 2005.
- [45] C. Robert and G. Casella. *Introducing Monte Carlo Methods with R*. Use R! Springer, 2010.
- [46] J. Schijve. *Fatigue of Structures and Materials*. Springer, 2009.
- [47] M. Shiao, K. Boyd, and S. Fawaz. A risk assessment methodology and tool for probabilistic damage tolerance-based maintenance planning. In *8th FAA/NASA/DoD Aging Aircraft Conference*, 2005.

- [48] M. Shinozuka. Durability methods development: volume 4. Initial quality representation. Technical report, Air Force Flight Dynamics Laboratory, United States Air Force, 1979.
- [49] B.D. Shook, H.R. Millwater, M.P. Enright, S.J. Hudak Jr., and W.L. Francis. Simulation of recurring automated inspections on probability-of-fracture estimates. *Structural Health Monitoring*, 7:293–307, 2008.
- [50] P.J. Shull. *Nondestructive Evaluation: Theory, Techniques, and Applications*. Dekker Mechanical Engineering Series. Marcel Dekker, 2002.
- [51] Standard practices for cycle counting in fatigue analysis. Technical Report E 1049-85, ASTM International, 2005.
- [52] R.I. Stephens, A. Fatemi, R.R. Stephens, and H.O. Fuchs. *Metal Fatigue in Engineering*. Wiley-Interscience Publication. John Wiley & Sons, 2000.
- [53] D. Straub and M.H. Faber. Risk based inspection planning for structural systems. *Structural Safety*, 27(4):335–355, Oct 2005.
- [54] S. Suresh. *Fatigue of Materials*. Cambridge Solid State Science Series. Cambridge University Press, 1998.
- [55] Y. Torng. Risk-based design and maintenance system (RBDMS), cited 2014. Software package, The Boeing Company.
- [56] W.N. Venables and B.D. Ripley. *Modern Applied Statistics With S*. Springer, 4 edition, 2003.
- [57] E.B. Wilson. Probable inference, the law of succession, and statistical inference. *Journal of the American Statistical Association*, 22:209–212, June 1927.
- [58] Y. Xiang, Z. Lu, and Y. Liu. Crack growth-based fatigue life prediction using an equivalent initial flaw model. Part I: Uniaxial loading. *International Journal of Fatigue*, 32(2):341349, 2010.

- [59] J.N. Yang, W.H. Hsi, and S.D. Manning. Stochastic crack propagation with applications to durability and damage tolerance analyses. Technical report, DTIC Document, 1985.
- [60] J.N. Yang and S.D. Manning. A simple second order approximation for stochastic crack growth analysis. *Engineering Fracture Mechanics*, 53(5):677–686, 1996.